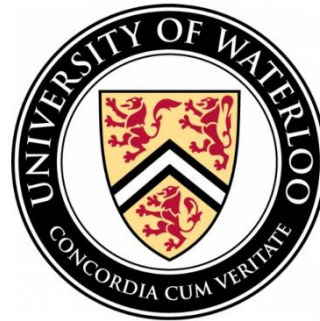


POLITECNICO DI TORINO
UNIVERSITY OF WATERLOO

**Corso di Laurea Magistrale
In INGEGNERIA MECCANICA**

Tesi di Laurea Magistrale

**“Through The Road” Hybrid configurations for
service vehicles: modelling and analysis**



Relatori

Prof. Andrea Tonoli
Prof. Amir Khajepour

Candidato

Andrea Pasca

A.A. 2018/2019

*Alla mia famiglia
E a chi mi è sempre stato accanto
in questo percorso*

Table of contents

| | |
|---|----|
| Table of contents..... | 3 |
| List of figures | 4 |
| List of tables | 7 |
| Introduction..... | 8 |
| 1. Literary review and background..... | 10 |
| 1.1 Degrees of Hybridization | 10 |
| 1.2 Parallel Hybrid configurations | 11 |
| 1.2.1 Parallel Hybrid architectures | 12 |
| 1.2.2 Operating modes..... | 13 |
| 1.3 Series Hybrid configuration..... | 14 |
| 1.3.1 Operating modes..... | 15 |
| 1.4 Parallel-Series Hybrid configurations (power split)..... | 16 |
| 1.4.1 E-CVT Transmission and Power split device (PSD) | 17 |
| 1.4.2 Operating modes..... | 18 |
| 1.5 Through-The-Road (TTR) Hybrid configuration..... | 19 |
| 1.6 Advantages of Hybrid Technology..... | 20 |
| 1.6.1 Optimization of the engine’s operating points | 20 |
| 1.6.2 Energy recuperation through Regenerative Braking..... | 24 |
| 1.6.3 Idling reduction | 26 |
| 1.6.4 Other advantages and challenges | 27 |
| 2. Drivetrain configurations and analysis tool..... | 28 |
| 2.1 “Through-the-Road” Hybrid Heavy Duty vehicles | 28 |
| 2.2 Analyzed configurations | 29 |
| 2.2.1 Single electric motor coupled through a differential | 29 |
| 2.2.2 Frameless wheel-motors..... | 30 |
| 2.3 Simulation Tools used | 32 |
| 2.3.1 Mechanical Simulation “TruckSim” suite | 32 |
| 2.3.2 Coupling with Matlab-Simulink environment | 36 |
| 2.4 Simulation procedures | 38 |
| 2.4.1 Heavy-Duty Diesel Truck Schedule..... | 38 |
| 2.4.2 Urban path test | 39 |
| 2.4.3 Food delivery path test..... | 41 |
| 2.4.4 Cruising path test | 43 |
| 3. Components and vehicle modelling | 45 |
| 3.1 Conventional vehicle modelling | 45 |
| 3.1.1 Sprung masses and payload | 45 |
| 3.1.2 Aerodynamics..... | 46 |
| 3.1.3 Tires specifications | 47 |
| 3.1.4 Internal combustion engine dataset | 49 |
| 3.1.5 Driveline dataset | 50 |
| 3.1.6 Suspension and steering dataset..... | 56 |
| 3.1.7 Simulink integration | 56 |
| 3.1.8 Food delivery truck modeling..... | 58 |
| 3.2 Single electric motor hybrid configuration – component sizing | 61 |
| 3.2.1 Electric machine | 61 |

| | |
|--|-----|
| 3.2.2 Battery pack..... | 64 |
| 3.3 Single electric motor hybrid configuration – modelling in Simulink | 66 |
| 3.3.1 Electric machine | 66 |
| 3.3.2 Battery pack..... | 71 |
| 3.3.3 Power management | 76 |
| 3.3.4 Model assembling | 82 |
| 3.3.5 Food delivery hybrid truck modelling | 84 |
| 3.4 Wheel motors hybrid configuration – component sizing..... | 85 |
| 3.4.1 Electric machine | 85 |
| 3.5 Wheel motors hybrid configuration – modelling in Simulink | 87 |
| 4. Simulations results, analysis and discussion | 89 |
| 4.1 Only-ICE architecture | 89 |
| 4.1.1 Urban path test results..... | 89 |
| 4.1.2 Food delivery path test results..... | 93 |
| 4.1.3 Cruising path test results..... | 96 |
| 4.2 Single electric motor architecture..... | 98 |
| 4.2.1 Urban path test results..... | 98 |
| 4.2.2 Food delivery test results | 105 |
| 4.2.3 Cruising test results | 108 |
| 4.3 Wheel motors architecture | 113 |
| 4.3.1 Urban path test results..... | 113 |
| 4.3.2 Urban path test results with re-sized battery pack..... | 117 |
| 5. Design feasibility study..... | 120 |
| 5.1 Single electric motor feasibility study | 120 |
| 5.2 Wheel motors architecture feasibility study..... | 123 |
| 5.2.1 Wheel subsystem | 125 |
| 5.2.2 Main hub subsystem | 126 |
| 5.2.3 Electric machine subsystem | 127 |
| 6. Conclusions and future work..... | 129 |
| 6.1 Conclusions..... | 129 |
| 6.2 Future work | 132 |
| Bibliography..... | 133 |
| Sitography | 134 |

List of figures

| | |
|---|----|
| Figure 1 - Parallel Hybrid schematic..... | 12 |
| Figure 2 - Parallel hybrid configurations (Yang Y., 2016) | 12 |
| Figure 3 - Series Hybrid schematic | 14 |
| Figure 4 - Parallel/Series Hybrid schematic..... | 17 |
| Figure 5 - PSD configuration schematic (Miller J. M., 2005) | 18 |
| Figure 6 - Mechanical efficiency as a function of imep..... | 22 |
| Figure 7 – Operating points of a D-segment passenger car on FTP-75 cycle (Eshani M., 2010)..... | 23 |
| Figure 8 - Regenerative braking torque vs vehicle speed (Khajepour A., 2014) | 25 |
| Figure 9 - Through the Road HD first configuration schematic..... | 30 |
| Figure 10 - Through the Road HD second configuration schematic..... | 30 |

| | |
|--|----|
| Figure 11 - TruckSim Run Control screen | 33 |
| Figure 12 – TruckSim Vehicle Configuration dataset | 34 |
| Figure 13 - TruckSim Simulated Test Specification screen | 35 |
| Figure 14 - TruckSim VS Visualizer..... | 36 |
| Figure 15 - TruckSim Run control with Simulink option | 37 |
| Figure 16 - External Simulink model (Mechanical Simulation, 2018)..... | 37 |
| Figure 17 - HHDDT Cruising mode..... | 39 |
| Figure 18 - HHDDT Transient mode..... | 39 |
| Figure 19 - Urban test speed profile | 40 |
| Figure 20 - Urban test ground elevation | 40 |
| Figure 21 - Urban test itinerary | 41 |
| Figure 22 - Food delivery test speed profile..... | 42 |
| Figure 23 - Food delivery test elevation..... | 42 |
| Figure 24 - Cruising test speed profile..... | 43 |
| Figure 25 - Cruising test elevation..... | 44 |
| Figure 26 - Tyre longitudinal force versus slip ratio | 48 |
| Figure 27 - Tyre's lateral force versus slip angle | 48 |
| Figure 28 - Tyre's aligning moment versus slip angle | 48 |
| Figure 29 - Detroit S50 efficiency map | 50 |
| Figure 30 - Driveline schematic (Mechanical Simulation, 2018) | 50 |
| Figure 31 - Driveline schematic, downstream of the clutch (Mechanical Simulation, 2018) | 51 |
| Figure 32 - Torque converter inverse capacity factor $1/K$ versus speed ratio | 53 |
| Figure 33 - Torque converter ratio versus speed ratio | 53 |
| Figure 34 - example of downshifting and upshifting strategies (Mechanical Simulation, 2018)..... | 54 |
| Figure 35 - Fuel consumption calculator subsystem..... | 57 |
| Figure 36 - External Simulink model for fuel calculation and data acquisition..... | 58 |
| Figure 37 - Refrigeration system power load cycle | 59 |
| Figure 38 - Simulink model extension for auxiliary device modeling..... | 60 |
| Figure 39 - Auxiliary device model | 60 |
| Figure 40 - HPEVS AC-51 characteristic curves (HPEVS, s.d.) | 62 |
| Figure 41 - AC-51 estimated efficiency map | 63 |
| Figure 42 - SOC limits for hybrid powertrain battery (Nelson F. R., 2000)..... | 65 |
| Figure 43 - Electric machine block..... | 66 |
| Figure 44 - Electric machine block design | 67 |
| Figure 45 - Electric motor block design | 68 |
| Figure 46 - Regenerative braking block design | 69 |
| Figure 47 - Average efficiency calculation subsystem..... | 71 |
| Figure 48 - Battery block | 72 |
| Figure 49 - Battery block design | 72 |
| Figure 50 - Circuit schematic (Khajepour A., 2014)..... | 73 |
| Figure 51 - Current calculator block | 73 |
| Figure 52 - Current saturation block | 74 |
| Figure 53 - State Of Charge calculation subsystem..... | 75 |
| Figure 54 - Optimization of the engine's operating points strategy | 76 |
| Figure 55 - Optimum engine torque curve..... | 77 |
| Figure 56 - Power management subsystem..... | 80 |
| Figure 57 - SOC control strategy subsystem | 81 |
| Figure 58 - Powertrain mode selection subsystem | 81 |

| | |
|--|-----|
| Figure 59 - Assembled Simulink model | 82 |
| Figure 60 - Front and rear differential schematic | 83 |
| Figure 61 - Auxiliary Device block..... | 84 |
| Figure 62 - wheel motors efficiency map | 86 |
| Figure 63 - Wheel motors Simulink block..... | 87 |
| Figure 64 - Urban path test, Only-ICE, vehicle speed versus target speed | 89 |
| Figure 65 - Urban path test, Only-ICE, speed target deviation | 90 |
| Figure 66 - Urban path test, Only-ICE, engine's output torque | 90 |
| Figure 67 - Urban path test, Only-ICE, engine's overall efficiency | 91 |
| Figure 68 – Urban path test, Only-ICE, engine's operating points | 92 |
| Figure 69 - Urban path test, Only-ICE, cumulated fuel consumption | 92 |
| Figure 70 - Food delivery test, Only-ICE, vehicle's speed versus target speed | 94 |
| Figure 71 - Food delivery test, Only-ICE, engine's overall efficiency..... | 94 |
| Figure 72 - Food delivery test, Only-ICE, cumulated fuel consumption..... | 95 |
| Figure 73- Cruising test, Only-ICE, vehicle's speed versus target speed | 96 |
| Figure 74 - Cruising test, Only-ICE, engine's efficiency | 96 |
| Figure 75 - Cruising test, Only-ICE, cumulated fuel consumption..... | 97 |
| Figure 76 - Urban path test results, first configuration..... | 99 |
| Figure 77 - Speed difference, Only-ICE vs HEV..... | 100 |
| Figure 78 - Engine operating points, ICE vs HEV | 101 |
| Figure 79 – Urban path test, first configuration, Engine average efficiency..... | 101 |
| Figure 80 – Urban path test, first configuration, Engine efficiency distribution..... | 102 |
| Figure 81 – Urban path test, first configuration, EM operating points..... | 102 |
| Figure 82 – Urban path test, first configuration, overall mechanical energy | 103 |
| Figure 83 – Urban path test, first configuration, Cumulated fuel consumption confrontation | 104 |
| Figure 84 – Food delivery test results, first configuration | 105 |
| Figure 85 – Food delivery test, first configuration, average efficiency | 106 |
| Figure 86 – Food delivery test, first configuration, Output mechanical energy | 107 |
| Figure 87 - Food delivery test, first configuration, Cumulated fuel consumption..... | 107 |
| Figure 88 – Food delivery test, first configuration, vehicle's speed and battery SOC | 109 |
| Figure 89 – Cruising test, first configuration, Engine operating points confront..... | 110 |
| Figure 90 – Cruising test, first configuration, Engine average efficiency confront | 110 |
| Figure 91 – Cruising test, first configuration, Mechanical energy confront..... | 111 |
| Figure 92 – Cruising test, first configuration, Cumulated fuel mass confront | 111 |
| Figure 93 - SOC confrontation, first vs second configuration | 113 |
| Figure 94 – Second hybrid configuration graphs | 114 |
| Figure 95 – Second configuration, Mechanical energy confrontation..... | 115 |
| Figure 96 – Second configuration, Electric motor operating points | 115 |
| Figure 97 – Second configuration, Cumulated fuel consumption confrontation | 116 |
| Figure 98 – Second configuration with resized battery pack, Battery SOC..... | 117 |
| Figure 99 – Second configuration with resized battery pack, Electric motor operating points..... | 118 |
| Figure 100 – Second configuration with resized battery pack, Mechanical energy | 118 |
| Figure 101 – Second configuration with resized battery pack, Cumulated fuel consumption | 119 |
| Figure 102 - Conventional axle rendering | 120 |
| Figure 103 - Mechanical connection between EM and differential..... | 121 |
| Figure 104 - Electric axle rendering..... | 122 |
| Figure 105 - Wheel motor configuration assembly..... | 123 |
| Figure 106 - Wheel assembly | 125 |

Figure 107 - Main hub assembly 126

Figure 108 - Electric machine assembly 127

Figure 109 - Complete assembly 128

List of tables

Table 1 - HDDT cycle characteristics 38

Table 2 - Vehicle's inertial properties..... 46

Table 3 - Detroit Diesel S50 characteristics..... 49

Table 4 - Differential and torque transfer case characteristics..... 55

Table 5 - HPEVS AC-51 specification (HPEVS, s.d.) 62

Table 6 - SOC control strategy parameters 78

Table 7 - Powertrain mode selection strategy 79

Table 8 - Wheel motor characteristics 86

Table 9 - Urban path, Only-ICE, test results 93

Table 10 - Food delivery test, Only-ICE, test results..... 95

Table 11 - Cruising test, Only-ICE, test results 97

Table 12 - First configuration model parameters..... 98

Table 13 – Urban path test, first configuration, results confrontation 104

Table 14 - Food delivery test results, first configuration 108

Table 15 – Cruising test results, first configuration..... 112

Table 16 – Second configuration model parameters 114

Table 17 – Second configuration, test results 117

Table 18 - Urban test results, second configuration with resized battery pack 119

Table 19 - List of components 124

Introduction

Since the invention of the first car, the historical Benz-Patent-Motorwagen, built in 1885, the automotive industry has encountered a substantial evolution during the twentieth and twenty-first centuries, revolutionizing our lives and changing forever our transportation habits.

Wheels-based transportation means have gained a predominant role in human lives and nowadays billions of cars, trucks, vans and motorcycles circulate all over the world, allowing us to move rapidly and comfortably from point A to point B, and to transport every kind of goods with ease.

Internal combustion engines based on fossil fuels have represented the main propulsion system to power every means of transport that circulates on the road. As a matter of fact, their favorable weight/power ratio, their relative simplicity and the huge energy density of fossils fuel compared to other energy sources have represented significant advantages that have decreed the undisputed domination of this technology.

However, if the advantages provided by internal combustion engines are undoubted, there are some drawbacks too. The disadvantages mainly rely on their dependence on fossil fuels. Beside the problems related to their availability, which is destined to reduce with time, the massive production of Carbon Dioxide due to the process of combustion, which is a strong greenhouse gas, and whose massive presence is negatively affecting the planet's climate equilibrium has to be considered. Furthermore, since the combustion process in engines is not ideal, several pollutant substances are produced together with CO₂. Carbon monoxide, unburnt hydrocarbons, nitrogen oxides and particulate matter are the main types of harmful substances emitted in the atmosphere by the engine exhaust system.

Because of the unsustainable problems that this type of propulsion involves, there is an increasing need to contain the use of fossils fuels by enhancing the engines' efficiency, and to reduce the emissions of pollutants, improving the after-treatment systems.

One of the alternatives is to substitute the internal combustion engine propulsion systems with electric motors, powered by a battery pack. Electric vehicles are nowadays starting to spread and they are gaining a considerable market share, but they still have to face many problems, such as the unfavorable energy density of batteries, the lack of infrastructures related to charging, and their price, still too high compared to traditional ICE powered alternatives.

One of the technologies that can improve the efficiency and emissions of vehicles, enhancing fuel saving, and maintaining the positive sides of traditional internal combustion engine powered vehicles, is represented by Hybrid Vehicles.

Hybrid Vehicles are generally considered as an effective intermediate solution between the technology of the past and the one of the future. Using electric power is a valid method to reduce the impact of internal combustion engines, and allows to grasp some interesting aspects that could be useful for future architectures and solutions.

In the last decade, Hybrid Electric Vehicles have spread worldwide in passenger cars applications, however, in the Heavy Duty market this technology is not as common, while it could represent an alternative to increase the overall efficiency of these vehicles.

Since Heavy Duty vehicles' lifespan is typically above one million kilometers, and their specific fuel consumption is much greater than passenger cars' vehicles, mainly because of their considerable mass and their higher aerodynamic coefficient, it is clear how even a slight increase in efficiency could represent a substantial economic advantage throughout the life cycle of the vehicle. Furthermore, it has to be considered that the CO₂ production is strongly related to the vehicle's fuel consumption.

The purpose of this Thesis is to explore the possibilities of electrification for heavy duty applications, and highlight the advantages that this technology can have, especially in terms of fuel economy and, therefore, carbon dioxide emissions.

In particular, a promising technology in this field is represented by "Through the Road" hybrid systems.

In this work two "Through the Road" HEV configurations will be analyzed and evaluated, consisting of a standard Internal Combustion Engine mounted on the front axle and powering two axles of the vehicle, and one or two electric motors mounted on the third rear axle. The term "Through the Road" indicates that the connection between the ICE and the electric motors is provided by the road's constraints. Therefore, no mechanical connection between the two powertrains is required, as it often happens in standard Parallel Hybrid Configurations.

Regarding the electric axle, two solutions will be discussed:

- *Single electric motor coupled with a differential.* In this configuration an electric motor will be coupled through conical gears to the differential crown. This configuration will require an electric motor capable of delivering a relatively low torque at higher speeds.
- *Two in-wheel electric motors.* In this configuration, two electric motors will be coupled to the wheels, without gear reductions. The motors will be two frameless motors capable of delivering high torque at low speeds.

The two hybrid configurations will be modeled through the use of "TruckSim" software by "Mechanical Simulations", coupled with Matlab-Simulink environment.

The two configurations and the standard ICE-only layout will be simulated in different situations and the results will be compared in order to highlight the fuel consumption advantages and the differences in the powertrain's behavior and performances.

Finally, for both configurations, a feasibility study will be conducted. In this phase, different design approaches for the architectures will be discussed. This is necessary to evaluate whether the solutions could be engineered without any critical issue, or if they have to be previously discarded because of obvious design difficulties.

1. Literary review and background

A Hybrid Vehicle is a vehicle that derives propulsion from multiple distinct types of energy sources, with the possibility of recovering friction energy using recuperation power systems, such as regenerative braking system (Khajepour, Fallah, & Goodarzi, 2014)

Hybrid Electric Vehicles combine the electric motor and high-voltage battery of a purely electric vehicle with the internal combustion engine of a conventional vehicle. On a fundamental level, Hybrid Electric Vehicles include a power unit, a propulsion system and an energy storage system.

Regarding the power unit, compression and spark ignition engines with fossil fuels, alternative fuels, and fuel-cells are all possible technologies. The propulsion system transfers the generated power to the wheels by a mechanical device, electric motor, or by a combination of both mechanical and electrical components. The electric machine is really versatile and can be used for both traction and generation phase.

Possible energy storage systems are ultra-capacitors, flywheels and, most commonly used, batteries.

1.1 Degrees of Hybridization

A first classification for hybrid vehicles can be done referring to different degrees of hybridization. In particular, we refer to:

- *Micro hybrid vehicles*: in this configuration an electric machine can work in applications such as stop/start and regenerative braking, but it can't supply an additional torque when the engine is running. Nowadays most of micro-hybrid applications are focused on small gasoline engines. The application of stop/start systems in diesel engines is a considerably greater challenge due to the much higher starting torque required.
- *Mild-Hybrid*: we refer to mild hybrid vehicles to indicate applications with an electric motor-generator integrated to provide up to approximately 10% of the maximum engine power as of an additional torque. Mild hybrid systems can provide some level of power assistance to the engine when it runs in low efficiency situations, and they can provide engine stop/start capability. Another possibility provided by these systems is to turn off the engine while idling and use electric power instead.
- *Full-Hybrid*: in a full-hybrid vehicle the electric motor typically provides at least 40% of the maximum engine power in the form of additional torque. In these applications, larger electric motors are used and usually the size of batteries has to meet acceleration requirements.

Moreover, a hybrid vehicle can be classified regarding its capability to be charged externally or not. We can distinguish:

- *HEV (Hybrid Electric Vehicles)*: A HEV doesn't have the possibility to be charged externally. In these vehicles, batteries act as an "energy buffer", in order to increase the engine's efficiency.
- *PHEV (Plug-in Hybrid Electric Vehicles)*: we refer to a PHEV to indicate a hybrid vehicle that can be externally charged. In a plug-in hybrid electric vehicle, fuel consumption and Tank-To-Wheel emissions are further reduced because of the increased possibility to be used as a purely electric vehicle.

1.2 Parallel Hybrid configurations

In a hybrid vehicle, there are several ways to couple the electric powertrain (electric motor-generator and batteries) and the internal combustion engine, in order to deliver the torque to the wheels.

For many manufacturers, parallel hybrid configurations have been the first step towards vehicle electrification. This architecture couples mechanically the two power sources, allowing their use either simultaneously or independently.

In this configuration the internal combustion engine is coupled with the electrical power output by mechanical devices such as torque couplers and speed couplers. The two machines work in an "in line" disposition, and the power is added up and transferred to the wheels via the transmission.

The internal combustion engine is the main source of power, and it delivers a continuative torque which is almost constant, while the electric motor has the task to compensate the lacks of the engine, for example during the launch of the vehicle, or during energy recuperation.

Considering the power output that can be delivered by the internal combustion engine and by the electric power source, in literature (Lukic & Emadi, 2004), a parameter, *HF (Hybridization Factor)*, can be defined:

$$HF = \frac{P_{motor}}{P_{ICE} + P_{motor}}$$

If *HF* is equal to zero, we have the limit case of a conventional vehicle powered by an internal combustion engine only. As *HF* increases, the on-board electric power increases and further electric operating modes are enabled.

If *HF* is equal to one, we have the limit case of a purely electric vehicle.

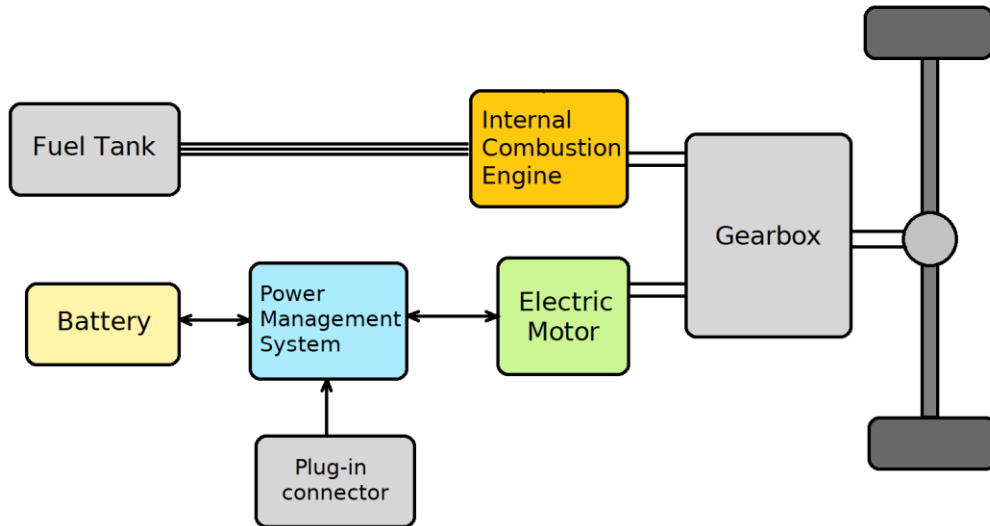


Figure 1 - Parallel Hybrid schematic

1.2.1 Parallel Hybrid architectures

Parallel hybrid configurations can be further classified depending on the relative position of the electric motor and the engine. Four categories can be distinguished, which are typically referred as P1 to P4, as shown in Figure 2 (Yang, Arshad-Ali, Roeleveld, & Emadi, 2016).

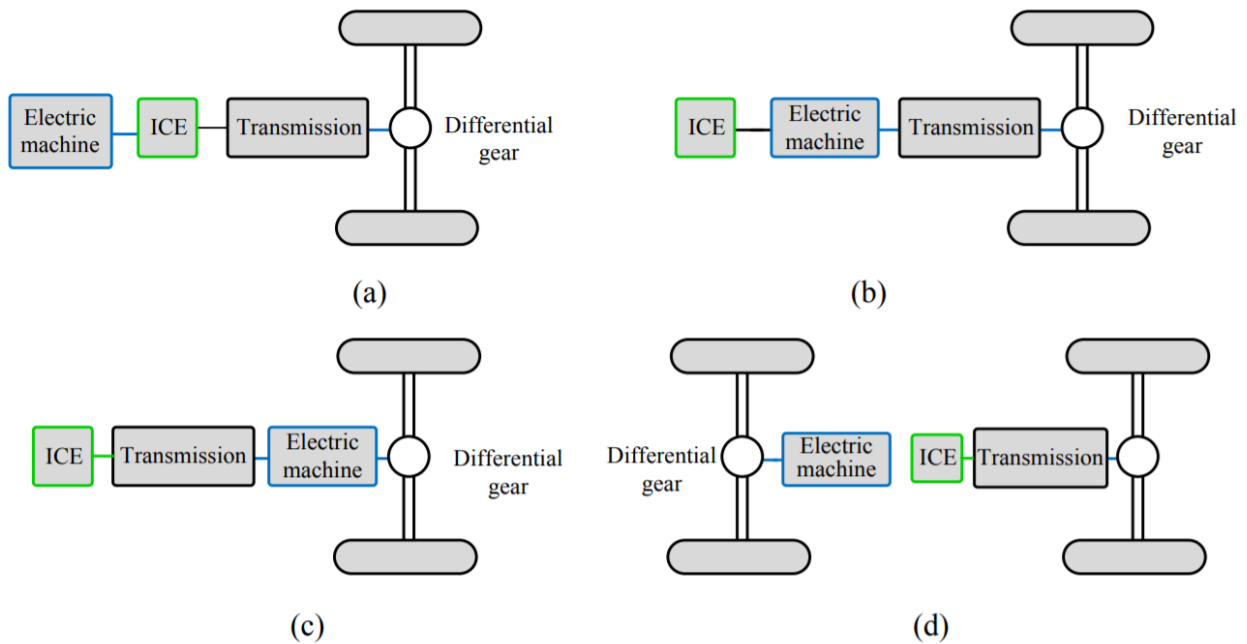


Figure 2 - Parallel hybrid configurations (Yang, Arshad-Ali, Roeleveld, & Emadi, 2016)

- (a) *P1*: we refer to P1 hybrid configurations to indicate an architecture in which the electric motor is mounted on the crankshaft, and therefore both the internal combustion engine and the electric machine have the same angular speed. In this case the motor can act as an engine starter and generator, powering the vehicle accessories. Furthermore, it allows the engine to shut off when the vehicle is stopped, saving fuel by preventing idling.
- (b) *P2*: a P2 configuration differs from the first one because the electric machine is mounted downstream of the clutch, right before the transmission input. The electric motor can provide assistance to the engine for greater acceleration or performance, or drive the vehicle in electric-only operation. The machine can operate as a generator while the engine provides power for traction and battery charging.
- (c) *P3*: this case is similar to a P2 architecture, but the electric motor is coupled to the transmission's output shaft. Therefore, the angular speed differs from the gearbox input shaft speed by a factor equal to the gear ratio.
- (d) *P4*: In this configuration the electric machine is placed either directly at the wheels (wheel-motors) or on a different axle. It is commonly referred as parallel "*Through-The-Road*" architecture. This solution allows to have an all-wheel drive powertrain mode, and at the same time isolates the electric power source from the internal combustion engine. The kinematical connection between the two power sources is provided by the constraints between the vehicle's wheels and the ground. This architecture is capable of the same operating modes as the conventional parallel powertrain, and it can also charge the batteries by applying a braking torque on the electrically powered axle.

1.2.2 Operating modes

In a parallel hybrid arrangement, it is possible to classify different operating modes (Khajepour, Fallah, & Goodarzi, 2014):

- *Engine alone traction mode*: in this mode, the total power is generated by the internal combustion engine alone, and the electric motor is off. This mode is activated when the engine is running close to its optimal operating point, for example when cruising.
- *Electric alone traction mode*: this mode is preferred when the engine would work at low efficiency values, for example when starting the vehicle or when the vehicle speed is low.
- *Hybrid mode*: in this mode, the wheels receive power from both sources. The internal combustion engine will provide an almost constant torque, while the electric machine

is responsible of managing the transitory phases, and forces the engine to work close to its optimal operating point, using the batteries as an energy buffer.

- *Engine traction and battery charging mode*: this mode is involved when the batteries' state of charge is low, and the engine produces more than the power required for vehicle motion. The additional power recharges the battery by switching the electric motor to operate as a generator.
- *Regeneration mode*: usually referred as regenerative braking, this mode is activated when the vehicle is braking or during downhill motion. It allows to recuperate the kinetic energy that would be wasted with regular braking mode.

1.3 Series Hybrid configuration

A series hybrid configuration is similar to a pure electric architecture. It's characterized by an electric motor, which provides traction to the wheels, and by a small internal combustion engine that drives an electric generator, providing power for the electric motor.

The main advantage of this configuration is the possibility to disconnect the internal combustion engine from the driving wheels, and therefore there is no more a kinematical relationship between the crankshaft and the driving axle, as it happens in regular vehicles.

Therefore, the combustion engine can operate in its most efficient range, regardless of the vehicle load and speed.

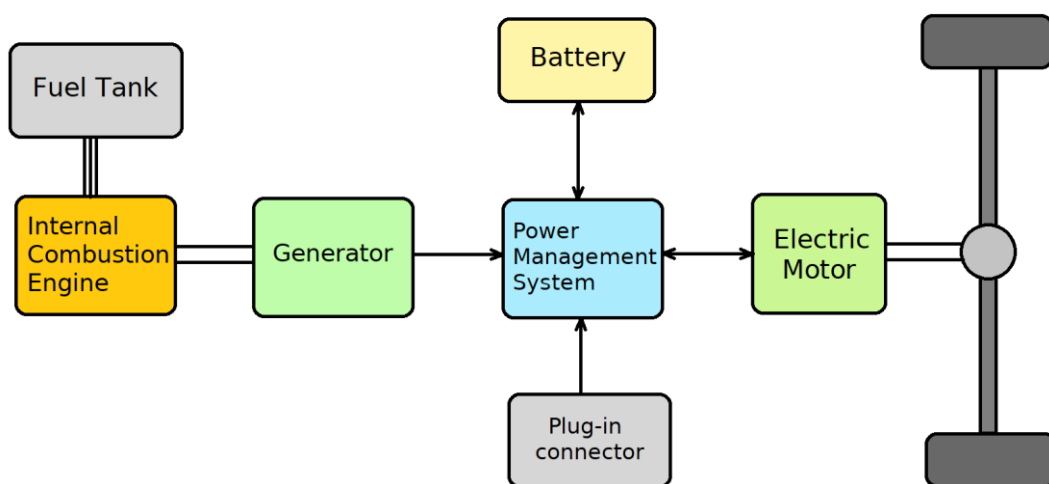


Figure 3 - Series Hybrid schematic

The difference with a parallel hybrid configuration resides on the electric motor and the transmission system. The electric machine used in these configurations must be significantly more powerful compared to parallel architectures, because it must be capable of providing all the necessary tractive power.

Regarding the transmissions systems, while in a parallel hybrid configuration there is the need for a more expensive multi-gear transmission to connect the engine to the wheels, in a series hybrid configuration the electric machine can be often directly coupled to the driving axle.

Considering the power output that can be delivered by the internal combustion engine and by the electric power source, as in the previous case of Parallel Hybrid configurations, HF (*Hybridization Factor*) is defined as (Lukic & Emadi, 2004):

$$HF = \frac{P_{ICE}}{P_{motor}}$$

This parameter allows to define the type of Series Hybrid vehicle. In the limit case of $HF=0$, the vehicle is purely electric. If $0 < HF < 1$, the vehicle is a Plug-in Hybrid Vehicle with a range extender. This means that the vehicle can act as an electric vehicle for a considerable amount of time, and the internal combustion engine is activated when the State of Charge of the battery is too low to guarantee an optimal traction.

If $HF = 1$, the vehicle a Series Hybrid with electric transmission. This means that the engine is still responsible of providing most of the power needed to traction, but it is disconnected by the drive axle.

1.3.1 Operating modes

Similarly to parallel hybrid powertrains, series hybrid configurations have different operating modes (Khajepour, Fallah, & Goodarzi, 2014):

- *Engine-alone traction mode*: in this mode, the internal combustion engine provides only the necessary power for the motion of the vehicle. The mechanical power is therefore converted into electric power by the generator and transferred to the electric motor, which converts it back into mechanical power and transfers it to the driving axle. In this mode the batteries neither provide nor receive any power from the drivetrain.
- *Electric-alone traction mode*: in this mode the engine is off and the batteries provides the necessary power to the electric motor in order to deliver traction to the wheels.
- *Hybrid mode*: in this mode, the engine-generator and batteries simultaneously deliver power to the driving axle, in order to provide traction.

- *Engine traction and battery charging mode*: when the batteries' state of charge is below the minimum acceptable level, the engine-generator provides a greater amount of power, in order to guarantee the vehicle motion and charge the batteries.
- *Regeneration mode*: the regenerative braking system charges the batteries during braking, decelerating and downhill travel. The traction motor operates as a generator and the engine-generator is not active.
- *Battery charging mode*: in this mode, the motor-generator stops and the batteries are charged by the engine-generator.
- *Hybrid battery-charging mode*: in this mode, both the engine and the motor-generator provide power to the batteries, charging them simultaneously.

1.4 Parallel-Series Hybrid configurations (power split)

Among all possible HEV architectures, power split ones are the most popular, since they are able to combine the best features of both series and parallel hybrid configurations.

In comparison with a parallel hybrid system, a series-parallel powertrain uses an additional electric motor that primarily functions as a generator.

It inherits from a series powertrain the possibility to run the internal combustion engine in order to generate a sufficient amount of current to charge the battery or to power the electric motor, which has the task to drive the axle. At the same time, it takes from a parallel architecture the ability to run simultaneously the electric motor and the engine in order to deliver traction to the wheels.

In other words, these systems split the power from the engine between two paths: one transfers the traction to the wheels through a mechanical gear system, and the other transfers the power to the wheels through a generator and an electric motor.

This architecture is able to guarantee a regenerative braking system, reducing the amount of energy dissipated through friction.

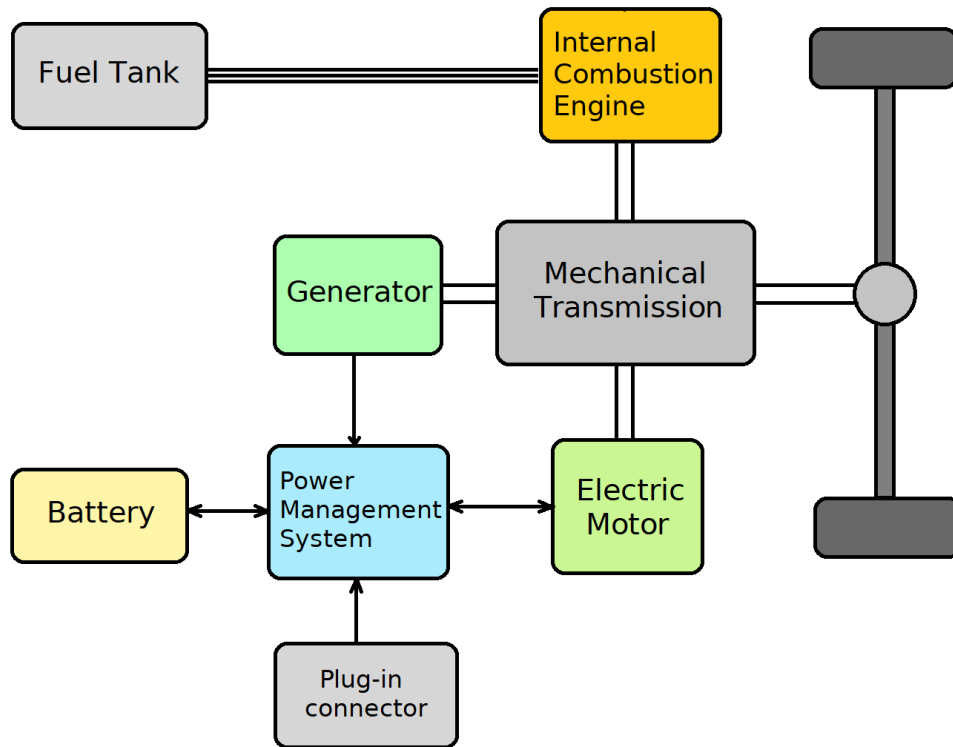


Figure 4 - Parallel/Series Hybrid schematic

1.4.1 E-CVT Transmission and Power split device (PSD)

The main drawback of a series-hybrid configuration compared to the previously discussed architectures is the complexity of its power transmission system.

There are several configurations that allow to mechanically connect the two power sources to the drive axle in a Series-Hybrid architecture.

One of the most common is *E-CVT* (Electric-Continuous Variable Transmission). It consists of a planetary gear set which makes possible to achieve a combination of either two input shafts and one output shaft, or one input shaft and two output shafts.

In Figure 5 (Miller, Ehsani, & Gao, 2005), a basic Power Split Device configuration is reported.

There are two electric motor-generator, $M/G1$ and $M/G2$ that circulate power from the engine via an electric path that is combined downstream of the driveline with mechanical power from the engine that follows a geared path.

The internal combustion engine output shaft is connected to the planetary gear set carrier, while the sun gear is connected to the first electric motor ($M/G1$).

The ring gear's motion is then transferred to the gearbox and then to the driving axle's differential.

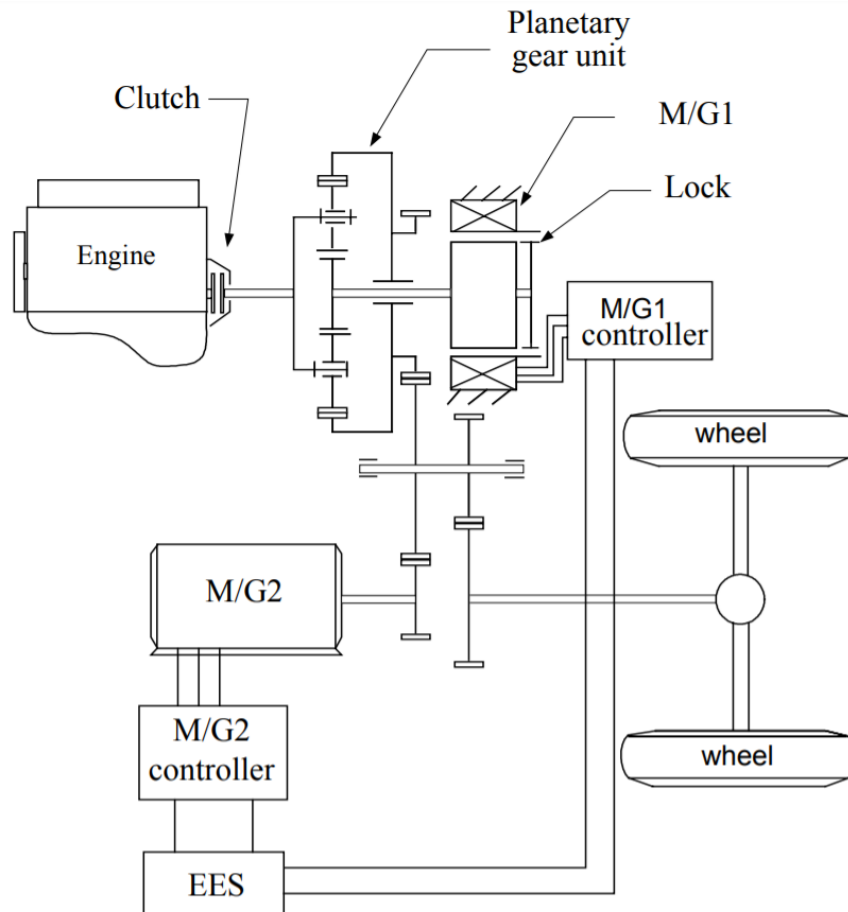


Figure 5 - PSD configuration schematic (Miller, Ehsani, & Gao, 2005)

1.4.2 Operating modes

- *Electric-alone traction mode:* in this mode, the internal combustion engine is shut off and the vehicle can run in pure electric mode. Referring to the above schematic, the engine clutch is disengaged while the power is transferred to the gearbox via M/G2 electric motor.
- *Engine traction/Hybrid mode:* locking the sun gear of the planetary gear set, the power can be delivered by the internal combustion engine alone, or by both the ICE and M/G2. We can therefore have an ICE mode or a combined (hybrid) mode.
- *Engine traction and power flow towards the electric motor-generator:* if the battery is sufficiently charged and the electric motor's current demand is too high to be sustained for long periods of time, the architecture can work as a series-hybrid: the engine transfers power both to the gearbox and the electric machine M/G1, and the electric power is then transferred to M/G2.

- *Engine traction and power flow towards the electric motor and the battery*: the internal combustion engine can be loaded by the electric machine M/G1 in order to work at its optimal operating point, while simultaneously transfer power to the drive axle. Excess energy can be stored in batteries and be used when there is the need.
- *Regenerative braking mode*: in this configuration, the system recovers energy with one or both electric machines, used as generators. The usage of the machines depends mainly on the vehicle's speed and on limits of energetic flows that the generators can handle.

1.5 Through-The-Road (TTR) Hybrid configuration

Among all the different hybrid configurations described above, in this Thesis work the attention will be focused to the so called “through-the-road” architecture.

This term refers to a “P4” parallel-hybrid configuration, where the internal combustion engine and the electric motor are independent and they are not coupled mechanically. Therefore, the thermal unit powers one or two axles of the vehicle (if we consider a heavy duty vehicle), while the remaining axle is electrically powered.

The two power source are still able to “communicate” and influence each other. In fact, the link between the two units is created by the road itself and by the constraints that the wheels have with the ground. If we suppose that the vehicle maintains a constant speed, its longitudinal acceleration is equal to zero and, therefore, the longitudinal equilibrium of the vehicles imposes that:

$$\sum_i F_i = ma_i = 0 \rightarrow F_{front} + F_{rear} - F_{ext} = 0$$

It is clear how the different axles of the vehicle are dynamically linked together and if a torque is applied on the electric axle which causes a change in F_{rear} (tractive force on the rear axle), F_{front} (tractive force on the front axle) has to change as well in order to maintain the vehicle's speed constant.

This equation is valid until the vehicle's wheels are in a pure rolling motion condition, or in the absence of macro-slip phenomena. It has to be noticed that a detailed analysis of the gearshift phase is required, in order to obtain the natural frequencies, modal shapes and frequency response functions of the overall system and optimize the drivability of the system (Galvagno, Morina, Sorniotti, & Velardocchia, 2013).

If the vehicle is equipped with an on-board power management electronics which allows to control its target speed based on the throttle pedal position, the electric power source can influence the thermal unit and vice-versa.

Therefore, all the operating modes described in paragraph 1.2.2 are achievable with this configuration.

1.6 Advantages of Hybrid Technology

1.6.1 Optimization of the engine's operating points

Conventional vehicles with internal combustion engines are designed to operate in a wide range of combinations of speed and load depending on the vehicle's mission profile.

Therefore, engines have to be capable of delivering a sufficient amount of torque to guarantee to the vehicle to reach an appropriate top speed suitable for highway cruising situations, and to have an appropriate acceleration.

The power delivered by the engine depends on two contributions, necessary to overcome the loads due to:

- 1) *Vehicle's motion opposition*, related to road's slope, rolling resistance and aerodynamic forces:

$$F_{res} = F_{roll} + F_{aero} + F_{slope} = \mu_r mg + \frac{1}{2} C_x \rho S v^2 + mg \sin(\vartheta)$$

- 2) Resistance related to *inertial effects*: this force has to take into account not only the vehicle's mass, but also every contribution related to rotating components:

$$F_{inertia} = m_{app} \frac{dv}{dt}$$

In order to determine the apparent mass, every rotating component has to be considered. Applying a kinematic equilibrium equation and reducing the complex system of rotating components into a simpler, lumped parameters system, we obtain:

$$\frac{1}{2} m_{app} v^2 = \frac{1}{2} m_v v^2 + \frac{1}{2} J_{eng} \omega_{eng}^2 + \frac{1}{2} J_{gb} \omega_b^2 + \frac{1}{2} J_{axle} \omega_{axle}^2 + \frac{1}{2} J_{wheel} \omega_r^2$$

Transmission and axle's inertia can be neglected if compared to engine and wheels inertia. Furthermore, we can consider that:

$$\omega_{wheel} = \frac{v}{R_0}; \quad \omega_{engine} = \omega_{wheel} * \tau_g * \tau_{final}$$

Therefore we have:

$$m_{app} v^2 = m_v v^2 + J_{eng} (\omega_{wheel} \tau_g \tau_{final})^2 + J_{wheel} \omega_{wheel}^2$$

$$m_{app} \approx m_v + \frac{J_w}{R_0^2} + J_{eng} \frac{\tau_g^2 + \tau_{final}^2}{2}$$

Finally, we can calculate the requested power for vehicles' motion:

$$P_{nec} = F_{res} v + m_{app} \frac{dv}{dt} v$$

$$P_{eng} = \frac{P_{nec}}{\eta_t} = \frac{1}{\eta_t} (F_{res}v + m_{app} \frac{dv}{dt} v)$$

From the above equations, it is possible to notice that the power that the engine has to deliver depends mainly on the vehicle's speed to the third power (v^3), on the road's slope (linearly), and on the vehicle's acceleration and current gear.

The high variability of the external conditions and driving situations determines the necessity to utilize engines capable of delivering high values of power and torque in order to face the most demanding situations (such as highway cruising and overtaking, still start with high road's slope and so on).

However, most of the time the engine will deliver lower values of torque, operating mainly in the lower-left area of its characteristic map.

Internal combustion engine's efficiency, on the other hand, is far from being constant. An engine will reach its maximum efficiency at high loads, while this will gradually decrease moving towards the bottom part of the engine's characteristic map, eventually reaching 0 at idling conditions.

This concept can be clarified by analyzing an internal combustion engine's efficiency.

In literature (Ferrari, 2014) an engine's overall efficiency is defined as:

$$\eta_u = \frac{W_u}{E_u} = \frac{W_u}{m_f H_i} = \frac{P_u}{\dot{m}_f H_i}$$

Where P_u is the engine's output power, \dot{m}_f is the fuel flow rate and H_i is the fuel's Lower Heating Value.

The overall efficiency, however, comprehend every loss involved in the process of converting the fuel's chemical energy into useful mechanical energy. In order to highlight why the engine's efficiency drops at low loads, we can further investigate its nature, by writing this value as:

$$\eta_u = \frac{W_u}{E_u} = \frac{W_u}{W_i} \cdot \frac{W_i}{W_{i,lim}} \cdot \frac{W_{i,lim}}{m_b H_i} = \eta_m \eta_{\theta i} \eta_{lim}$$

The cause of this efficiency drop has to be attributed mainly to the mechanical efficiency η_m .

Referring the Brake Work, the Indicated Work and the Friction Work to the engine's displacement and then substituting into the expression of η_m , we obtain:

$$bmep = \frac{W_u}{V_d} \quad imep = \frac{W_i}{V_d} \quad fmep = \frac{W_f}{V_d}$$

$$\eta_m = \frac{bmep}{imep} = 1 - \frac{fmep}{imep}$$

The friction mean effective pressure (*f MEP*) is indicative of the energy wasted in order to overcome the engine’s mechanical losses, and to power all the auxiliary devices necessary to keep the engine and the vehicle running (such as the fuel pump, the oil pump, eventual air conditioning system and so on).

An experimental measure of the friction mean effective pressure can be provided by the Chen-Flynn relation, which states that:

$$f MEP = A + B p_{max} + C \left(n \frac{c}{2} \right) + D \left(n \frac{c}{2} \right)^2$$

Where *p_{max}* is the maximum value of the pressure reached inside the cylinder for a given value of the engine’s rotating speed, *n* is the engine’s rotating speed, *c* is the engine’s stroke, and A,B,C and D are experimental constants.

It is clear from this expression that *f MEP* does not depend from the engine’s load (except for the term related to *p_{max}* which is negligible compared to the other terms). Therefore, if we decrease the engine’s load, *IMEP* decreases, while *f MEP* remains almost constant.

We can conclude that when the engine’s load is low, the engine’s mechanical efficiency η_m and its overall efficiency η_u decrease, increasing specific fuel consumption.

Plotting the engine’s mechanical efficiency to the value of *IMEP* at constant angular speed, we obtain:

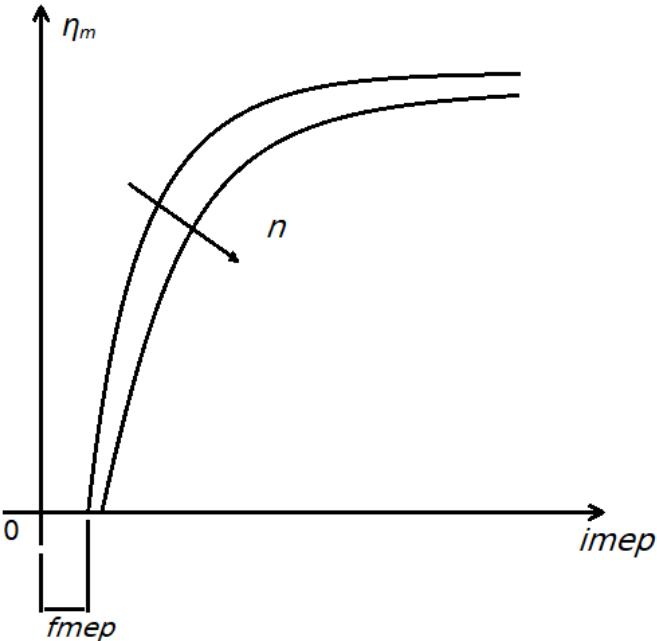


Figure 6 - Mechanical efficiency as a function of *IMEP*

Despite the wide range of operating points that the engine has to be capable of in order to guarantee the necessary amount of power to the vehicle for every external condition, the

most common driving scenarios involve operating points which are far from the optimal conditions.

The following graph illustrates the operating points of the internal combustion engine of a D-segment passenger car vehicle on the FTP-75 driving cycle (Ehsani, Gao, & Emadi, 2010)

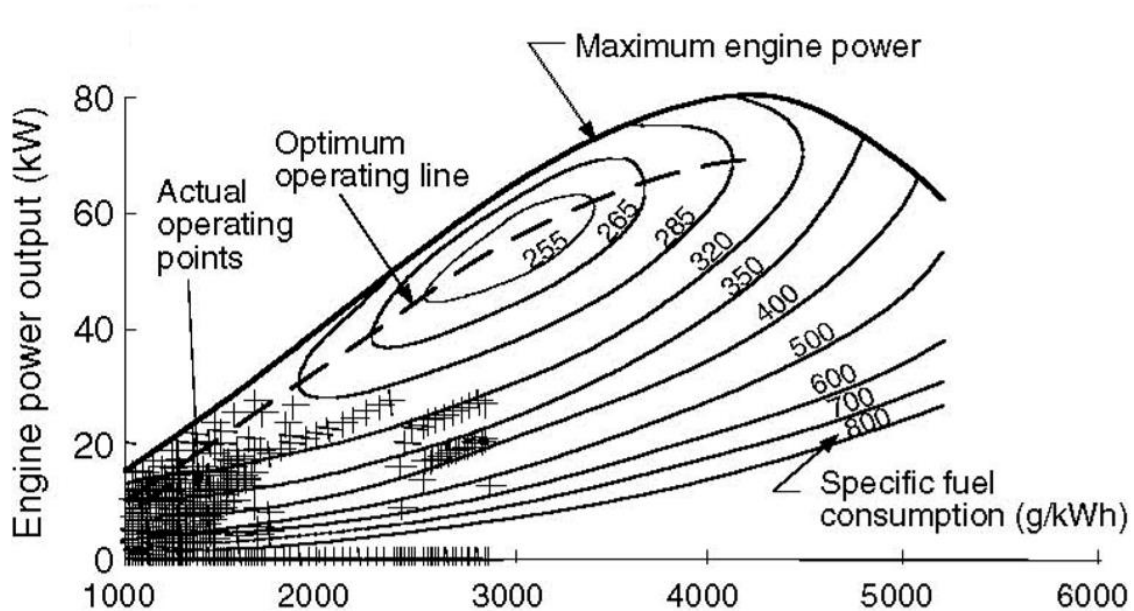


Figure 7 – Operating points of a D-segment passenger car on FTP-75 cycle (Ehsani, Gao, & Emadi, 2010)

As explained before, most of the time the engine works far from the optimum operating line, which guarantees the minimum specific fuel consumption. Therefore, the average efficiency of engines is most of the time much lower than the maximum.

With Hybrid Powertrains, it is possible to reduce this effect taking advantage of the electric power source.

We can analyze two scenarios:

- 1) *Engine's output torque is less than the optimal torque for a given speed.*

This situation is very common when the vehicle is engaged in urban driving, when its load is a small percentage of the maximum.

In this scenario, the on-board electronics of a hybrid system can estimate the difference between the optimal torque and the actual delivered torque of the engine (which can be estimated by a look-up table giving as an input the throttle pedal position and the engine's rpm).

Then, ideally, the electric motor can generate a load on the engine's crankshaft (or, in the case of a *through-the-road* system, on the electrified axle) equal to the difference

previously calculated, causing the engine to increase the output torque and therefore its efficiency.

The excess energy produced by the electric machine (which works as a generator in this case) is stored in batteries and can be used in other occasions. Obviously this strategy isn't always convenient, since storing the excess energy in batteries requires some energy conversion, and therefore involves losses.

2) *Engine's output torque is more than the optimal torque for a given speed.*

This situation is less common in urban driving, and can occur during demanding accelerations. In this case, the electric machine can act as a motor, reducing the load on the internal combustion engine exploiting the energy previously stored in the battery.

Since the first situation is more common than the second, sometimes this can result in an excessive increase of the battery's State Of Charge (SOC), and after some time the powertrain could not be able to continue with this strategy.

In order to avoid this effect, the Optimum Torque can be calculated as a fraction of the torque that guarantees the maximum efficiency for a given speed. This will result in a minor advantage, but determines a better balance of the SOC.

Another way to balance the SOC is to switch to *electric-only* mode at low speeds, performing an idling control. This strategy will be discussed later.

1.6.2 Energy recuperation through Regenerative Braking

In conventional vehicles, the braking system imposes a braking torque to the wheels, converting the vehicle's kinetic energy into thermal energy, dissipating it. With hybrid powertrains, it is possible to exploit the electric machine in order to convert significant amounts of kinetic energy into other types of energy that can be stored in energy-storage devices, such as batteries.

However, using batteries as an electrical energy storage device can impose some limitations to the system, mainly because batteries are not capable of absorbing excessive amounts of energy in a limited amount of time. An alternative solution is the use of ultra-capacitors which, however, are very expensive.

Regenerative braking systems typically operate when the driver presses the brake pedal while decelerating, or when releasing the accelerator pedal to generate the same deceleration feeling as in conventional ICE vehicles.

In these circumstances, the electric machine works as a generator, creating a braking torque that resists the forward momentum and eventually stops the car.

If the regenerative braking torque is not enough to meet the driver's demand for braking torque, the conventional friction braking system is combined with the regenerative one, in order to provide the additional torque to generate the requested deceleration.

Moreover, the conventional braking system provides the total desired braking torque if the receptive sources have a full charge and therefore regenerative braking is no longer applicable.

The torque limitations for a regenerative braking system follow the electric machine torque curve: at low speed, after a threshold speed value, the maximum regenerative torque is almost constant (machine in *constant-torque mode*), while after another speed threshold, the maximum regenerative torque is hyperbolic (machine in *constant-power mode*).

The following figure illustrates the distribution of regenerative and hydraulic braking torque given a requested braking torque input from the driver (Khajepour, Fallah, & Goodarzi, 2014):

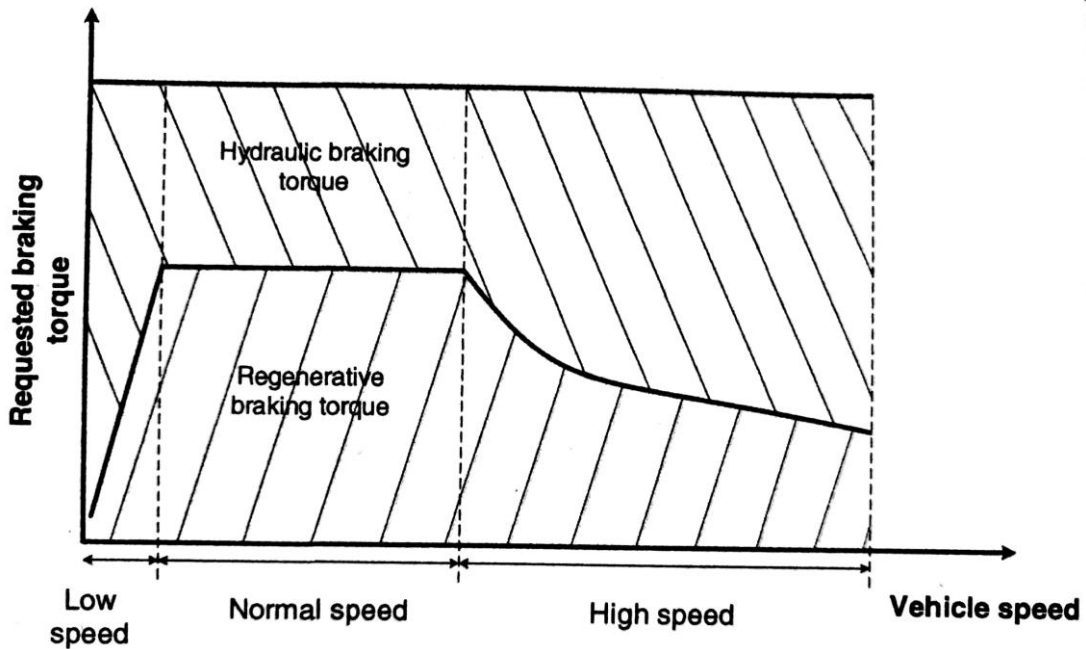


Figure 8 - Regenerative braking torque vs vehicle speed (Khajepour, Fallah, & Goodarzi, 2014)

In a regenerative braking system, energy conversion occurs four times: mechanical to electric, electric to chemical, chemical to electric and electric to mechanical. As a result, its overall efficiency can be quite low.

The efficiency of the generator can be defined as:

$$\eta_{gen} = \frac{W_{out}}{W_{in}}$$

Where W_{out} is the energy produced by the generator and W_{in} is the work introduced in the generator, which is equal to the difference of kinetic energy of the vehicle between the start

and the end of the braking process (assuming that conventional friction braking doesn't take part in the process).

Therefore, we have:

$$W_{in} = \frac{1}{2} m \Delta v^2$$

$$W_{out} = P_{gen} \Delta t$$

$$\eta_{gen} = \frac{P_{gen} \Delta t}{\frac{1}{2} m \Delta v^2} \rightarrow P_{gen} = \frac{\eta_{gen} m \Delta v^2}{2 \Delta t}$$

In the process of storing the energy into the batteries, we have to consider the energy losses due to the imperfect conversion of the electric energy into chemical energy.

The efficiency of the battery can be described as:

$$\eta_{batt} = \frac{P_{out}}{P_{in}}$$

Where

$$P_{in} = P_{gen} \quad P_{out} = \frac{W_{out}}{\Delta t}$$

Substituting in the previous equation and recalling the expression for P_{gen} previously calculated, we obtain:

$$W_{out} = \frac{\eta_{gen} \eta_{batt} m \Delta v^2}{2}$$

This expression represent the amount of energy that we are able to store into the batteries during the process of pure regenerative braking.

1.6.3 Idling reduction

Vehicle idling is a condition that occurs when the engine of a vehicle is running but is not engaged with the transmission or is simply not in gear (Shancita, et al., 2014).

Vehicle idling is a common condition in urban driving, when the vehicle has to perform several stops during its advancement, or in situations where the vehicle has to stop for a long time, but the engine has to keep running in order to provide power for auxiliary equipment.

As illustrated in paragraph 1.6.1, this situation is detrimental for the engine's overall efficiency, because the engine is forced to run at very low loads with a consequent increase in specific fuel consumption.

While for conventional vehicles there is no way to prevent this condition, with a huge impact on fuel economy and pollutant emissions, hybrid powertrains can avoid this situation,

resorting exclusively to the electric source to power the vehicle and shutting off the thermal unit. The energy required to run the vehicle is therefore drained from the batteries, and has been previously stored by regenerative braking or by loading the engine working at higher efficiency. Therefore, this technique can have a substantial impact on the powertrain efficiency.

1.6.4 Other advantages and challenges

As illustrated in the previous paragraphs, hybrid powertrains can be a valid solution to impact on the major drawbacks of a conventional ICE vehicle. The improvement on the engine's operating points, regenerative braking and idling reduction are the most important aspects that this technology can influence, and they will be continuously taken as a reference during the developing of this work.

However, hybrid technology can have many other positive aspects and can improve the overall behavior of a vehicle in many other different ways. Some of them are listed below:

- *ICE downsizing/downspeeding*: due to the assistance of the secondary power source, a smaller internal combustion engine or a longer final drive can be chosen without affecting the vehicle's performance;
- *Eliminating or mitigating the "clutching" losses*: these losses can be reduced by not engaging the engine until the speeds are matched and do not require any slip;
- *Potentially continuously varying gear ratio*: since in an hybrid vehicle all the power management is achieved by a powerful on-board electronics, these powertrain can be matched with continuously varying gear ratio transmission (such as EVT like in Toyota Prius, Ford Escape, and so on).

Other than that, hybrid vehicles have still to encounter some critical issues, which are the main challenges that are been currently addressed. Here are some of the most significant:

- HEV are currently more expensive than conventional vehicles;
- They are heavier than conventional vehicles, due to additional weight from secondary power sources and energy storage system;
- High cost of components;
- Reliability is still under study;
- More complex control systems are required to optimize fuel efficiency;
- They might have drivability issues.

2. Drivetrain configurations and analysis tool

2.1 *“Through-the-Road” Hybrid Heavy Duty vehicles*

Hybrid technology became widespread in the automotive world in the late 1990s. The “Toyota Prius” was the first mass-produced hybrid passenger-car, and its production started in Japan in 1997.

After that, more and more passenger cars constructors have entered the market with hybrid models, and hybrid vehicles’ sales have significantly increased during the last two decades, from less than 10 000 models sold in the United States in the year 2000 to almost 500 000 vehicles sold in 2013 (Block, Harrison, Brooker, Center, & Dunn, 2015).

However, in the Heavy Duty industry, this technology has had a much less significant impact on the market.

The first application of hybrid technology in the light-duty market was introduced by Mercedes Benz with the Sprinter, in 2004, followed by the “Daily Bimodale”, by Micro-Vett SPA (Fiat).

Nowadays, Coca-Cola Enterprise has the largest fleet of hybrid heavy-duty delivery trucks in North America, with a number of 327 units in 2009.

The main constructors of hybrid powertrains for heavy duty trucks are Eaton Corporation, ZF Friderichshafen, Azure Dynamics, and their solutions are based mainly on series-parallel configurations with power-split mechanical systems.

Hybrid Technology could represent an excellent way to improve heavy-duty trucks’ average efficiency, especially in cases where the vehicles’ mission profile is characterized mainly by urban routes, such as in food delivery applications.

Even a slight improvement in a heavy duty vehicle’s efficiency could in fact represent a significant economic advantage throughout the entire truck’s lifespan.

As a matter of fact, a heavy duty vehicle’s lifespan is much greater than a passenger car’s one, and can easily exceed one million kilometers. Therefore, even a few percentage points advantage in its specific consumption can determine a cumulative fuel advantage of thousands of liters throughout the truck’s life cycle.

In terms of hybrid configurations, in technical literature there is a lack regarding the configuration described in paragraph 1.2.1 (d) as “parallel hybrid P4 configuration”, or “trough-the-road” architecture. However, this solution may represent an optimal architecture in this field for a number of reasons:

- It is a relatively simple solution to design and manufacture
- There is no mechanical connection between the two power sources;
- The electric axle can be designed as an independent and all-inclusive unit;
- The electric powertrain adds two (or more) tractive wheels to the vehicle;
- It can be possible to retrofit the system to older conventional trucks without re-designing the entire driveline.

2.2 Analyzed configurations

As described before, in a “through-the-road” hybrid configuration the electric machine is placed directly on the electric drive-axle, which is not mechanically linked to the ICE powered axles. The connection between the two power sources is provided by the constraints between the vehicle’s wheels and the ground.

All the operating modes seen for parallel hybrid configurations are achievable in this scheme.

In this work, two hybrid through-the-road configurations will be analyzed.

2.2.1 Single electric motor coupled through a differential

In the first configuration proposed, the third idle axle of the truck is substituted by the electric axle of the hybrid powertrain, which is powered by a single AC electric motor. The machine is mounted to the axle and connected through conical gears to a standard open differential. The differential is responsible of splitting the torque to the wheels and ensuring their kinematical decoupling, necessary when the vehicle is turning. The gear ratio between the motor’s pinion and the differential crown has to be dimensioned considering the ideal range of speeds at which the electric machine can work at maximum efficiency.

The electric machine has to be chosen in order to fit the range of speeds involved in the vehicle’s advancement, and its output power should guarantee a good hybridization factor.

This solution is the simplest between the two proposed, both in terms of axle design and power management, since there is only one electric motor to manage and the design of the axle can be taken over from a regular mechanical axle.

Furthermore, thanks to the pinion-crown coupling between the electric machine and the axle, the motor can work at high speed and, therefore, it can deliver a significantly smaller amount of torque in order to provide the desired power.

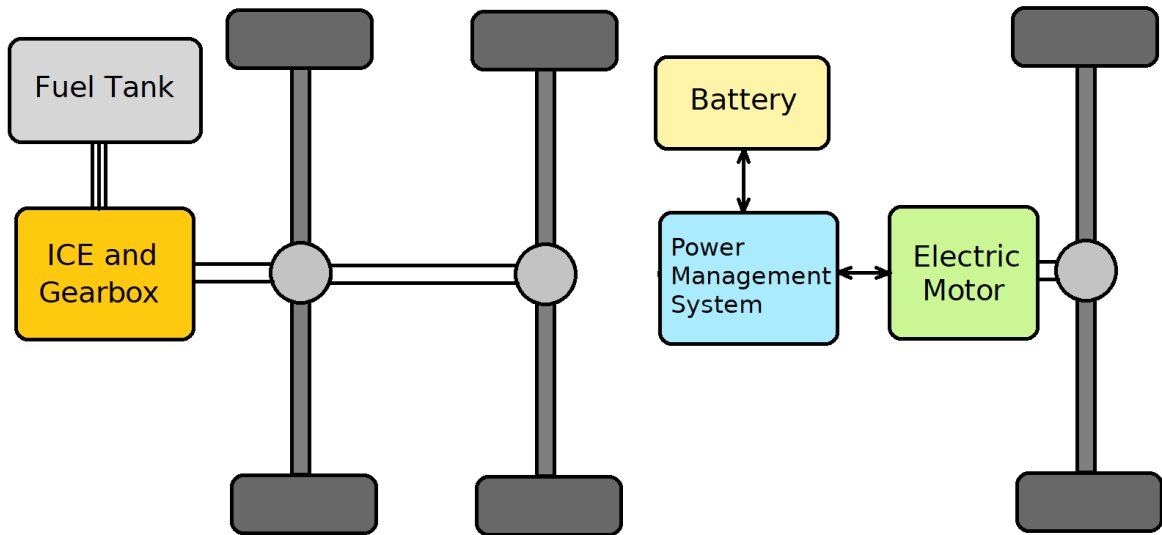


Figure 9 - Through the Road HD first configuration schematic

2.2.2 Frameless wheel-motors

The second configuration that will be analyzed is characterized by two wheel motors directly connected to the wheels instead of a single electric motor coupled to the wheels through a differential.

The absence of the pinion-crown gear reduction ratio determines that the angular speed of each motor has to match the wheel's angular velocity. Therefore, in order to provide the same amount of power, the motors have to deliver a much greater torque.

Thus, the motors' voltage will increase significantly compared to the first solution.

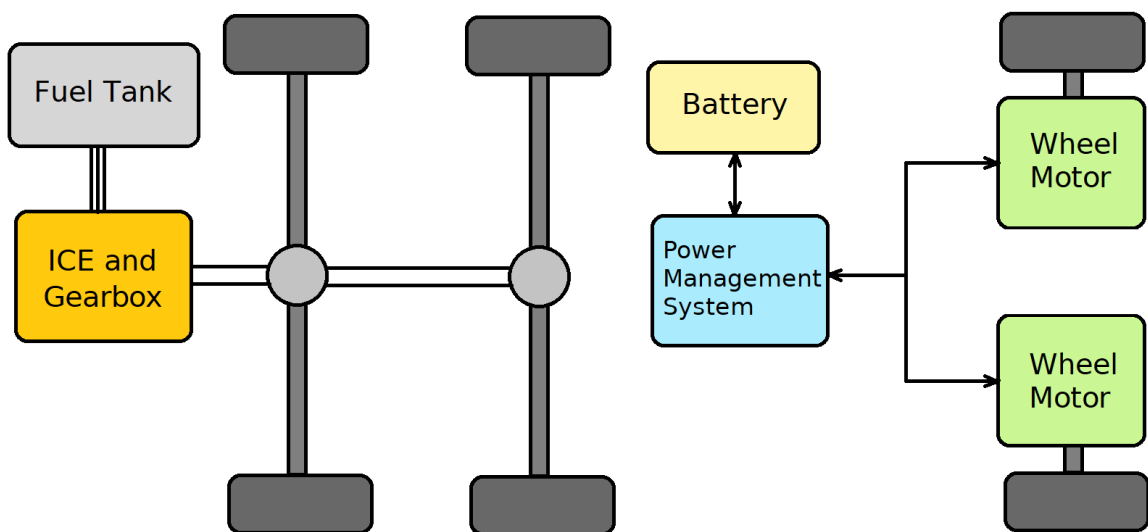


Figure 10 - Through the Road HD second configuration schematic

The motor involved in this configuration are specific frame-less, liquid cooled, AC motors, capable of very high torque at low speed.

The higher performances of frame-less motors, and the fact that we have one motor per wheel determines a greater hybridization factor for the second configuration and, therefore, a greater impact on power management strategies.

In fact, if the motors are capable of delivering a greater amount of torque, their impact on the engine's operating points will be higher, and therefore there will be a greater possibility to "force" the engine to work closer to the optimal torque. Furthermore, if the electric machines are more performant, regenerative braking will be more effective, and they will be more capable of reducing the vehicle's idling phase.

Also, the absence of the differential and the direct connection of the motors' rotor with the wheels determine a higher mechanical efficiency related to the kinematical chain.

Finally, the presence of two independent motors that control the two separate wheels allows the implementation of traction control strategies for the vehicle, enhancing its safety.

Despite all the advantages highlighted for the second solution, the main drawback of this configuration is the significantly higher cost of the components. In fact, frameless, high-performance motors are much more expensive than a regular AC motor, and the greater voltage of the batteries determines their increased cost. Finally, there is the need to design from scratch the full electric axle, which involves further expenses.

Comparing these two architectures, we can conclude that they are significantly different in terms of capabilities, performances, and costs. While the first one is less expensive but less performant, the wheel-motors solution should be much more performant and efficient, it can open various new possibilities regarding traction control strategies, but at the same time its cost will be definitely higher.

2.3 Simulation Tools used

2.3.1 Mechanical Simulation “TruckSim” suite

The evaluation of each configuration’s behavior through defined procedures has been carried on with the software suite “*TruckSim*” by *Mechanical Simulation*. In this section, the main capabilities and functionalities of the suite will be presented (Mechanical Simulation, 2018).

TruckSim provides to the engineers an accurate, detailed and efficient method for simulating the performance of multi-axle commercial and military vehicles.

The vehicle’s dynamics behavior can be reproduced within the software by efficient parametric math models, under the control of a specific *Graphic User Interface*.

TruckSim suite consists of three main tools:

- *VS Browser*: it consists of a custom GUI, and allows the user to define every aspect of the system intended to be simulated, from the vehicle’s characteristics to the event’s procedures.
- *VS Solvers*: its purpose is to calculate time histories of variables in math model. Those variables involves the vehicle’s *kinematics* (coordinates, angles, speeds, accelerations), its *dynamics* (forces and moments), and different other types of information. The math models within the solvers are customized to define parameters based on physical properties familiar to users. Once that every parameter has been set, the solver proceeds to implement the desired equations and solves them in an efficient way, generating the output variables.
- *VS Visualizer*: once that the output quantities have been determined, they can be easily visualized using this tool. It provides plots for every set parameter versus simulation time, and animation of the vehicle during the test procedure.

TruckSim uses standard VS library routines for processing input files, reading all input from text files that are normally generated automatically by the software. These files can be also compiled manually for more advanced applications. Input files follow a simple keyword-based format called *Parsfile*.

In TruckSim software, every model, procedure or parameter defined is related to a specific *dataset*.

Each dataset contains a set of parameters and is related to a specific mathematical model. The user can define the type of dataset to implement, and can manipulate it modifying the parameters in order to create the desired model.

Every dataset is then linked to multiple sub-datasets, everyone with a defined structure and representing a particular aspect of the vehicle or procedure.

The main dataset which contains all the parameters and specifications of every TruckSim model is visualized as a “Run Control Screen”. It represents the home screen and it is linked to sub-datasets for simulated systems, procedures, plot settings, and other settings related to the simulation run environment.

In figure 11, a standard example of a TruckSim Run Control Screen is represented.

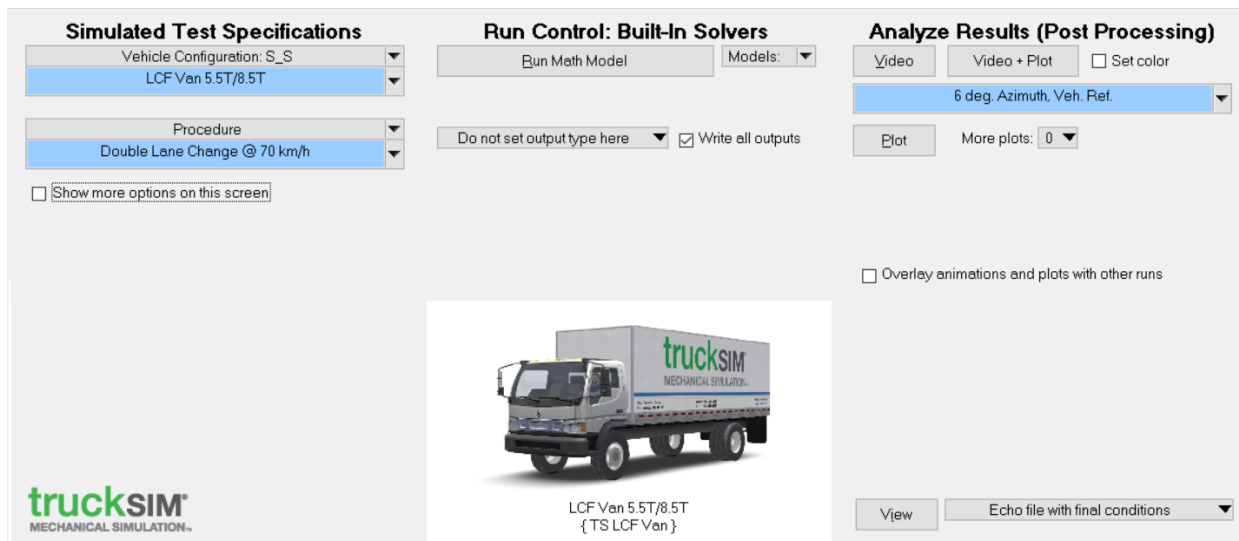


Figure 11 - TruckSim Run Control screen

The model’s home screen is divided into three main areas:

- *Simulated Test Specifications;*
- *Run Control;*
- *Post Processing.*

The first area (*Simulated Test Specifications*) allows to define the characteristics of the vehicle, the procedure test and optional datasets that may be used in the simulated run.

The center area of the home screen is linked to the VS Solver environment. From the “Run” button it is possible to start the simulation with TruckSim solver or, alternatively, with eventual external Solvers if the model is linked to third party environments.

The right-hand region allows the user to visualize the results in a graphic interface which includes a 3D animator, and to plot the output variables.

In the Simulated Test Specifications area, two important links can be found: *Vehicle Configuration* and *Procedures*.

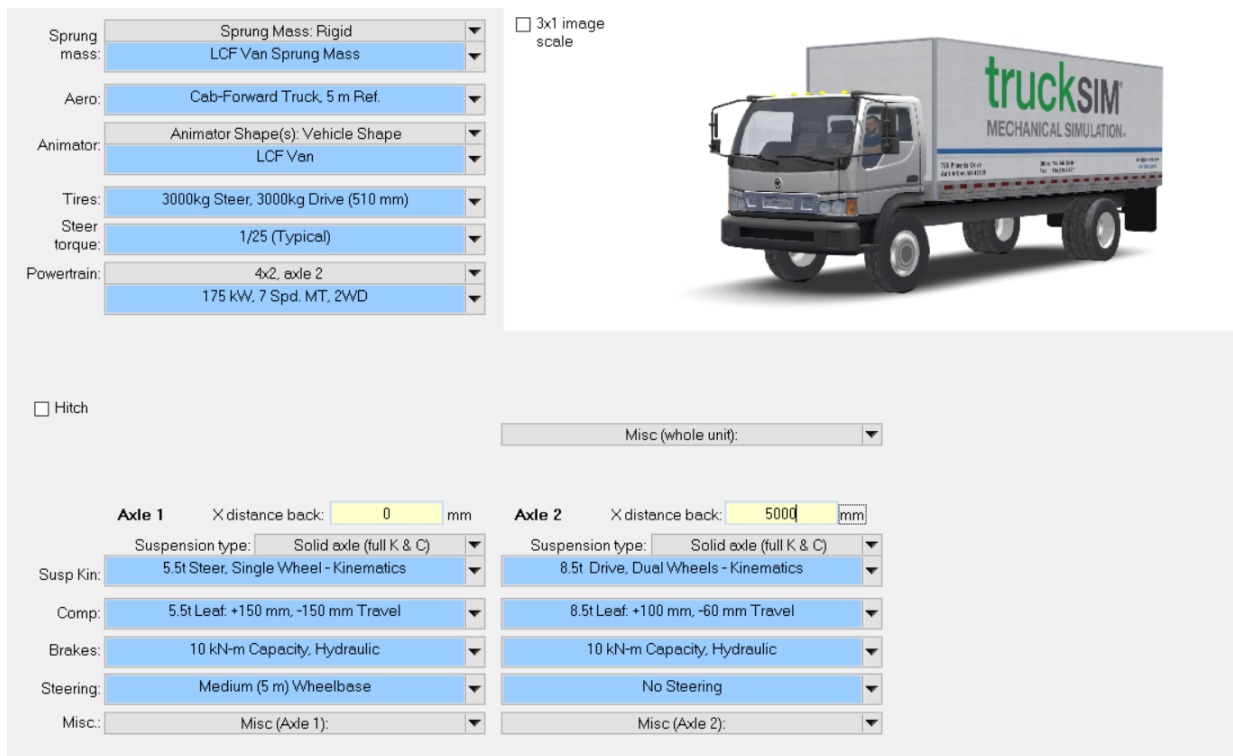


Figure 12 – TruckSim Vehicle Configuration dataset

The *Vehicle Configuration dataset* contains several sub-datasets, which describe the vehicle’s subsystem. The “*sprung mass*” subsystem defines the vehicle’s inertial properties, such as its mass, its inertia tensor, and the position of the center of mass.

The “*Aero*” dataset defines the aerodynamic coefficients of the vehicle in a Cartesian reference system, while the “*Tires*” subsystem allows to describe the tires’ properties in terms of rolling radius (effective and unloaded), spring rate, reference vertical force, width, and so on.

Particularly important is the “*powertrain*” dataset. In this section, it is possible to insert all the data that define the vehicle’s powertrain, from the internal combustion engine to every other component of the driveline.

In this subsystem it is possible to model the clutch, the gearbox (defining a shifting strategy as well), the transfer case and the differentials, and the internal combustion engine.

The vehicle’s ICE is modeled by its torque curves and by the fuel consumption map. The first defines the engine’s output torque related to the crankshaft speed and the throttle position, while the second includes the values of the engine’s fuel consumption rate, and allows the software to calculate the fuel consumption during the test.

The second main block of the “*Simulated Test Specification*” area is the *Procedure dataset*. This dataset is essential to define every aspect of the procedure test that the vehicle has to perform. Its main block is the *Driver Controls*, which determines the target variables that the models tries to chase by modifying the related vehicle’s quantities.

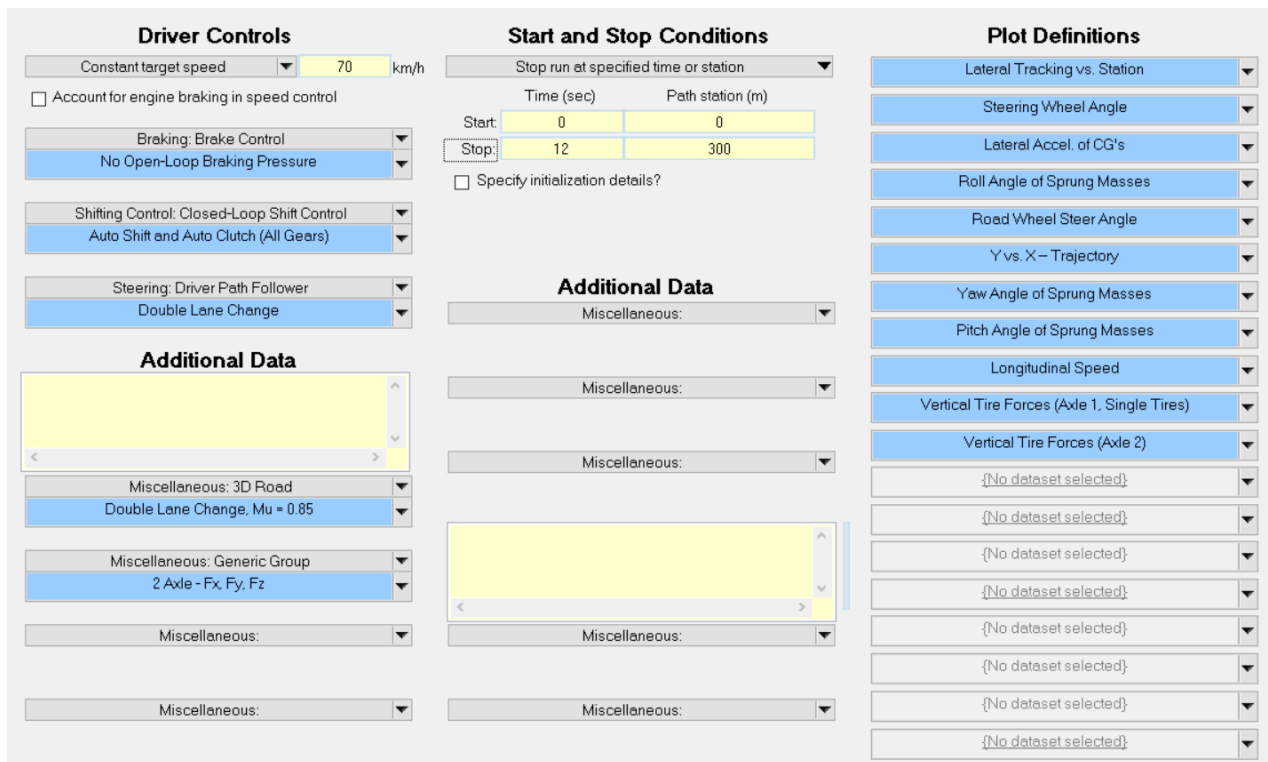


Figure 13 - TruckSim Simulated Test Specification screen

These target variables typically address to longitudinal dynamics (throttle and speed control, braking control), and lateral dynamic (steering and trajectory control). Possible target variables can be a constant speed (as shown in the example figure), a speed profile, a throttle profile, a defined trajectory, a steering angle profile and so on.

The dataset can be populated with numerous miscellaneous sub-datasets, which can help to define a particular situation or event, wanted to be evaluated. An example of additional sub-datasets that can be included is the road characteristics, from its friction coefficients to its elevation profile, to even its 3D topology (this information will be used in the VS Visualizer animations).

In the center part of this section, Start and Stop Conditions and the output variables that will be visualized in the VS Visualizer environment can be specified.

Once that every dataset has been created and the mathematical model which represents the test procedure has been completely defined, the mathematical model can be run.

The VS Solver then solves the equations that the software has generated and produces an output that can be visualized and post-processed in the VS Visualizer environment.

As shown in the following picture, all the output quantities are plotted and a graphic visualization of the test procedure is created, in order for the user to properly evaluate the model and verify if the results are plausible.

TruckSim offers also the possibility to export the output variable, in order to process them with third party software as Matlab.

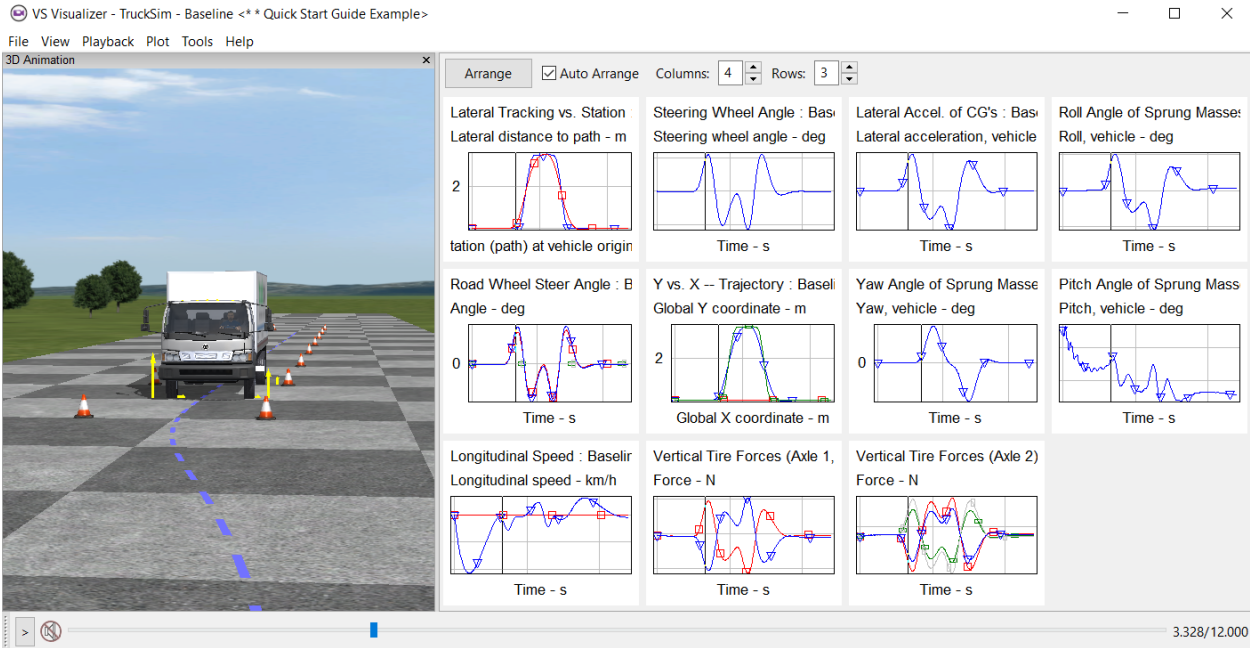


Figure 14 - TruckSim VS Visualizer

2.3.2 Coupling with Matlab-Simulink environment

Despite TruckSim suite offers a wide possibility to create different models and datasets and allows to simulate most of the common driving situations for trucks and passenger cars, there could be some specific situations which are not possible to recreate within the software.

Some hybrid powertrain configurations are an example. TruckSim offers some datasets to simulate hybrid powertrains, but unfortunately the suite doesn't include the configurations that this thesis work aims to analyze.

However, the software offers the possibility to co-operate with third party software, such as the Matlab-Simulink environment by MathWorks.

In fact, in TruckSim it is possible to set an external Run Control with Simulink. In this mode, Import and Export channels can be set up, defining which variable we would like to send to the external environment and process in Simulink.

Once that those variables have been defined, the software generates a Simulink block with an input and an output signal, as shown in figure 16. The dimension of the signals depends on the number of I/O variables previously defined in TruckSim.

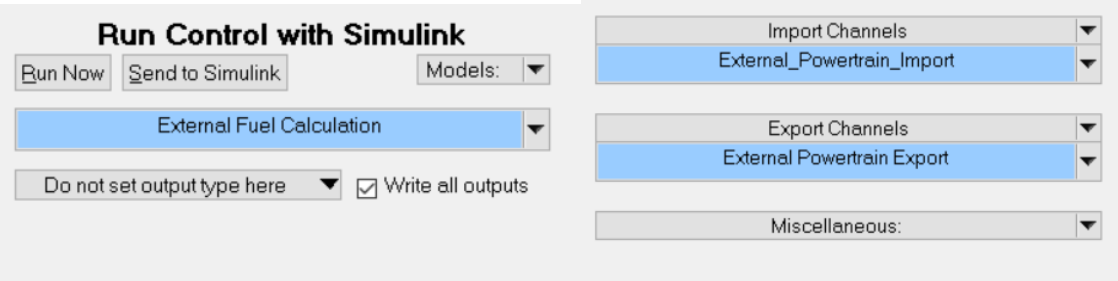


Figure 15 - TruckSim Run control with Simulink option

Those vectorial signals can be splitted into double type signals by using a “demux” function, and they can therefore be processed and manipulated in Simulink.

Finally, the signal can be fed back into the TruckSim block and the simulation is then ran into the Simulink environment.

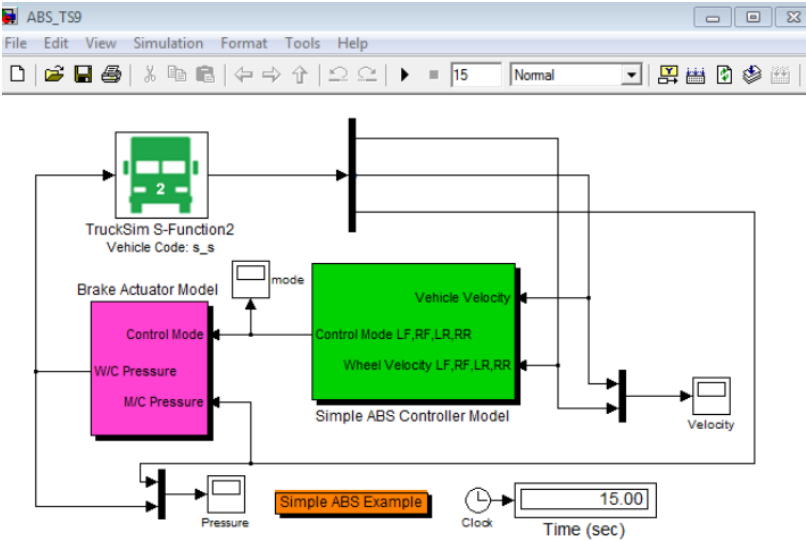


Figure 16 - External Simulink model (Mechanical Simulation, 2018)

The opportunity to couple the TruckSim suite with Matlab-Simulink environment also allows to have a better management of the post-processing phase.

2.4 Simulation procedures

In order to simulate the systems' behavior in TruckSim, the first step is to define the model datasets. These regard mainly the vehicle's layout and the test procedures.

This paragraph aims to describe the implemented procedures to evaluate the hybrid architectures discussed before. The main parameter which will be taken as a reference to compare the different powertrains will be the *fuel rate* and the *cumulated fuel consumption* on standard paths, each one representative of a common real life situation. The expectation is that the hybrid powertrains will guarantee an overall fuel saving compared to the conventional configuration.

2.4.1 Heavy-Duty Diesel Truck Schedule

The point of reference for the driving cycle that the truck has to follow in the simulations is represented by the *Heavy Heavy-Duty Diesel Truck (HHDDT) Schedule*, developed by the California Air Resources Board (CARB) with the cooperation of West Virginia University (Heavy Heavy-Duty Diesel Truck (HHDDT) schedule by California Air Resources, s.d.).

This study was conducted in order to understand in-use Heavy-Duty Diesel Vehicles (HDDV) emissions in California and though-out the country, and was part of a larger effort to expand the CARB's current HDD inspection and maintenance program in California (Durbin, Johnson, Miller, Maldonado, & Chernich, 2008).

The HHDDT Schedule is the result of years of investigation on actual on-road driving behavior of HDDVs, by using chassis dynamometer test data, and provides a valid instrument for investigating real on-road performances of heavy duty vehicles in North America. The test consists of four speed-time modes: idle, creep, transient and cruise. The following table resumes the main characteristics of the different modes:

Table 1 - HDDT cycle characteristics

| Parameter | HHDDT Creep mode | HHDDT Transient mode | HHDDT Cruise mode |
|----------------------------------|-------------------------|-----------------------------|--------------------------|
| Duration [s] | 253 | 668 | 2083 |
| Distance [mi] | 0,2 | 4,59 | 37,17 |
| Average speed [km/h] | 2,85 | 24,78 | 64,21 |
| Stops/kilometer | 38,9 | 2,9 | 0,42 |
| Maximum speed [km/h] | 13,26 | 76,44 | 95,43 |
| Max acceleration [km/h·s] | 3,7 | 4,8 | 3,7 |
| Max deceleration [km/h·s] | -4,07 | -4,5 | -4,02 |
| Percent idle | 42,29 | 16,3 | 8 |

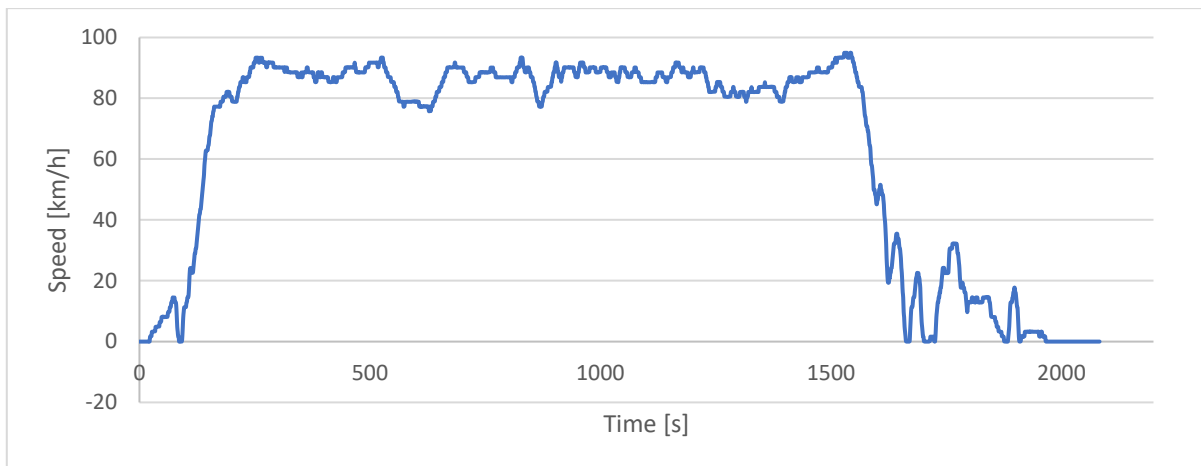


Figure 17 - HHDDT Cruising mode

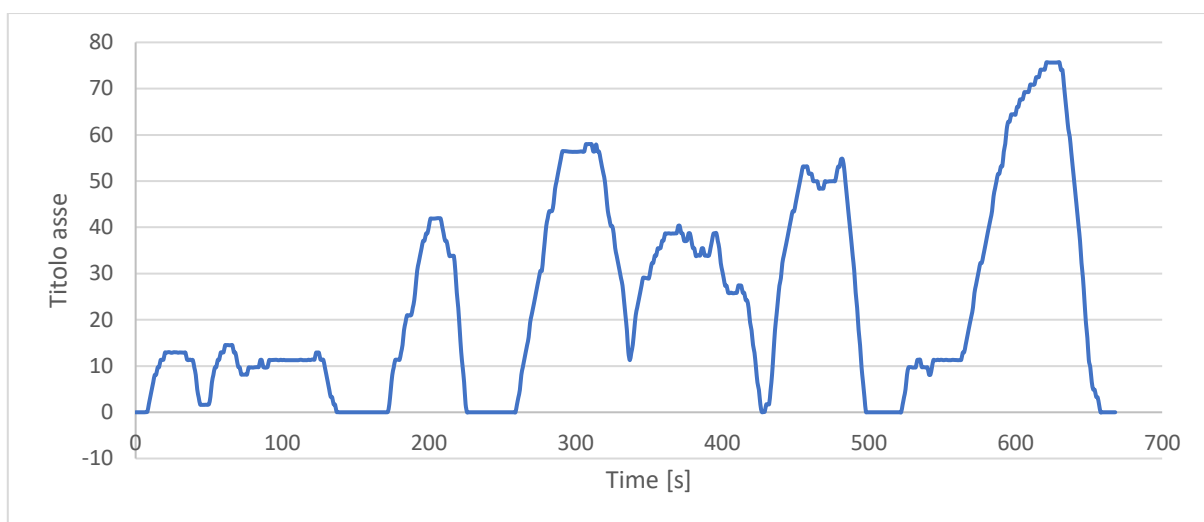


Figure 18 - HHDDT Transient mode

2.4.2 Urban path test

The first test proposed to evaluate the powertrains' performance is based on an urban route. In this situation a conventional vehicle is far from its optimal operating conditions, due to frequent braking, idling segments and low loads and a hybrid powertrain should guarantee the best advantages.

In order to simulate a real-driving urban situation, a city route commonly traveled by commercial vehicles has been chosen. Based on that, a custom drive cycle has been created, taking as a reference the HHDDT Transient Cycle, and reiterating it in order to match the route's length.

Another element that was considered in the realization of this procedure test is the road's elevation. This factor plays an important role in the definition of the external torque request, and especially its derivative (road slope), as evidenced in the first equation of paragraph 1.6.1.

The selected route for the urban test is a common city path that commercial vehicles follows in the heart of Toronto metropolitan area. It is a 18,4 kilometers itinerary that links two DHL shipping centers, from Englemount – Lawrence to Discovery District.

In the following graphs its main characteristics are highlighted.

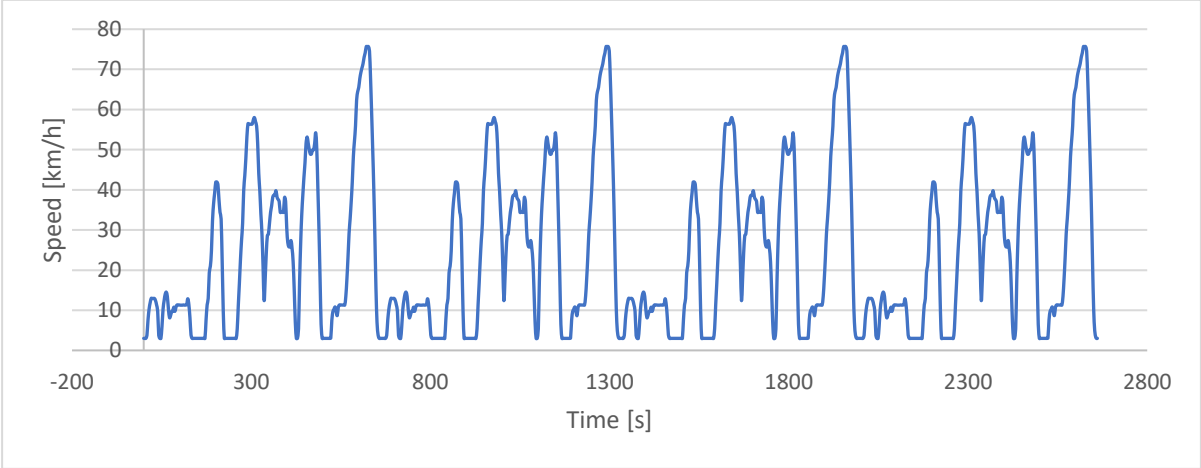


Figure 19 - Urban test speed profile

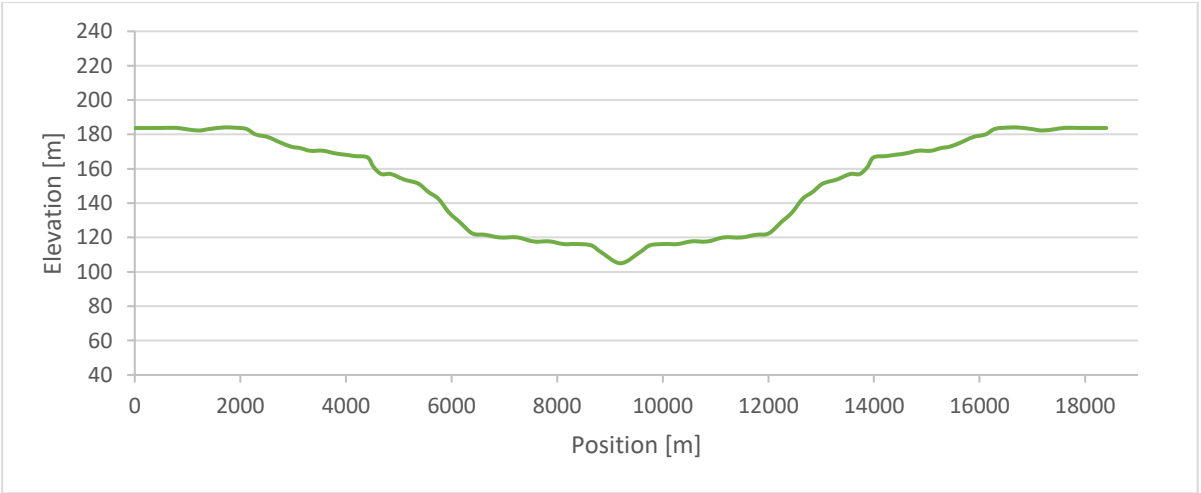


Figure 20 - Urban test ground elevation

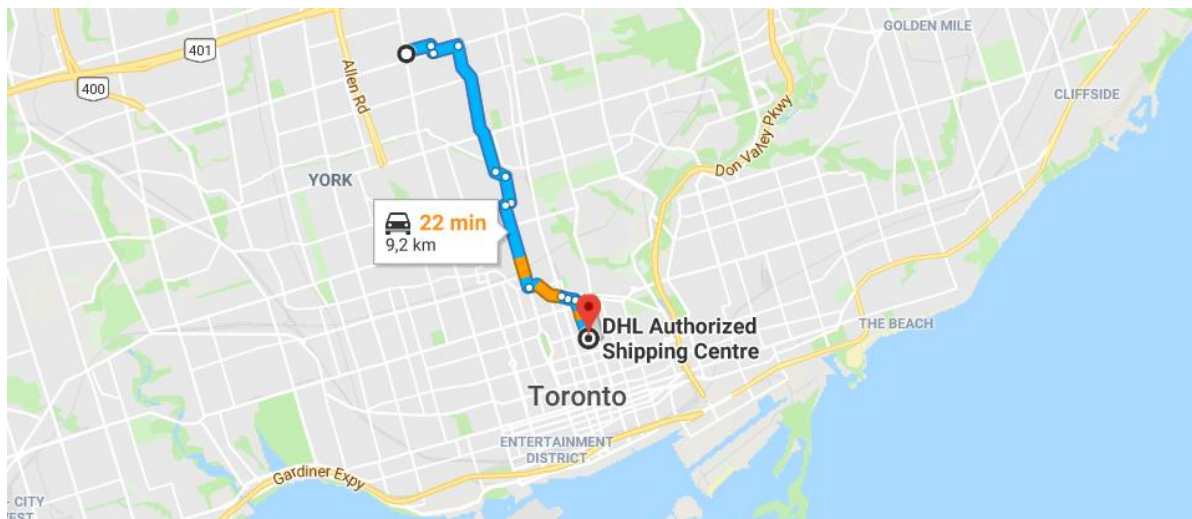


Figure 21 - Urban test itinerary

The selected itinerary consists of a 9,2 kilometers path for each trait, and the same distance can be obtained by reiterating two times the HHDDT transient cycle. A remark that the selected speed profile matches the real-driving conditions is given by the correspondence by the duration of the custom cycle and the estimated time proposed by Google Maps, both equal to 22 minutes.

The path has a slight uphill profile, with a total altitude increase of 73 meters, which corresponds to an average slope of 0,79%. The roundtrip total altitude difference is, of course, equal to zero.

2.4.3 Food delivery path test

A typical situation for Heavy Duty vehicles is represented by the food delivery process. In this condition, the vehicle has to perform several stops during which the refrigeration system has to keep running in order to maintain adequate conditions in the cold room in which the food is stored.

This circumstance is particularly unfavorable for conventional vehicles. In fact, regular ICE powered trucks are not equipped with capacious batteries that could power the auxiliary devices. As a result, during the delivery phase the truck's engine has to be on in order to provide the necessary power to the system.

This working condition is extremely inefficient, since the engine's load is close to the minimum.

If the vehicle is equipped with a hybrid powertrain, during the food delivery phase the internal combustion engine can be turned off, and the auxiliary systems can be powered exploiting the charge previously stored in the batteries in high engine efficiency conditions, or derived by

energy recuperation strategies such as regenerative braking. This can lead to a substantial fuel saving.

In order to simulate this situation, another procedure test has been defined, taking as a starting point the urban city path described in the previous paragraph.

The new cycle has been assembled as a sequence of three urban paths interspersed with ten minutes stop intervals, which represent the loading/unloading procedure.

In terms of elevation, the former elevation profile has been reiterated three times to simulate the extended cycle. The results in terms of speed profile and elevation are represented below:

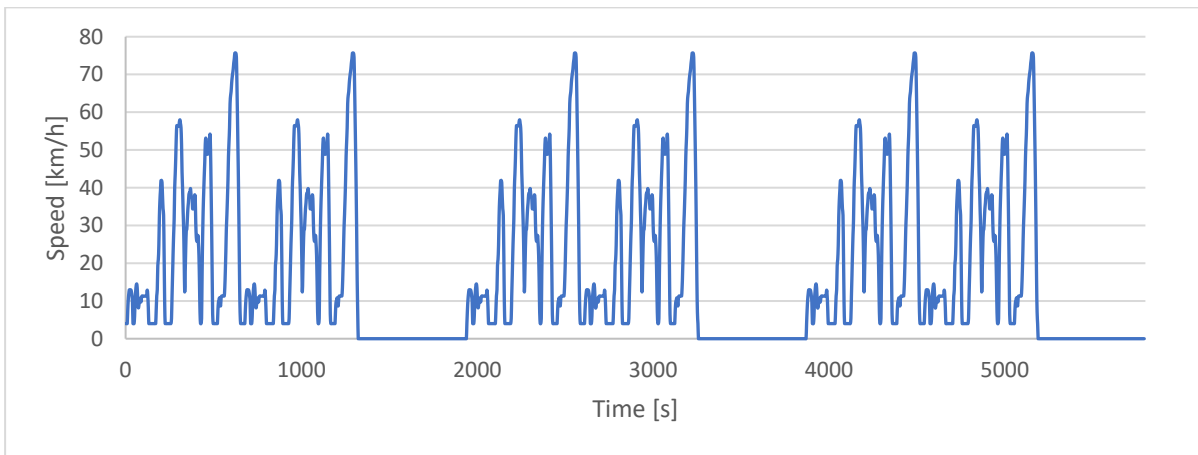


Figure 22 - Food delivery test speed profile



Figure 23 - Food delivery test elevation

2.4.4 Cruising path test

The last test procedure to which the models will be submitted is a highway cruising route. In this situation a conventional vehicle works at its optimum efficiency, since its internal combustion engine has been designed to operate at a high load and, therefore, at its maximum efficiency.

Furthermore, the minimum presence of braking implies no energy recuperation through regenerative braking.

It is legit to suppose that in this condition a hybrid powertrain will not be able to ensure any fuel saving. However, even during cruising mode the vehicle does not travel at constant load, but there will be some fluctuations related to the change in road elevation, slight variations of the vehicle's speed related to traffic, and so on.

The aim of this test is to evaluate whether the capabilities of a hybrid system can allow to obtain a certain fuel saving even in highway cruising conditions, or, conversely, if the energy conversion inefficiencies will determine a disadvantage compared to a conventional solution.

If that's the case, the best option is to deactivate the hybrid powertrain whenever the power management system detects a cruising scenario, switching to Engine alone traction mode.

This test procedure has been created taking as a reference the HDDT cruising cycle, reiterating it in order to match the length of an itinerary between Toronto and Ottawa.

The elevation profile has been calculated using Google Maps in the same way as the former procedures. The results are shown in the following graphs.

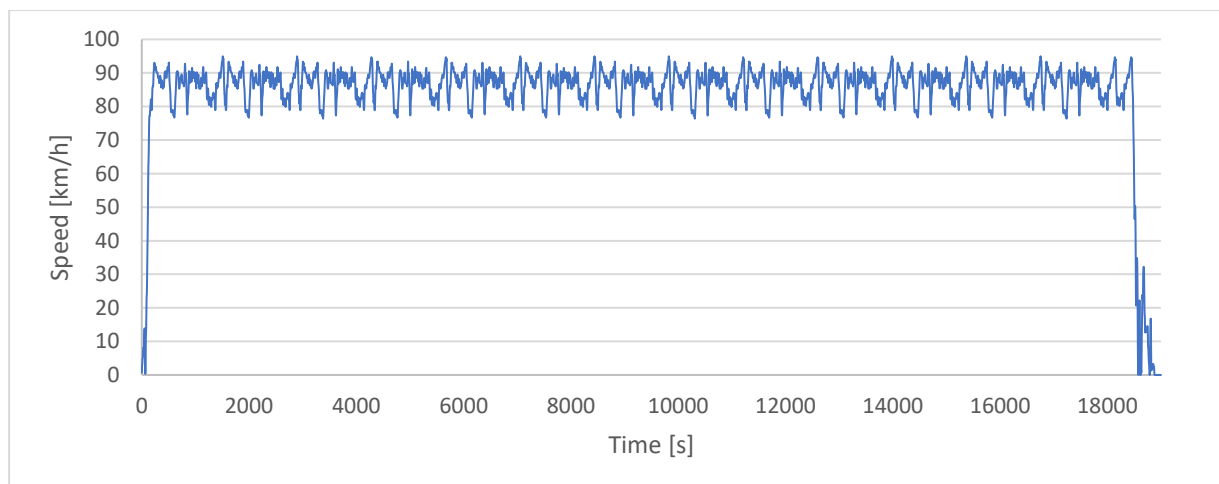


Figure 24 - Cruising test speed profile

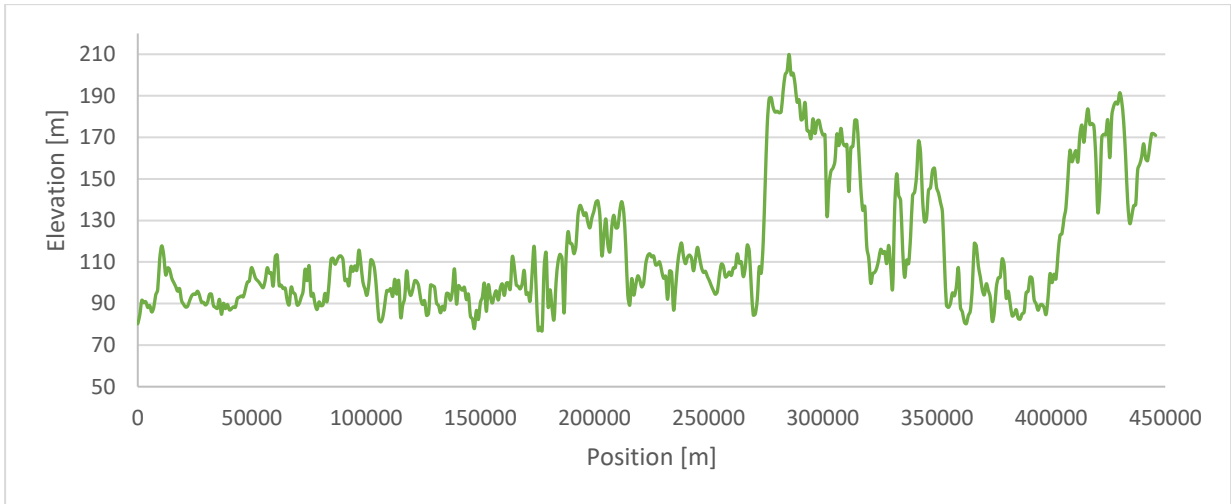


Figure 25 - Cruising test elevation

3. Components and vehicle modelling

In this chapter the attention will be focused on creating the required dataset in TruckSim in order to model a conventional service vehicle and run the simulations on the test procedures described above.

Modelling and simulating a conventional only-ICE truck is a step required to obtain benchmark data to compare with the hybrid powertrain models, and to have the base model needed to configure the hybrid architectures.

3.1 Conventional vehicle modelling

3.1.1 Sprung masses and payload

The first step of the creation of the only-ICE model's dataset is defining the vehicle's inertial properties, its aerodynamics and the tires specifications.

The modeled vehicle falls into the Medium Heavy-Duty Vehicle class 5 category according to the US classification. In this class are included trucks as Ford F-550, GMC 5500 and Ram 5500.

This category comprises trucks with GVWR (gross vehicle weight rating) range between 7258 and 8845 kilograms. For this model, the *Ford F-550* has been taken as a reference to define the vehicle's inertial specifications (Ford, 2018).

Therefore a standard 3-axles truck model has been selected from the available TruckSim datasets, and its sprung mass specifications have been modified in order to match with the Ford F-550 data. In particular, while the mass has been changed to 8845 kilograms, the vehicle's radii of gyration and position of the center of mass has remained unchanged.

The software has then provided to calculate the vehicle's inertia tensor, based on the relation $I_i = MR_i^2$

We must keep in mind that for the aim of this simulation, giving exact values of the vehicle's inertial properties in the three spatial dimensions is not a fundamental requirement, while its mass has a much greater impact on the simulations' result. However, providing accurate values of the trucks' rotational inertial properties helps us to avoid unwanted phenomena, such as unexpected tire locking or a wrong braking force distributions.

In addition to the inertial properties related to the vehicle's cab, a payload has been added to the model, in order to simulate the truck's advancement at full load.

Based on the Ford F550 specifications about the maximum value of the payload, which cannot exceed 5774 kilograms, a 5000 kilograms payload has been chosen and added to the model.

The payload has been modeled as a simple 3000x2000x1000 mm parallelepiped, with its center of mass coincident with its geometric center (constant density hypothesis has been applied). The following table describes the inertial characteristics of the vehicle's sprung masses.

Table 2 - Vehicle's inertial properties

| | |
|---|-------|
| Cab sprung mass [kg] | 8845 |
| Roll Inertia [kg·m²] | 9640 |
| Pitch inertia [kg·m²] | 30436 |
| Yaw inertia [kg·m²] | 27554 |
| Center of mass height [mm] | 1020 |
| Center of mass z coordinate [mm] | 1385 |
| Payload mass [kg] | 5000 |
| Payload center of mass height [mm] | 1800 |

3.1.2 Aerodynamics

Aerodynamic effects are represented by a force vector and a moment vector acting on the sprung mass. The force vector is applied at the aerodynamic reference point, defined by coordinates in the sprung-mass coordinate system.

The components of the force and moment in the body-fixed sprung mass frame are calculated as functions of the aerodynamic side slip angle beta:

$$\begin{aligned}
 F_x &= -C_{fx}(\beta) \cdot A \cdot Q & F_y &= -C_{fy}(\beta) \cdot A \cdot Q & F_z &= C_{fz}(\beta) \cdot A \cdot Q \\
 M_x &= C_{mx}(\beta) \cdot A \cdot l \cdot Q & M_y &= -C_{my}(\beta) \cdot A \cdot l \cdot Q & M_z &= -C_{mz}(\beta) \cdot A \cdot l \cdot Q
 \end{aligned}$$

Where $Q = \frac{Dv^2}{2}$, D is air mass density, set to 1,206 kg/m³, A is the frontal area, equal to 10 m², l is the reference length, equal to 5000 mm and v is the relative air speed.

The aerodynamic coefficients are dimensionless and are defined as functions of beta.

3.1.3 Tires specifications

Tires data are referred to a standard radial tire model proposed by the software. Specifically, every truck's tire is a 385/65R22.5 with a nominal load rating of 3500 kg. Each tire has an unloaded radius of 538 mm, a spring rate of 1350 N/mm, while the effective rolling radius is equal to 528 mm.

The main parameters that play an important role in the determination of the total resistance forces to the vehicle's advancement (and therefore in the determination of the engine's required torque and on the overall fuel consumption) are the rolling resistance moment and the wheel's spin inertia.

Even in this case, the default values proposed by TruckSim has been used. In particular, the rolling resistance moment coefficient values amount to:

$$R_{r_c} = 0.0041 \quad [-] \quad R_{r_v} = 0.09216 \left[\frac{S}{km} \right]$$

The determination of the longitudinal and lateral forces and the aligning moment takes place on the base of the Pacejka model.

According to this model (Pacejka, 2005), the *longitudinal force* that the tractive tire is able to exchange with the ground can be described as a polynomial function of the tire's *absolute slip ratio* (k) and the *normal force* that is applied to the tire.

Similarly, the absolute *lateral tire force* and the *aligning moment* are functions of the *absolute slip angle* (α) and of the tire's load.

During the simulation, the software calculates real-time the values of the tire's absolute slip ratio and slip angle, and determines the dynamic action that are exchanged with the ground. If the values of slip ratio or slip angle are too high, the forces exchanged saturate, and the tires slip.

In the following graphs are reported the aforementioned relations between forces and moments exchanged with the ground and slip ratio and angle implemented in the truck's model.

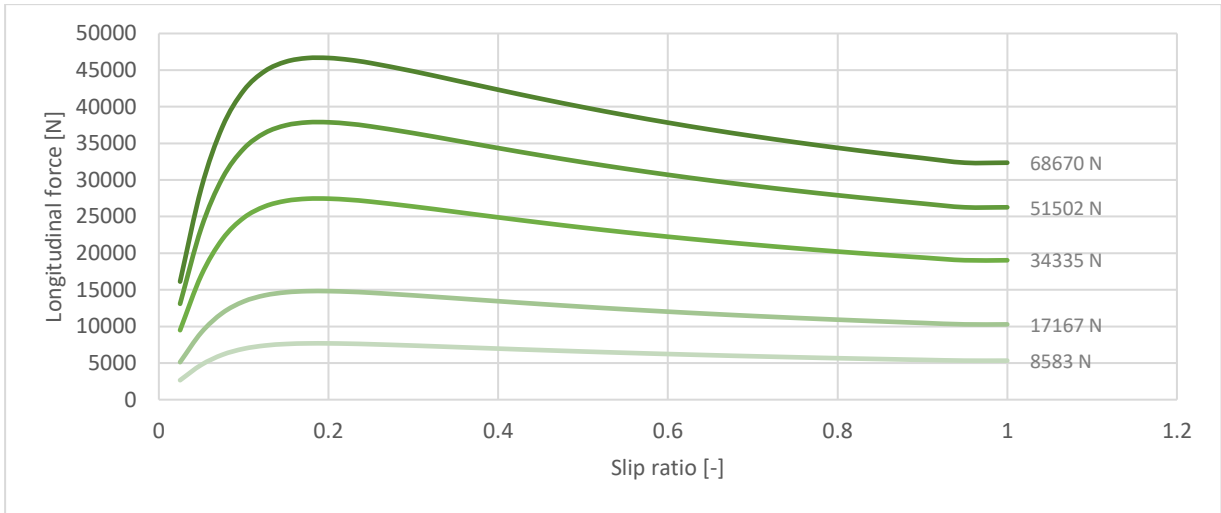


Figure 26 - Tire longitudinal force versus slip ratio

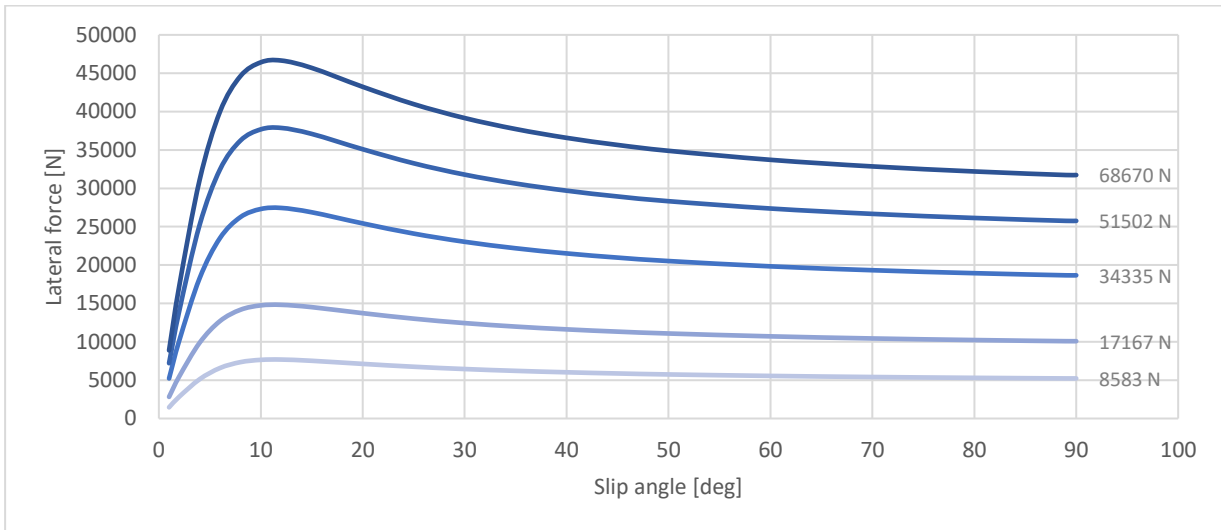


Figure 27 - Tire's lateral force versus slip angle

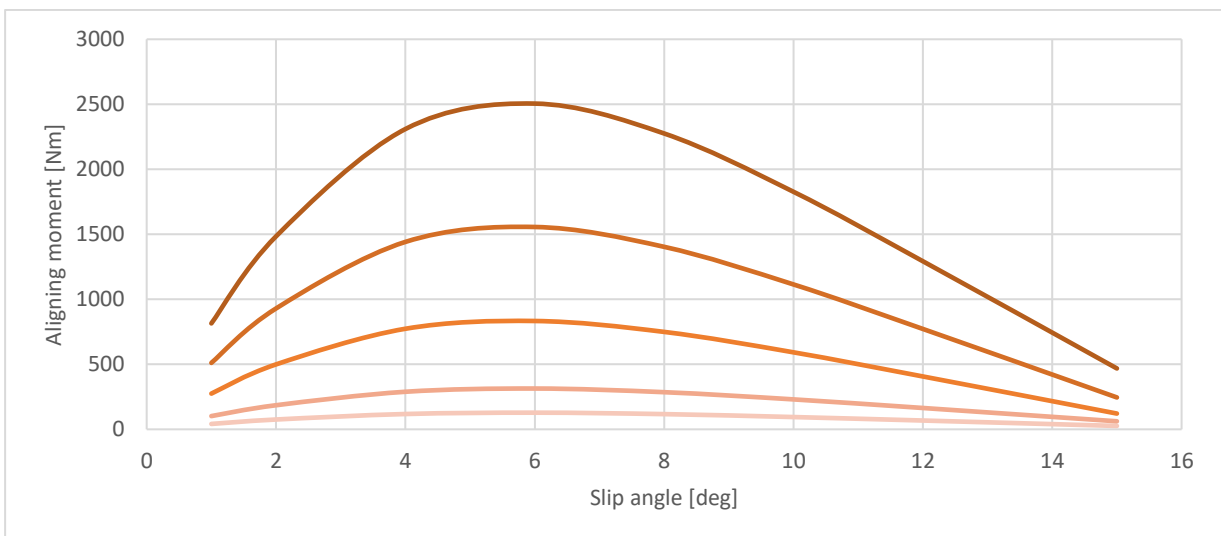


Figure 28 - Tire's aligning moment versus slip angle

3.1.4 Internal combustion engine dataset

In this model, the internal combustion engine is the only power source available. In TruckSim, the engine model is described by relating the output engine torque to the throttle position and the rotational speed. These properties are defined in a lookup table of torque versus engine speed for different throttle settings.

Another fundamental data is the engine's inertia, related to the engine's crankshaft. If we define the engine's moment of inertia as I_e , the moment of inertia of torque transfer device engine side as I_{tc_in} , the engine angular acceleration as α_e and torque transfer device input torque as T_{tc_in} , we can express the engine's angular acceleration as:

$$\alpha_e = \frac{T_e - T_{tc_in}}{I_e - I_{tc_in}}$$

Engine angular speed is obtained in each time step by integrating the differential equation:

$$\dot{\omega}_e = \alpha_e = \frac{f(\text{throttle}, \omega_{e_present}) - T_{tc_in}}{I_e - I_{tc_in}}$$

Therefore, TruckSim requires data related to the engine's torque map, its moment of inertia and eventual dynamic throttle delays (not implemented in this model).

The engine selected for the truck model was chosen since its torque, power and, displacement and general characteristics are typical of medium heavy-duty applications of this class. It is a Detroit Diesel S50, an 8.5 liters engine capable of delivering a maximum power of 205 kW. Its main characteristics are reported in the following table:

Table 3 - Detroit Diesel S50 characteristics

| Detroit Diesel S50 | |
|----------------------------|------------------------|
| Number of cylinders | 4 |
| Total displacement | 8500 cm ³ |
| Idle speed | 650 rpm |
| Maximum speed | 2100 rpm |
| Maximum power | 205 kW |
| Maximum torque | 1200 Nm |
| Engine inertia | 0.35 kg·m ² |
| Engine mass | 861 kg |

This engine is specifically designed for heavy duty applications, and its overall efficiency is particularly high in a limited area of its map, where it can reach 41%.

The engine map is shown below. The maximum torque curve (corresponding to full throttle) and the isoefficiency curves have been represented.

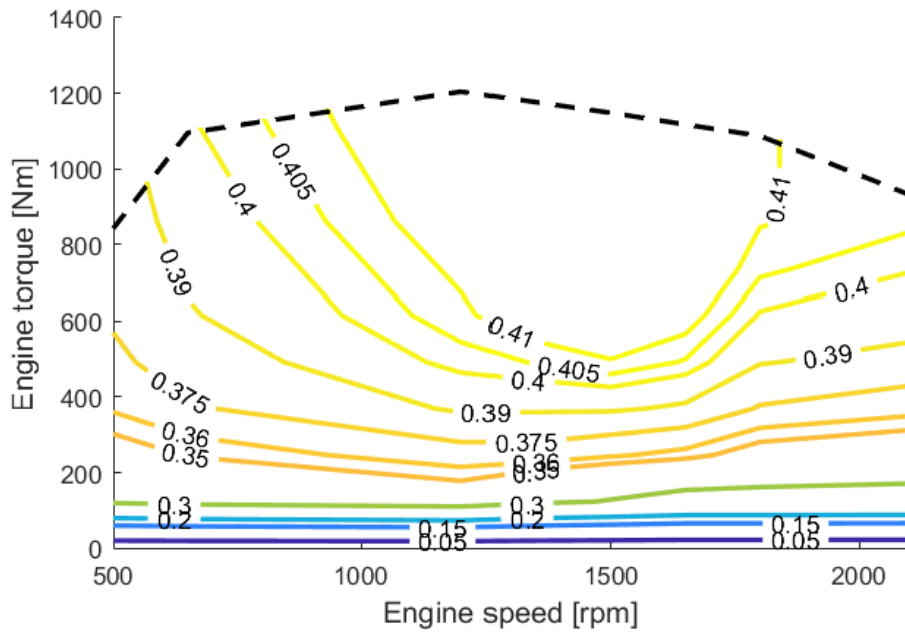


Figure 29 - Detroit S50 efficiency map

3.1.5 Driveline dataset

Once that the engine dataset has been created, the next step was to define the vehicle's complete driveline, from the engine output to the tires. The TruckSim powertrain model includes the engine, a torque transfer device (which can be either a torque converter or a mechanical clutch), transmission, a transfer case (for 4WD vehicles as in this case), and differential gears on the front and on the rear axles.

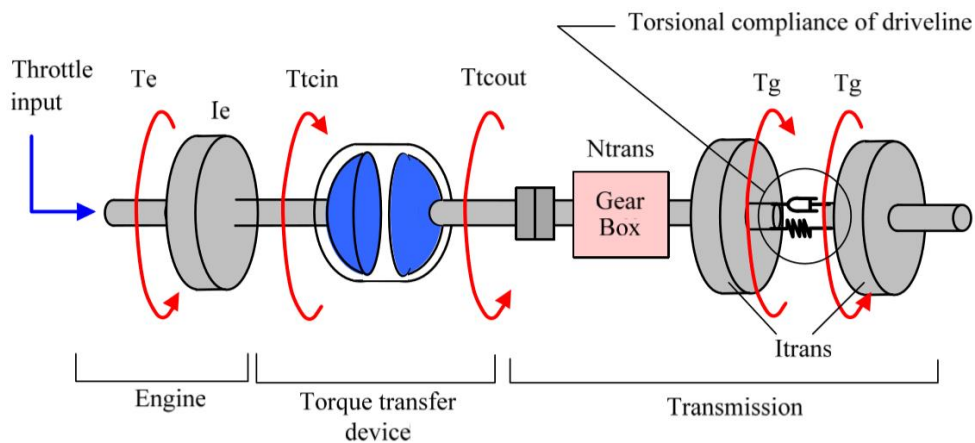


Figure 30 - Driveline schematic (Mechanical Simulation, 2018)

In Figure 30 is represented a schematic of the driveline, from the throttle input to the vehicle's transmission. Downstream of the transmission output, the torque is then transferred to the two axles via the transfer case, as shown below:

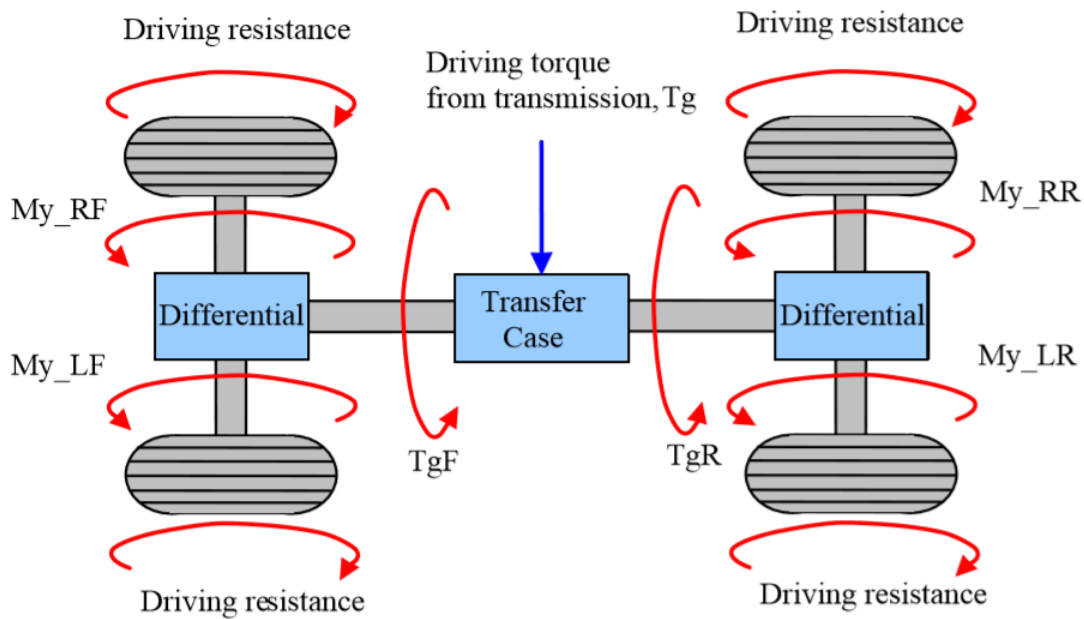


Figure 31 - Driveline schematic, downstream of the clutch (Mechanical Simulation, 2018)

3.1.5.1 Driveline inertia, stiffness and damping

A vehicle's driveline is not completely rigid and each part has some compliance due to its torsional flexibility. In TruckSim, the driveline flexibility is modeled using a lumped element approach: a single spring-damper unit, located after the transmission gearbox as shown in figure 30 is used to represent the torsional flexibility of the driveline.

The user input parameters are the driveline *natural frequency* and its *damping ratio*, which are converted automatically to the torsional stiffness and damping coefficient in the model, using the following equations:

$$K_{driveline} = \omega_{n\ driveline}^2 \cdot I_{driveline}$$

$$D_{driveline} = 2\zeta_{driveline} \cdot \omega_{n\ driveline} \cdot I_{driveline}$$

The front end of driveline inertia (engine side) is calculated as:

$$I_{driveline\ front\ end} = I_{tc\ out} \cdot N_{trans}^2 + 0.5 \cdot I_{trans}$$

Regarding the rear end of driveline inertia, in the case of a four wheel drive vehicle, it should account the torque bias ratio of the central transfer case, $T_{bias\ to\ rear}$, such as:

$$I_{driveline\ rear\ end} = 0.5 \cdot I_{trans} + \frac{I_{axle\ F} \cdot I_{axle\ R}}{I_{axle\ R} \cdot (1 - T_{bias\ to\ rear})^2 + I_{axle\ F} \cdot T_{bias\ to\ rear}^2}$$

The total driveline inertia, $I_{driveline}$, is derived by the following equation:

$$\frac{1}{I_{driveline}} = \frac{1}{I_{driveline\ front\ end}} + \frac{1}{I_{driveline\ rear\ end}}$$

We note that while the torsional stiffness and damping coefficient may change with the shift position, the user defined natural frequency and damping ratio is maintained during the simulation.

Furthermore, the torsional stiffness and damping coefficient used in this model are linear. However, TruckSim gives the user also the possibility to use non-linear characteristics, using non-linear tables for the torsional stiffness and damping of the transmission.

3.1.5.2 Torque converter

In the model created, torque is transmitted from the engine to the transmission by a hydraulic torque converter. The torque at the output side of the torque converter is given by the product of the characteristic table (f_{tr}), which represents the torque ratio ($T_{tc\ in}/T_{tc\ out}$) as a function of the speed ratio (S_{tc}), multiplied by the input side torque:

$$T_{tc\ out} = f_{tr}(S_{tc}) \cdot T_{tc\ in}$$

Furthermore, torque at the input side of the torque converter can be obtained by the torque load on the engine given by the characteristic table (f_{tki}), which is the inverse torque capacity ($1/K$), function of the speed ratio, multiplying angular speed of the engine:

$$T_{tc\ in} = sign\{f_{tki}(S_{tc})\} \cdot \{f_{tki}(S_{tc}) \cdot \omega_e\}^2$$

Generally, a torque converter is characterized by its torque capacity K . However, it is difficult to describe an engine braking model in terms of K , since this value normally tends to infinity as the angular speed of the torque converter and the angular speed of the engine assume an equal value. Therefore, the capacity is described by a table for $1/K$ as a function of the speed ratio (ω_{tco}/ω_e). When the speed ratio is negative, the sign of K is assumed to be negative, thus exerting a retarding torque on the transmission and the wheels.

The characteristic tables f_{tr} and f_{tki} implemented in the TruckSim torque converter dataset are shown in the graphs below:

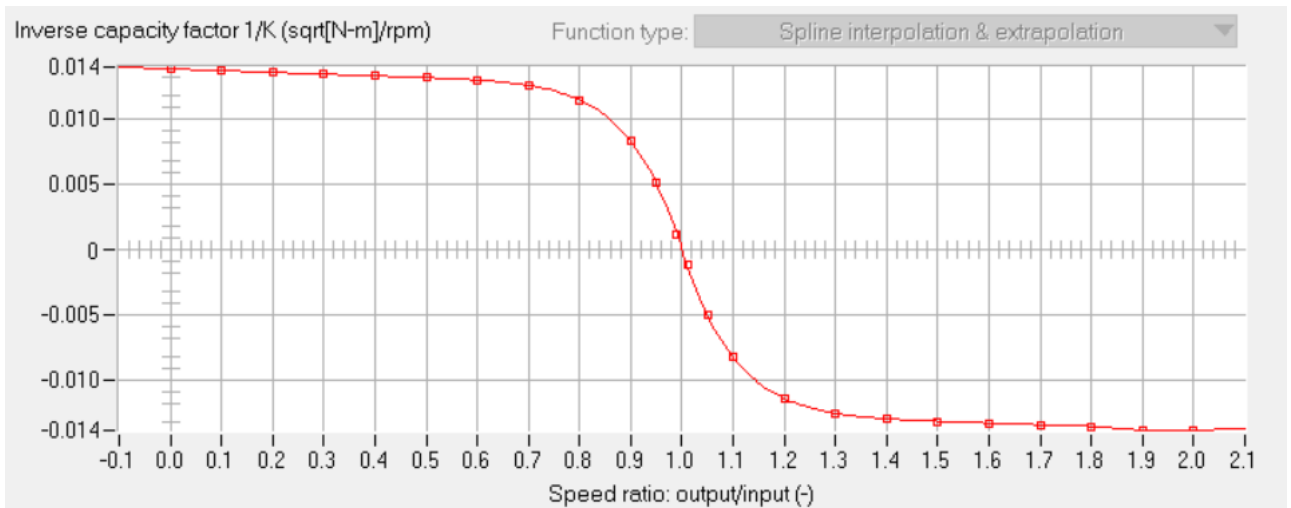


Figure 32 - Torque converter inverse capacity factor 1/K versus speed ratio

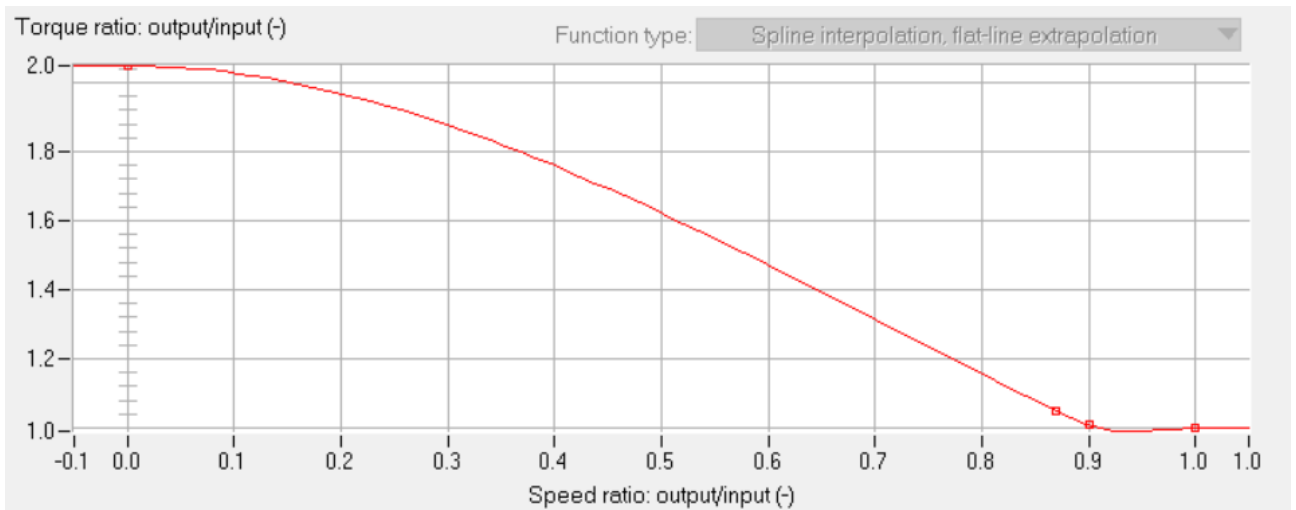


Figure 33 - Torque converter ratio versus speed ratio

3.1.5.3 Transmission and shift schedule

Regarding the transmission, an automatic 7-speed gearbox has been modeled. The transmission gear ratio (N_{trans}) is associated with the selected gear number. The output torque of the transmission gearbox is given by the torque transfer device output torque ($T_{tc\ out}$), gear ratio and the gear efficiency, depending on whether the engine drives the wheel or the wheels drive the engine, such as:

$$T_{gr\ out} = N_{trans} \cdot T_{tc\ out} \cdot \eta_{trans} \quad (T_{tc\ out} \geq 0)$$

$$T_{gr\ out} = \frac{N_{trans} \cdot T_{tc\ out}}{\eta_{trans\ rev}} \quad (T_{tc\ out} < 0)$$

The gear of the transmission is determined by the transmission's mode of operation. There are different operating modes in TruckSim: if mode 1 is selected, the gear is defined by an open loop function of time as specified in the "Control: shifting (open loop)" screen.

Mode 0 refers to a neutral gear, while mode -1 engages reverse gear. Mode 2 to 7 (the one used in this model), cause gears to be changed automatically according to the upshift and downshift schedule tables linked to the transmission screen.

If the mode selected goes from 2 to 7, the mode number defines the upper boundary for the maximum gear selectable.

The gear selection criteria is defined by the *shifting schedule*: for every currently engaged gear and throttle position, two boundary values of the engine angular speed are defined. The first corresponds to a downshift, the second one to an upshift.

Generally, if the throttle position percentage increases, also the two speed boundaries are greater, and vice versa. In the following images are reported two examples of upshift and downshift diagrams.

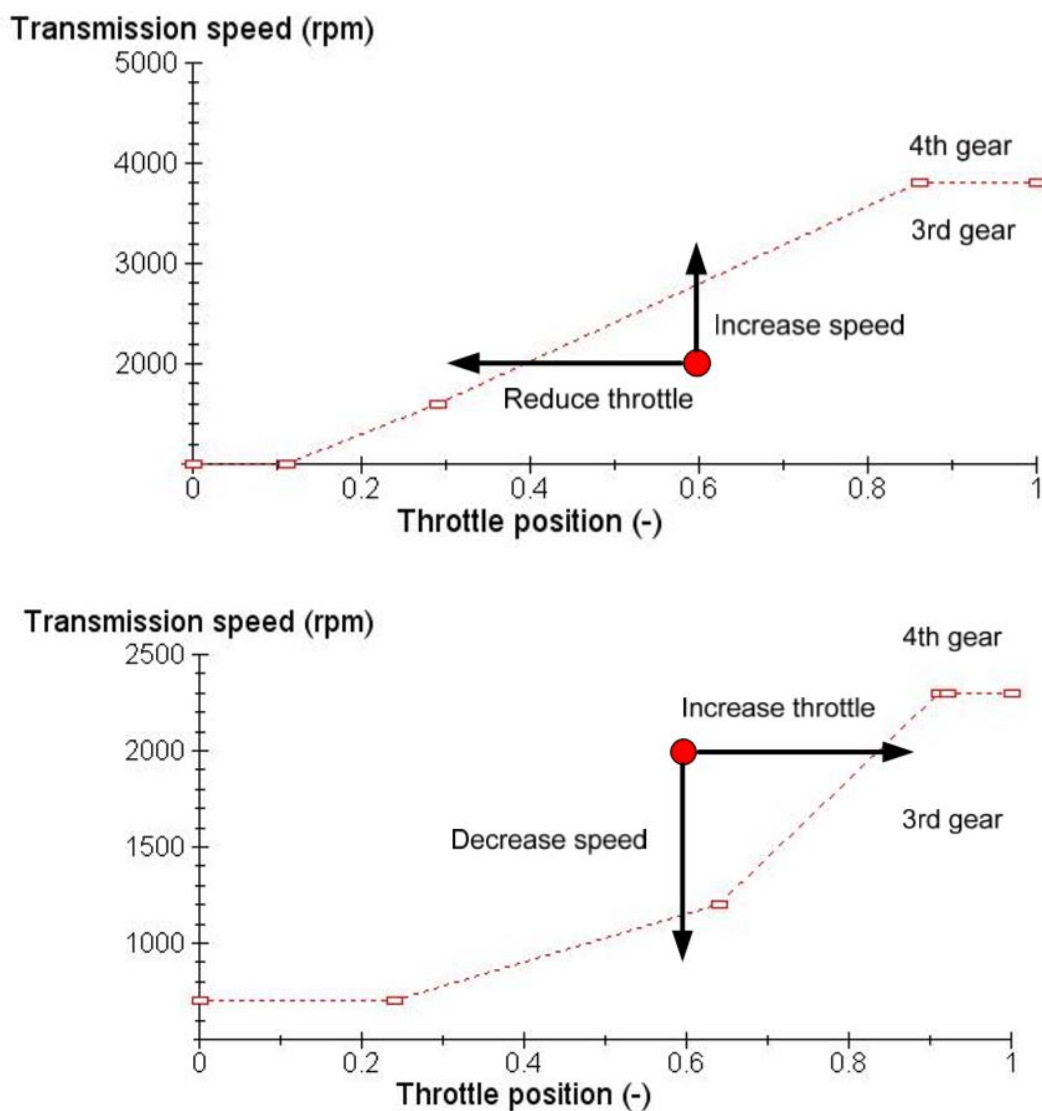


Figure 34 - example of downshifting and upshifting strategies (Mechanical Simulation, 2018)

In the model, a 7 speed transmission dimensioned for a truck with similar engine specifications has been selected. The dataset included inertias, gear ratios and efficiencies (driving and coasting) values, as well as shifting schedules.

3.1.5.4 Differentials and Torque transfer case

For the front and rear differentials and for the central torque transfer case, regular open architectures have been chosen. Therefore, if we define the *Torque Bias Ratio (TBR)* for a general LSD differential as:

$$TBR = \frac{T_{high}}{T_{low}}$$

We can assume that the TBR for the used differentials and torque transfer case can be approximated to 1. In the test procedures analyzed in this thesis, since the vehicle is not engaged in any cornering event, a LSD differential would behave in the same way as an open differential, and the impact on the fuel consumption estimations would be negligible.

Therefore, the output torques and speeds are related to the input values by the following equations:

$$T_{left} = T_{right} = 0.5 \cdot T_{input} \cdot \eta_{diff}$$

$$\omega_{diff} = \frac{\omega_{left} + \omega_{right}}{2}$$

The differentials and torque transfer case specifications are summarized in the following table:

Table 4 - Differential and torque transfer case characteristics

| | Differential | Torque transfer case |
|--|---------------------|-----------------------------|
| Gear ratio | 4.4 | 1 |
| Stiffness | 80 | 80 |
| Damping | 0.8 | 0.8 |
| Efficiency ratio (driving) | 0.99 | 0.99 |
| Efficiency ratio (coasting) | 0.99 | 0.99 |
| Drive shaft spin inertia | 0.013 | - |
| Shaft to left wheel spin inertia | 0.009 | - |
| Shaft to right wheel spin inertia | 0.009 | - |
| Torque distribution | 50% | 50% |

3.1.6 Suspension and steering dataset

TruckSim math models support many different suspension design, using data that can be obtained from real or simulated kinematics and compliance tests. In TruckSim approach, detailed specifications as linkage geometry, bushing properties and so on are not needed, since the behavior of the suspension system and its impact on the vehicle response is described with more generic system-level parameters and nonlinear tables.

This approach reduces the number of suspension models to just a few types, based on fundamental kinematical behavior. The available math models for suspensions are two: *independent* and *solid axle*.

In an independent suspension the vertical movement of one wheel does not cause noticeable movement of the other wheel on the same axle (except in the case of the presence of a roll-bar).

In contrast, a solid axle suspension has an actual axle or linkage system that causes both wheels to roll together.

For the purpose of this simulations, an accurate modelling of the truck's suspensions is not required, since in any case we do not have any turning event, and the terrain is perfectly symmetric in relation to the longitudinal median plane of the vehicle.

Therefore, solid axle suspension type has been chosen for all three axles of the truck, setting the weight of the unsprung masses to 595 kilograms.

Regarding the steering system, similarly to suspensions, a standard 6 meters wheelbase steering system dataset has been chosen. The choice of the steering system does not affect at all the simulation, since the steering angle is always set to zero.

3.1.7 Simulink integration

As soon as the truck's model has been created and every dataset have been defined, the dataset related to the test procedures have been generated, defining the three different scenarios discussed in paragraph 2.4.

After that the simulated test specifications in the main dataset screen have been completely defined (both vehicle configuration and procedure), the next step was to set up the run control section.

In TruckSim, the data relative to the engine's fuel efficiency, necessary to calculate its fuel rate and the cumulative fuel mass consumed during the test, can be defined as a 2D look-up table which gives as an output the value of the instantaneous fuel rate, taking as inputs the throttle position and the current engine angular speed.

However, this way to proceed is inconvenient in our case. In fact, the fuel efficiency data available for the selected engine are in the form of a 2D look-up table that takes as inputs the engine output torque and its current angular speed, giving the fuel rate as an output. Therefore, in order to create the correct engine dataset for the fuel consumption calculation, a data conversion is required.

Furthermore, when the model relative to the hybrid configurations will be created, the throttle position value will no longer be uniquely associated with the engine's output torque. Therefore, TruckSim method for fuel consumption calculation will not provide accurate results.

Nevertheless, TruckSim provides the possibility to interact with Matlab-Simulink environment, as described in paragraph 2.3.2, and this allows to implement the aforementioned look-up table and calculate the fuel rate externally, using the available engine data, in a simple and efficient way.

Moreover, in a Simulink environment it is possible to acquire all the variables generated during the simulation run, and log them into the Matlab workspace. This can simplify the post processing and data analysis procedure, since all the variables of interest will be automatically recorded as Matlab arrays.

For these reasons, the TruckSim solver block has been included in a Simulink model, and a fuel consumption calculator subsystem has been defined as well. This subsystem takes as inputs the engine's angular speed and its output torque (which come from the TruckSim solver), and determines the current fuel rate by the 2D look-up table. This value is then integrated by an integrator block, obtaining the fuel mass consumed at every instant, as shown in the figure below:

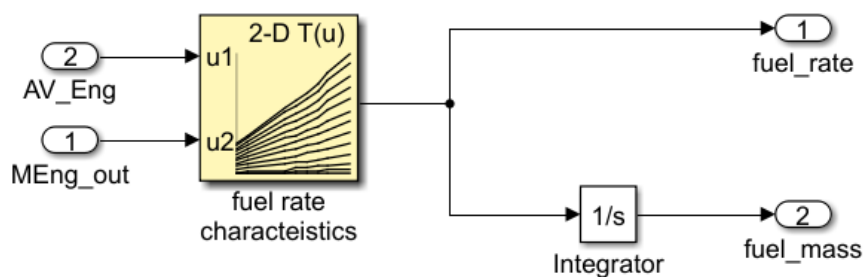


Figure 35 - Fuel consumption calculator subsystem

Additionally, other interesting quantities are calculated by the model:

- *Engine cumulated output mechanical energy*: obtained by integrating the engine power output, inferiorly saturated at zero:

$$E_{out} = \int_{t_0}^{t_{end}} P_{out_{pos}} \cdot dt$$

- *Engine instantaneous overall efficiency*: calculated by implementing the definition of overall efficiency:

$$\eta_u = \frac{P_{out}}{\dot{m}_{fuel} \cdot LHV}$$

- *Speed target deviation*: it expresses the difference between the target speed and the vehicle's actual speed.

In the next figure the complete Simulink model for the “Only-ICE” configuration is represented.

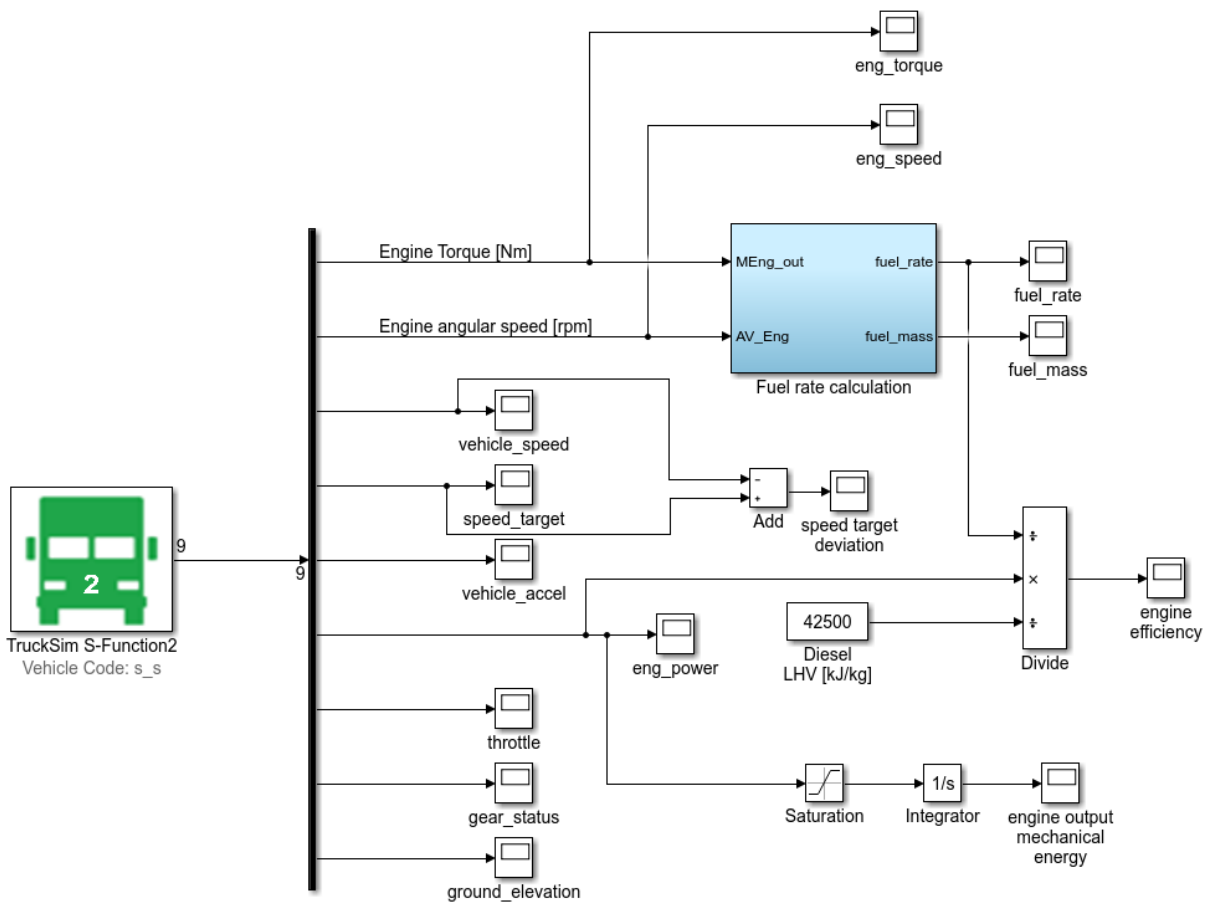


Figure 36 - External Simulink model for fuel calculation and data acquisition

3.1.8 Food delivery truck modeling

The second procedure that has been implemented in the model is the food delivery test, described in paragraph 2.4.3. The test consists of three identical urban-speed profiles interspersed with 10 minutes stops where the food delivery procedure happens.

In contrast with the previous simulations, the truck simulated in this test is a food delivery truck, equipped with a 10 kW refrigeration system, whose load cycle is characterized by 5 minutes of activity and 5 minutes of inactivity, as shown in the following figure.

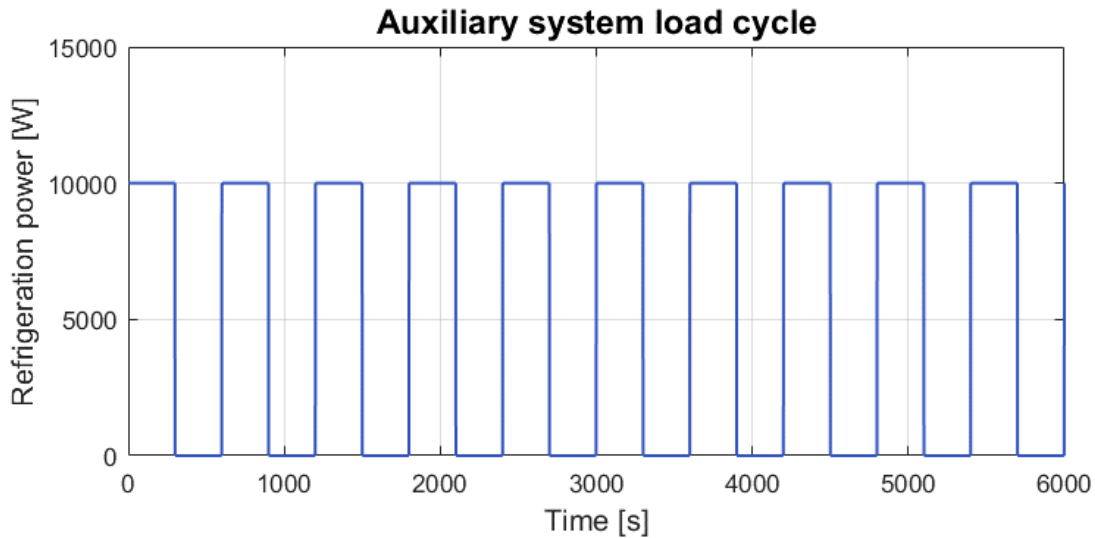


Figure 37 - Refrigeration system power load cycle

Since the standard configuration does not include high capacity batteries, the auxiliary system has to be powered directly from the internal combustion engine, which keeps running for all the duration of the test.

In order to perform this simulation, the Simulink model has been modified, including a subsystem that generates an external torque related to the auxiliary system.

Since in TruckSim is not possible to add an import channel to simulate a torque applied directly on the engine's crankshaft, the input torque has been referred to the four front wheels, as it follows:

$$T_{wheel} = - \frac{P_{aux} \cdot \tau_{diff} \tau_{gear} \cdot \delta_{brake}}{4}$$

Where δ_{brake} is a parameter which is equal to zero when the truck is performing a brake, and one in every other case. This prevents the system to become unstable during a braking maneuver.

The following figures show the modifications applied to the previous Simulink model in order to include the auxiliary devices (figure 43), and how the subsystem has been designed (figure 44).

3.2 Single electric motor hybrid configuration – component sizing

Once that the conventional vehicle model has been finalized, the subsequent step was to create the first hybrid configuration model in Simulink and integrate it with the TruckSim conventional vehicle model.

The Simulink model has to simulate all the mechanical and electrical components of the electric axle, taking as inputs the outputs generated by the TruckSim solver. Then, two torque signals are generated in Simulink, which represent the torque transferred at the two wheels of the third axle of the vehicle.

These signals are fed back into the TruckSim block, which adapts its parameter in order to chase the target speed profile defined into the procedure dataset. The goal of this paragraph is to describe the modelling phase of the first hybrid powertrain configuration (single EM).

3.2.1 Electric machine

As described in the previous paragraphs, this configuration is characterized by a hybrid driveline, in which the ICE is assisted by the action of an electric motor, coupled via a differential to the rear axle. As assessed by A. Khajepour, S. Fallah and A. Goodarzi in “Electric and Hybrid Vehicles”, the primary requirements and specifications associated with a proper selection of the electric motor are:

- To have a sufficient Hybridization Factor in order to provide an adequate assistance to the ICE and allow to achieve optimal fuel saving values. A range of HF which guarantees optimal performance is between 0,1 and 0,3 (Somà, Bruzzese, & Viglietti, 2015) (Buecheler, Bolvashenkov, & Herzgov, 2009);
- To provide high efficiency over wide speed and torque ranges for the reduction. This requisite is fundamental to avoid major energy losses when converting mechanical energy into electrical energy and vice versa, and thus enhancing overall fuel saving;
- To provide high controllability, high steady state accuracy and good dynamic performance;
- To provide sufficient robustness against high temperature, vibration and bad weather conditions.

Among all possible solutions available, we can distinguish different major types of electric machines:

- *DC motors*: these motors are characterized by a set of coils, a rotor, a commutator and optional brushes. The set of coils generates the magnetic field that provides the

torque. The best use of these motors is for short bursts of acceleration, however they may suffer from being heavy, not particularly efficient and relatively unreliable.

- *AC motors*: the structure of these motors is similar to DC motors, but there is no need for a commutator and brushes due to the periodic nature of the alternative current. These motors have the advantage of providing higher efficiency, they have lower operating costs, they are lighter and don't require high levels of maintenance. The main drawback of this solution is that it requires a more complex on board power electronic device. In fact, DC battery current has to be converted into AC current to feed the motor, and vice versa during generator mode.

3.2.1.1 HPEVS AC-51

Based on the previous requirements, the electric machine chosen to be equipped in the hybrid powertrain model was the AC-51 by HPEVS.

The HPEVS AC-51 is an 8'' alternative current electric machine, equipped with a Curtis 108 Volt controller, capable of producing a peak power of 55 kW and a peak torque of 204,2 Nm at 0 rpm. It can provide a maximum hybridization factor of 0,21. The specifications of the motor are summarized in the following table and graph:

Table 5 - HPEVS AC-51 specification (HPEVS, s.d.)

| | |
|------------------------|----------------------|
| Peak power | 55.53 kW at 2950 rpm |
| Peak torque | 204.2 Nm at 0 rpm |
| Peak DC current | 607.8 A |
| Battery voltage | 108 V |
| Weight | 52.2 kg |

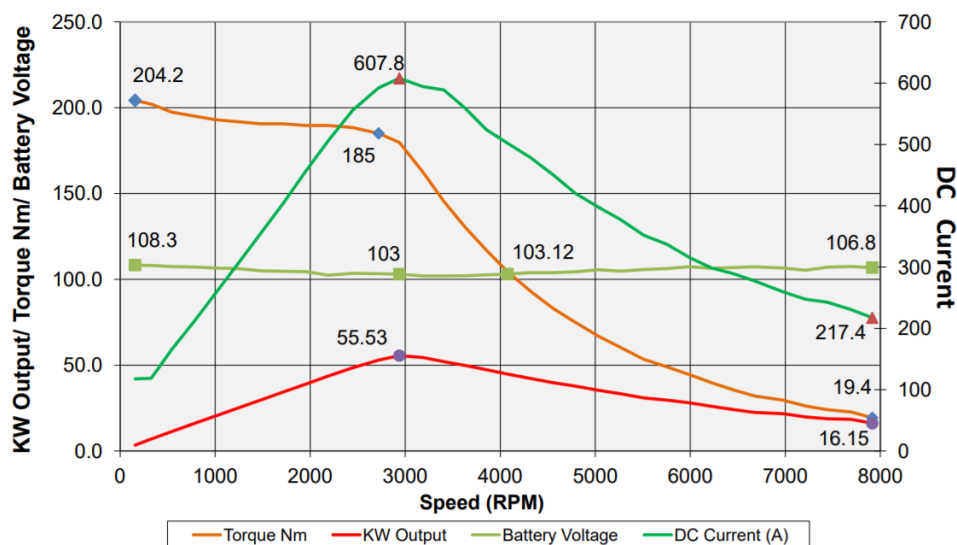


Figure 40 - HPEVS AC-51 characteristic curves (HPEVS, s.d.)

A fundamental quantity that characterizes the motor and has to be implemented in the Simulink model is the machine's efficiency.

Unfortunately the constructor does not provide an efficiency map for this model. However, this map can be estimated referring to similar machines with similar characteristics.

The following graph reports the actual machine's operating field (delimited by the two peak torque curves), and the estimated efficiency map.

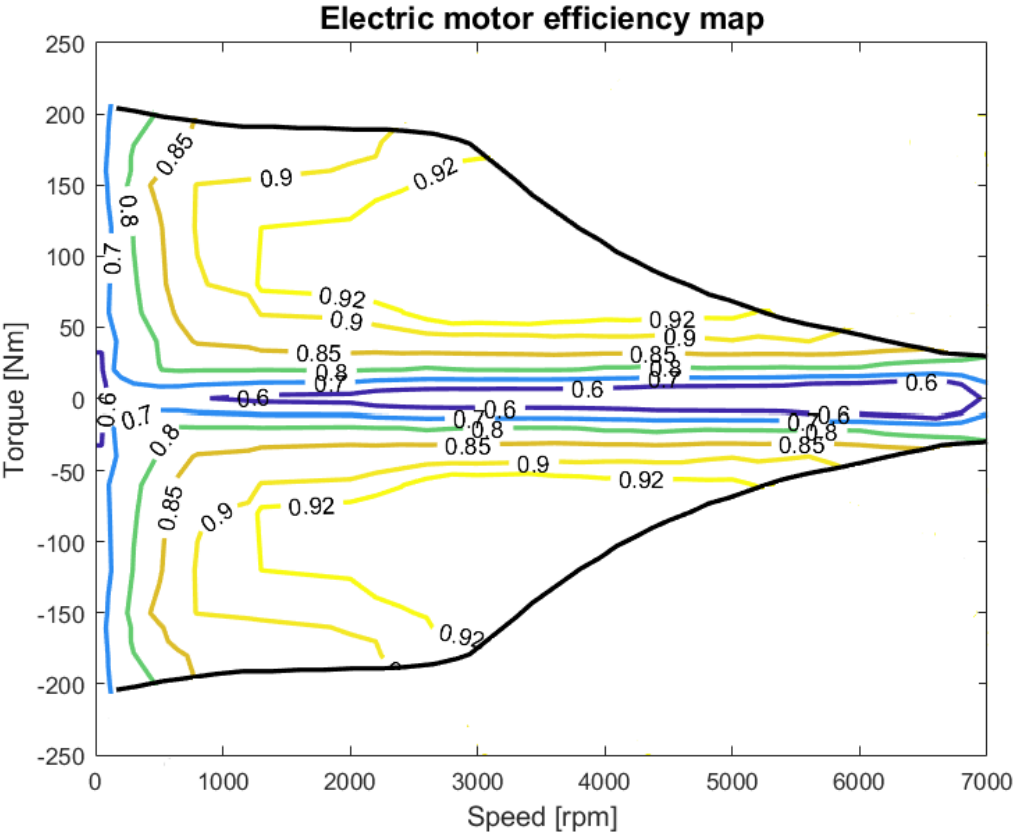


Figure 41 - AC-51 estimated efficiency map

3.2.1.2 Coupling with the differential

Once that the electric machine has been chosen, it is important to define how this machine will be coupled with the differential that is then responsible of delivering the traction to the wheels.

In particular, the main parameter that has to be defined is the gear ratio between the motor's pinion and the differential crown.

The criterion behind the determination of the gear ratio is ensuring that the speed range of the machine is included in the high efficiency area of the motor's map. At the same time, when the vehicle is at its top speed, the motor's angular speed should not outmatch its maximum speed.

Therefore, it is necessary to relate the motor's angular speed to the vehicle's longitudinal speed in the first place.

Assuming that the vehicle is not involved in any cornering event, if R is the radius of the rear wheels, the angular speed of the rear axle can be expressed as:

$$\omega_{rear\ axle} = \frac{v}{R}$$

This value coincides with the differential crown angular speed, since we have:

$$\omega_{diff} = \frac{\omega_{left} + \omega_{right}}{2}$$

Finally, we can express the motor's angular speed as:

$$\omega_{motor} = \tau \cdot \omega_{rear\ axle} = \tau \cdot \frac{v}{R} \rightarrow n_{motor} = \tau \cdot \frac{v}{2\pi R}$$

From the motor's efficiency map we can notice that the best values of efficiency are achieved at higher speeds. Therefore, it is possible to choose τ in order to match the vehicle's top speed (of 120 km/h) with the motor's maximum angular speed (8000 rpm).

Substituting those values in the previous equation and solving for τ , we obtain $\tau = 13,27$.

A reasonable value of τ that allows us to maximize the motor's efficiency and at the same time comply with the constraints in terms of maximum motor speed can be 12.

This value will be further verified once that the model is complete and the simulations are ran. At this stage, in fact, it will be possible to analyze the actual operating point of the motor.

3.2.2 Battery pack

A fundamental component of the system is the battery pack, which is the energy accumulation system used by the configuration to store energy and use it when necessary. Among all the technologies used for batteries in Hybrid Electric Vehicles, nowadays the most diffused one is represented by Lithium-Ion batteries.

This type of battery technology offers very high energy density, good high temperature performance, high specific energy and power and long cycle life.

For the purpose of this study, this parameters have been taken into consideration in order to properly size the battery pack:

- *Capacity*. It is a measure of the maximum energy that can be stored into the battery, usually expressed in [Wh] or its multiples. The battery has to be sufficiently capacious in order to ensure a good range of operation during the vehicle's advancement, and in order to avoid to reach the upper and lower boundaries for the battery's SOC.

The optimal range for the battery's SOC is represented in the following figure (Nelson, 2000)

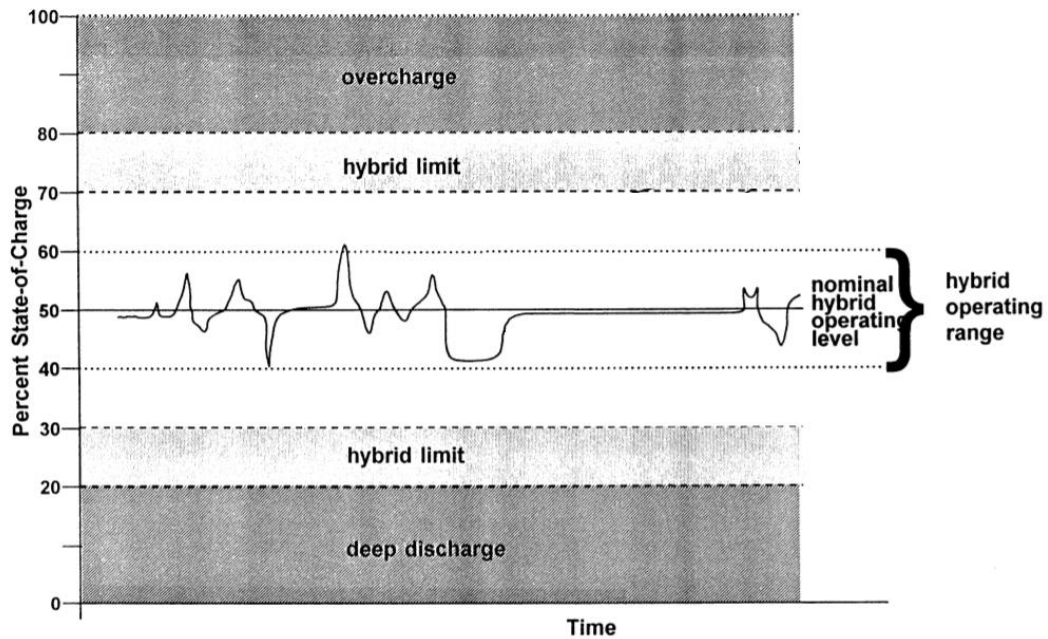


Figure 42 - SOC limits for hybrid powertrain battery (Nelson, 2000)

If the battery SOC exceeds the lower value of 30%, or the upper value of 80% it is necessary to intervene with specific power management strategies in order to restore the regular battery SOC. However, this operations reduce the capability of the system, so it is important to find a balance between the power management actions and the battery capacity.

- *Maximum power.* Every battery is capable of delivering or storing energy with a certain maximum rate. The current that the battery can handle in this processes is limited. Therefore, the electric machine's power could be limited by the maximum charge or discharge power imposed by the battery's characteristics.

This reduces the powertrain capabilities to influence the engine's operation and to increase its efficiency, and reduces the ability to store energy through regenerative braking.

Lithium-Ion batteries are composed by modules (or banks), made up by unitary cells. Cells are connected in series, so a single module delivers a voltage which is the sum of the voltage provided by the single cells.

Modules are connected in parallel. This allows to increase the battery capacity and the maximum charge and discharge power, but the total voltage remains equal to each module's voltage. The determination of the number of cells per bank, and the number of modules is conducted in parallel with the simulations, adopting an iterative approach. In this way, it is possible to converge to the optimal capacity and maximum power that allow to have good performances and an optimal operation between the two SOC boundaries.

3.3 Single electric motor hybrid configuration – modelling in Simulink

The step further to the choice of the components that constitute the electric axle (in particular the electric machine and the battery pack) was the realization of the hybrid powertrain in Simulink.

Then, once that the model has been completed and tested, the scenarios introduced in section 2.4 could be simulated and the results analyzed.

3.3.1 Electric machine

The first component that was modeled in Simulink was the electric machine (HPEVS AC-51).

This Simulink block has the task to calculate the torque and the power delivered or absorbed by the electric machine during its operation.

The machine can either work as a motor or generator, depending on the driving situation. When the machine works in motor mode, it delivers a positive torque to the rear axle and reduces the torque that the engine has to deliver in order to make the vehicle advance, following a particular speed profile.

When the machine works in generator mode, it delivers a negative torque (braking torque). Therefore, the torque required by the engine in order to follow that same speed profile increases.

Another situation during which the machine works in generator mode is regenerative braking. In this case, in fact, the braking torque produced by the generator is needed to reduce the amount of braking torque supplied by the conventional braking system. As a result, the battery SOC increases.

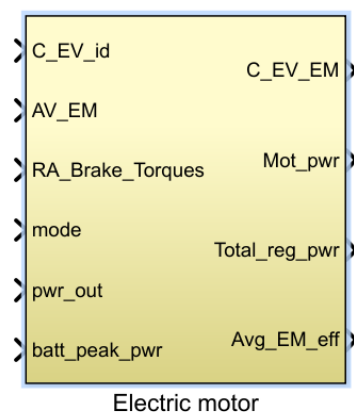


Figure 43 - Electric machine block

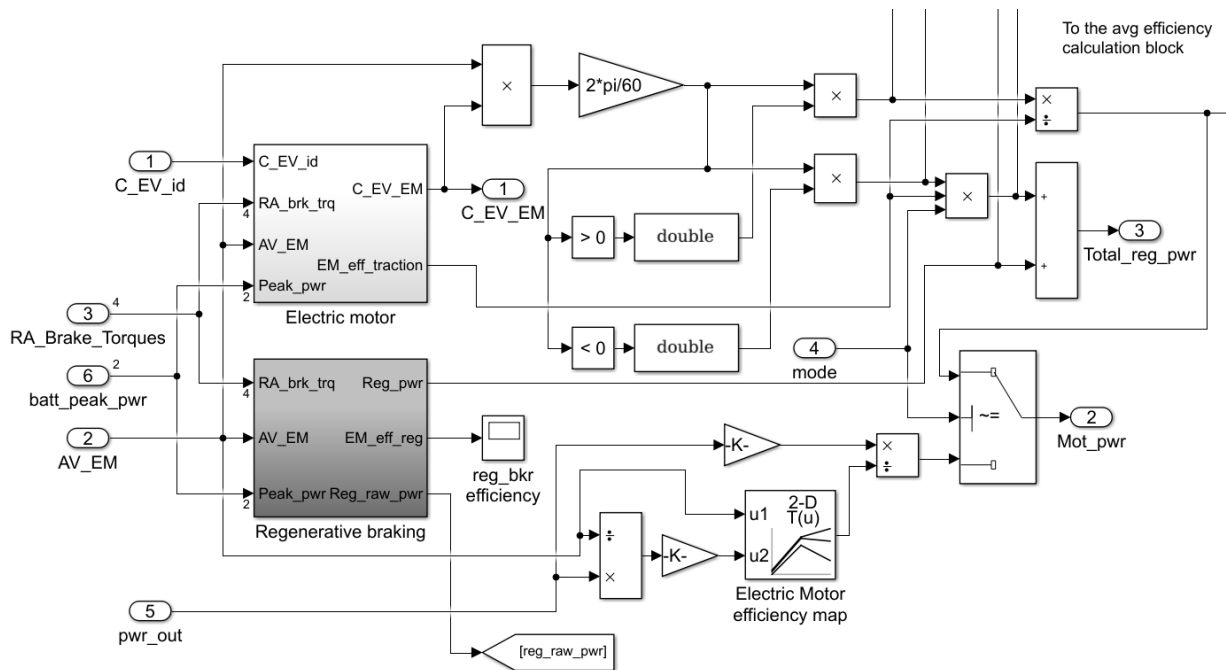


Figure 44 - Electric machine block design

The block inputs are:

- *Ideal electric torque (C_EV_id)*: this input represent the value of the ideal torque that the machine has to provide to the axle in order to fulfill the requirements of the power management.

However, sometimes this value cannot be achieved, because it exceeds the capabilities of the machine.

- *Angular Speed of the motor's pinion (AV_EM)*: in order to determine quantities such as mechanical or electric power delivered, or the machine's efficiency, it is important to know the motor's angular velocity.

This value is calculated in the rear differential block, as explained in section 3.2.1.2.

- *Rear Axle braking torque (RA_Brake_Torque)*: this quantity represents the overall braking torque delivered at the rear axles during a braking event. It is a TruckSim output and it refers to conventional braking. In the Simulink model, this value is used to determine the regenerative braking torque (which is a fraction of that quantity) that the electric machine is able to deliver.

It is to be noticed that with this approach the braking distribution between the front axle and the rear axle is not modified. The overall braking torque of the rear axle is

simply redistributed between conventional and regenerative braking, but the sum of the two values remains identical.

- *Mode*: this parameter represents an output from the power management block, and it defines the hybrid mode currently active.
- *Engine output power (pwr_out)*: this quantity is necessary when the mode selected is “full electric”. In this case, in fact, the model considers the power delivered by the engine as if it has been delivered by the electric motor.
- *Battery peak power (batt_peak_pwr)*: this value is needed to saturate the regenerative or motoric torque to the maximum value that produces the maximum current that the battery can manage.

The electric machine block includes three subsystem:

- *Electric motor*: this subsystem is necessary to calculate the machine’s efficiency, its torque and power delivered while functioning. Despite the block’s name, it calculates all these quantities both in motor and in generator mode.
- *Regenerative Braking*: this subsystem calculates the afore-mentioned quantities when the machine is operating in regenerative braking mode.
- *Average efficiency*: this block is used to calculate the average efficiency of the electric machine (in both modes) throughout the operating cycle. This value is important to evaluate the correct functioning of the electric machine, and is also necessary to determine the *equivalent fuel mass* in the battery block.

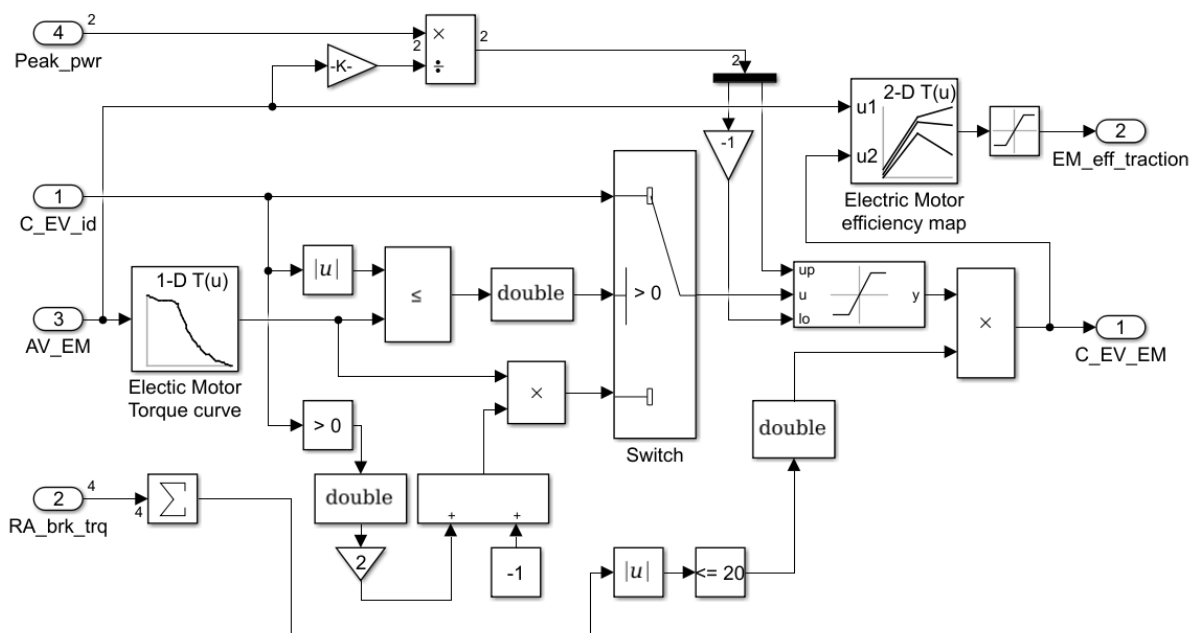


Figure 45 - Electric motor block design

The first subsystem that will be analyzed is the “Electric motor block” (Figure 45).

Going into details for what concerns this specific block, the first operation that is possible to highlight is the determination of the maximum torque that the machine can deliver for a given angular speed. This operation is carried on by a simple 1-D look-up table.

Then, the absolute value of the torque that the motor has to deliver (input C_EV_id) is compared with the calculated value of maximum torque by a logic operator (\leq). This element gives as an output a Boolean value of “1” if the statement is correct. Otherwise it returns “0”. This Boolean operator is then converted into a “double” value, and it constitute the discretional criterion for the subsequent switch block.

The switch allows to saturate the ideal request of electric torque to the maximum value that the machine is capable of delivering, both in motor and generator mode.

Then, another saturation block is added, in order to keep in account the maximum power that the battery can handle (calculated in the battery block). The peak power is a two dimensional vector that contains the values of the maximum power that the battery can absorb/deliver in charging/discharging mode.

These values are algebraically divided by the motor’s angular speed in order to obtain the maximum torque that the machine can process. The two obtained values of torque are used as constraints in a dynamic saturation block.

Furthermore, the output torque is set to zero if the vehicle is braking, and the machine switches to “regenerative braking mode”. To achieve this, the sum of the braking torque is simply confronted to a threshold value (20 Nm) by a Boolean operator. Its result is converted into a “double” signal and multiplied by the output torque.

Finally, this block calculates the current efficiency of the electric machine, using a 2-D look-up table, which takes as inputs the motor’s angular speed and its current torque.

This value is then given as an output in order to calculate the actual power drained or stored into the battery.

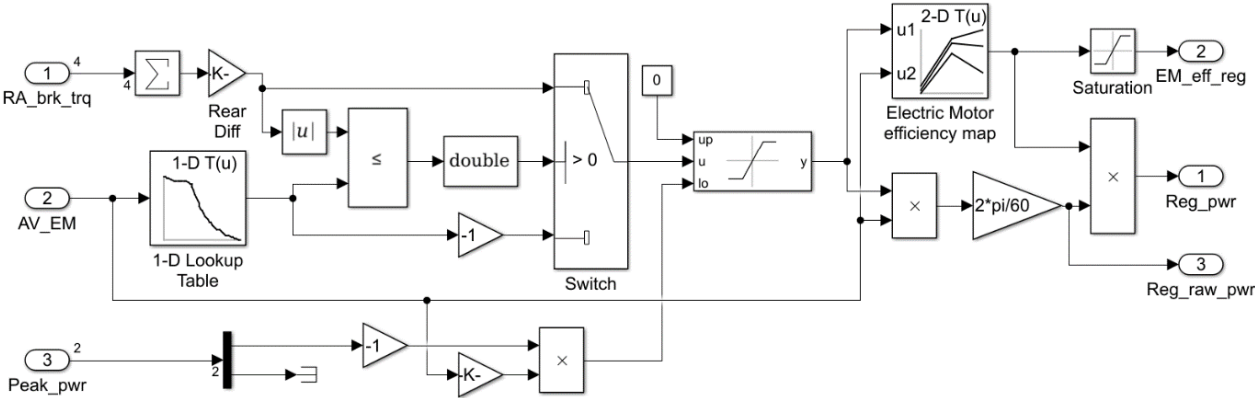


Figure 46 - Regenerative braking block design

The “Regenerative braking” block (Figure 46) is in all respects similar to the previous one. The main difference is that the input torque is the rear axle braking torque, divided by the conical gear ratio between the motor’s pinion and the crown differential.

This value of torque is then saturated to the maximum torque manageable by the electric machine and then to the maximum torque allowed by the battery, in the same way of the previous block. Finally, the generator efficiency is calculated using the same 2-D look-up table seen before, and the regenerative braking power is determined.

Once that the mechanical quantities related to the electric motor have been calculated, they are combined and processed in the main “Electric machine” block and given as output in the model.

Looking back at Figure 44, it is possible to see how the output torque from the first block is used to calculate the power delivered or absorbed by the electric motor, by the multiplication by the motor’s speed and the application a specific gain to match the physical dimensions.

Then, two Boolean operator determine the sign of the output power, in order to determine whether it is a tractive or a braking power. If it is a tractive power (>0), it is divided by the motor efficiency and then sent to a switch. If it is a braking power (<0), it is multiplied by the generator efficiency, added to the regenerative braking power and sent as an output (Total regenerative power).

Finally, it is possible to notice a “mode” input in the block. This input is equal to 0 if we are in full electric mode, and it is equal to 1 if we are in hybrid mode.

So, when the power management switches to *full electric mode*, the previous block are excluded from the calculation, and the output ICE power is treated as if it’s coming from the electric source. As in the previous cases, this power (which is only motoric) is divided by the engine efficiency and given as an output for the SOC calculation in the battery block.

The last block to be analyzed is the “Average efficiency” block (Figure 47), which is responsible of calculating the electric machine’s efficiencies both in motor and in generator mode.

The average motoric efficiency of the electric machine is calculated as:

$$\eta_{mot} = \frac{E_{mot}}{E_{batt_mot}}$$

Where E_{mot} is the mechanical energy delivered by the motor throughout the cycle, while E_{batt} is the electrical energy drained from the battery during the cycle. These two quantities are calculated by integrating the respective powers, which are inputs of the block:

$$E_{mot} = \int_0^{t_{fin}} P_{mot} dt \quad E_{batt_mot} = \int_0^{t_{fin}} P_{batt} dt$$

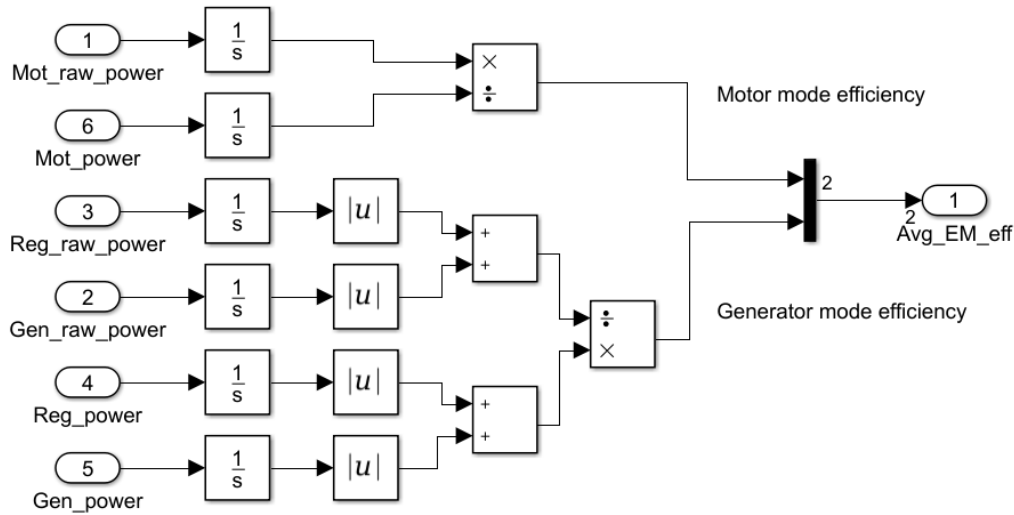


Figure 47 - Average efficiency calculation subsystem

For what regards the generator efficiency, this value is determined by the following equations:

$$\eta_{mot} = \frac{E_{batt_gen}}{E_{gen}}$$

Where E_{batt_gen} is the energy delivered to the batteries during the cycle, while E_{gen} is the mechanical energy introduced in the generator. These energies have to take into account both the functioning of the electric machine as a generator during the vehicle's advancement and the regenerative braking phase. So we have:

$$E_{gen} = \int_0^{t_{fin}} (P_{gen} + P_{reg})dt \quad E_{batt_mot} = \int_0^{t_{fin}} (P_{batt_gen} + P_{batt_reg})dt$$

The two efficiencies are then arranged in a two dimensions vector by a mux operator, and sent as an output.

3.3.2 Battery pack

The Battery block is responsible of simulating the battery functioning and calculating the main characteristic quantities related. The block takes as inputs the electrical power demand or supply from the electric machine block, and from eventual auxiliary devices blocks, as well as the electric machine's efficiency.

Starting from these quantities, it calculates the current that the battery delivers or receives, its voltage (both open circuit and terminal voltage), the peak power that the battery can handle and, primarily, the battery's SOC (State Of Charge).

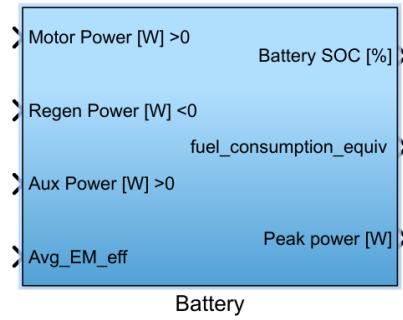


Figure 48 - Battery block

The block gives as output the Battery SOC in percentage, the equivalent fuel consumption and the peak power.

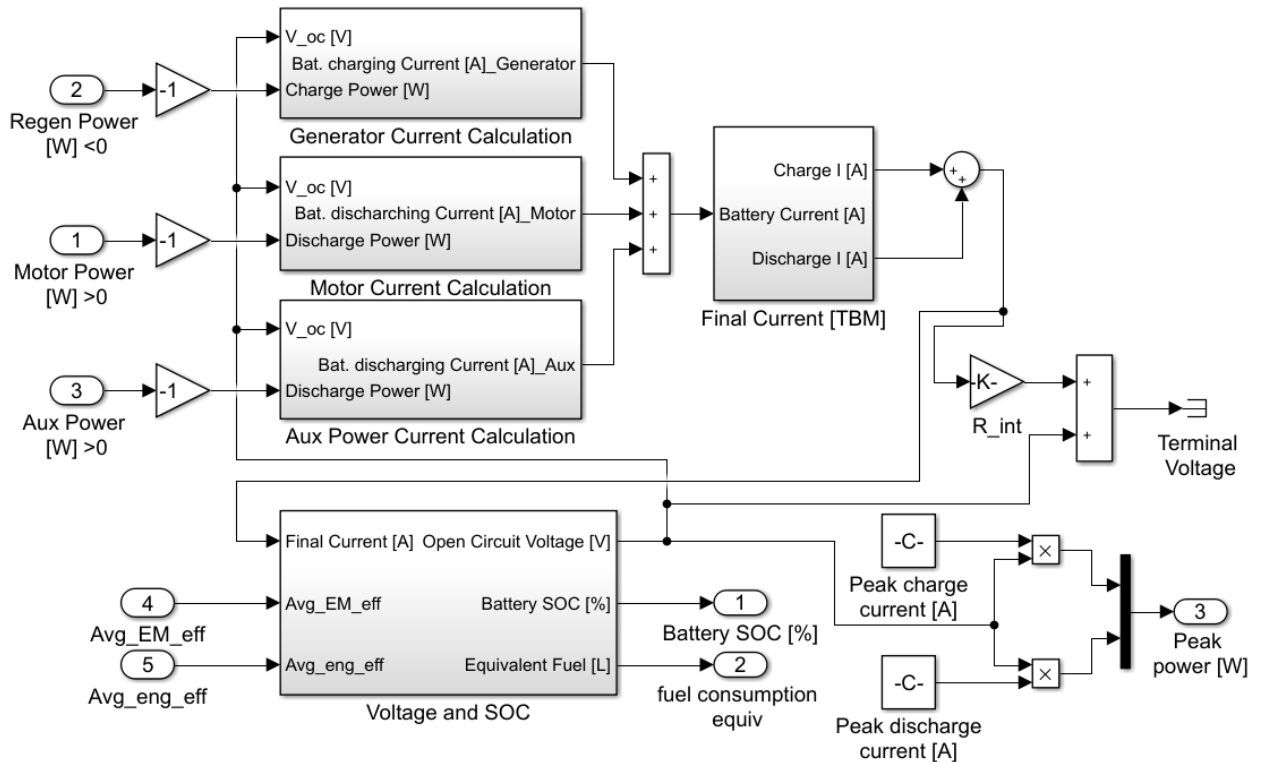


Figure 49 - Battery block design

Analyzing the battery model design (Figure 49), it is possible to notice the organization in different subsystems. In the top left part of the model we have three subsystems dedicated to the calculation of the current flowing from one pole to the other.

The circuit constituted by the battery and the electric machine can be schematized as it follows:

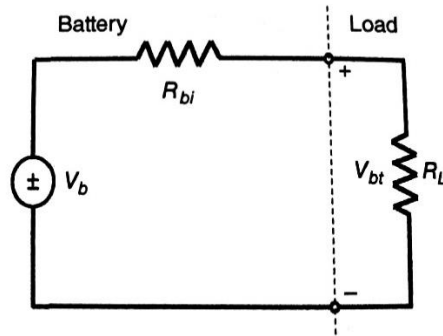


Figure 50 - Circuit schematic (Khajepour, Fallah, & Goodarzi, 2014)

The battery can be schematized by a voltage generator (V_b) and an internal resistance (R_{bi}), while the motor can be represented as an external load (R_L).

Applying Kirchhoff's voltage law to the circuit, we have:

$$V_{bt} + R_{bi}i - V_b = 0$$

Multiplying this equation by the terminal battery voltage (V_{bt}), and introducing the terminal battery power ($P_b = V_{bt}i$) we have:

$$V_{bt}^2 + R_{bi}V_{bt}i - V_bV_{bt} = 0 \rightarrow V_{bt}^2 + R_{bi}P_b - V_bV_{bt} = 0 \rightarrow V_{bt} = \frac{V_b \pm \sqrt{V_b^2 - 4R_{bi}P_b}}{2}$$

Using Ohm's law and assuming constant internal resistance, we achieve the current flowing in the circuit:

$$i = \frac{V_b \pm \sqrt{V_b^2 - 4R_{bi}P_b}}{2R_{bi}}$$

Modelling this equation in Simulink we obtain:

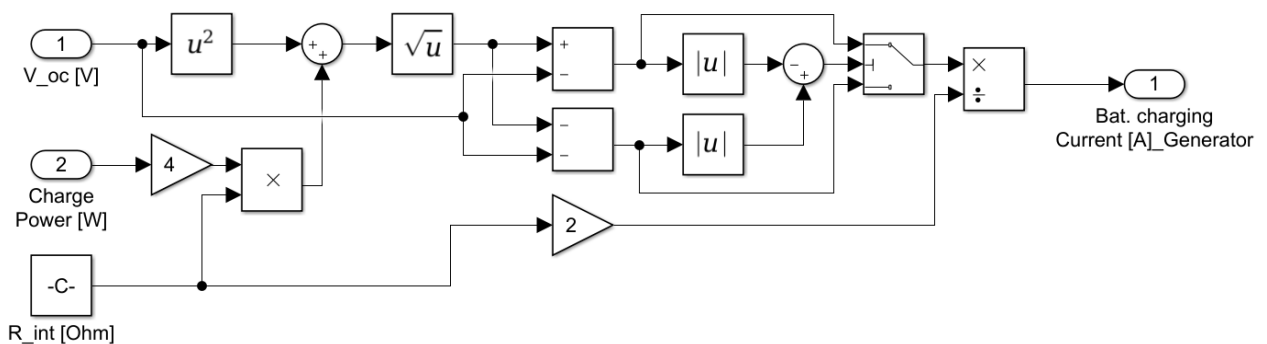


Figure 51 - Current calculator block

After that the current has been calculated, the three contributions from the motoric and generation phase and the auxiliary device are added up together and sent to the next block.

The aim of this subsystem is to saturate the current calculated to the peak current manageable by the battery, and to split it into charge current (positive) and discharge current (negative):

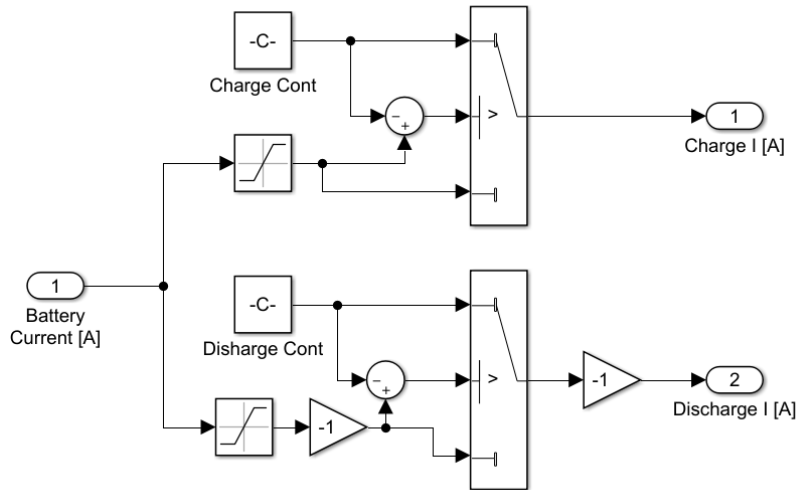


Figure 52 - Current saturation block

Finally, the last subsystem is necessary to determine the battery open voltage, the state of charge (SOC), and the equivalent fuel consumption.

The State of Charge is a measure of the residual capacity of a battery after the discharge from the fully charged condition. It is expressed as a percentage of the battery capacity, which unit of measurement is the same of an energy (Joule [J] or typically Kilowatt-hours [kWh]).

The first step of the calculation is to determine the amount of energy delivered or stored from the beginning of the cycle, and add it up to the initial energy available.

To do so, the cumulative energy is calculated as:

$$E_b = \int_{t_0}^{t_{fin}} P_b dt = \int_{t_0}^{t_{fin}} i \cdot V_b dt$$

Then, using a sum and a memory block, the ΔE for every iteration is determined, and it is added up to the initial energy contained in the battery.

Finally, the total energy is divided by the *battery rated capacity* and then converted into a percentage, obtaining the SOC:

$$\Delta E_i = E_{b_i} - E_{b_{i-1}} \quad E_{batt} = E_{init} + \sum_i \Delta E_i$$

$$SOC = 100 \cdot \frac{E_{batt}}{C_{batt}} [\%]$$

The Battery SOC is given as an output of the block, and it is also used to determine the open circuit voltage (V_b). This calculation is done implementing a 1-D look up table which contains the empirical relation between the battery voltage and its state of charge.

The last quantity that the block calculates is the *equivalent fuel consumption*. This parameter represents the amount of fuel energetically equivalent to the energy stored or drained from the battery during the test. This value is calculated as it follows:

$$\begin{cases} m_{feq} = \frac{\Delta E_{batt} \cdot H_i}{\eta_{avg_{eng}}} & \Delta E_{batt} > 0 \\ m_{feq} = \Delta E_{batt} \cdot H_i \cdot \eta_{avg_{discharge}} & \Delta E_{batt} < 0 \end{cases}$$

$$\Delta E_{batt} = E_{batt_{fin}} - E_{batt_{in}}$$

We notice that if we have an overall excessive energy storing throughout the test cycle, it can be used to power the vehicle with an efficiency that can be estimated as the average discharging efficiency of the electric motor.

However, if $\Delta E_{batt} < 0$, we would have to charge the battery in order to restore the initial SOC. This operation involves the engine efficiency, which can be estimated as the average engine efficiency throughout the cycle.

The following figure reports the final design of the SOC calculation subsystem.

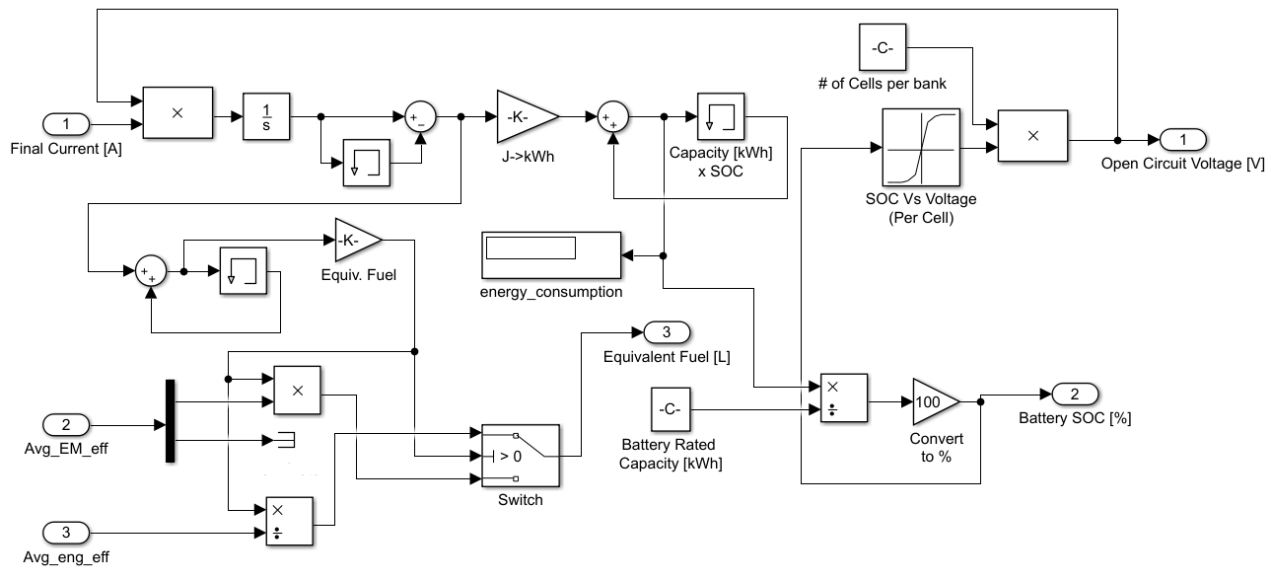


Figure 53 - State Of Charge calculation subsystem

3.3.3 Power management

The term “power management” refers to the design of the higher-level control algorithm that determines the power flows between the power sources.

Different power control strategies can be used to regulate the power flow to and from different components. These strategies can be addressed to satisfy four key goals (Chau & Wong, 2002):

- Maximum fuel economy;
- Minimum emissions;
- Minimum system costs;
- Good driving performance.

In this model, the main goal of the power management strategy was to maximize the fuel economy, and minimizing the size of the electrical components, reducing the system cost. Emissions and drivability were not taken into account in this preliminary modelling procedure.

3.3.3.1 Optimal engine operating points

The strategy implemented in this model is simple and based on a static optimization method. As discussed in paragraph 1.6.1, an ICE’s operating points vary during the vehicle’s advancement, and most of the times the ICE does not operate at its optimal efficiency. So, if the engine is operating above the optimum curve, the electric axle can work in motoric mode, delivering a tractive positive torque to the rear wheels. This reduces the amount of torque that the engine has to provide in order to match the external torque demand, and the operating point shifts towards the optimum curve.

On the other hand, if the engine is working below the optimum curve, the electric axle switches in generator mode, imposing a braking negative torque to the rear wheels. In order to provide the same amount of torque to match the external demand, the engine has to increase its load and even in this case the operating point shifts closer to its optimal value.

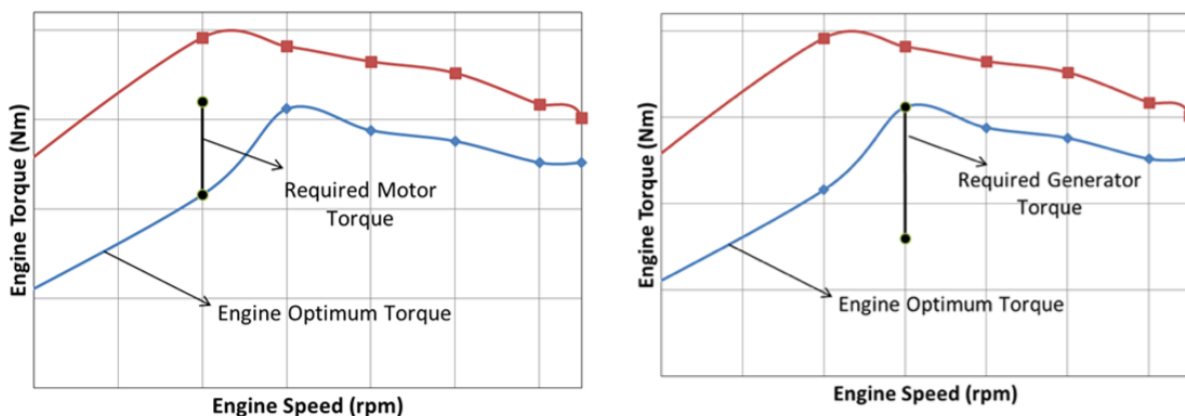


Figure 54 - Optimization of the engine's operating points strategy

To determine the amount of ideal torque that the electric axle has to provide in order to follow this strategy, two quantities are required at any given time:

- *External torque demand*: this is the value of the overall torque needed to follow the target speed profile.
- *Optimal torque*: this is the value of torque which guarantees the optimal efficiency for a given angular speed.

The *external torque demand* can be estimated using different approaches. It is possible to calculate it in analytical ways, as described in paragraph 1.6.1, but in this case another approach has been used. Since different models have been realized for all the different driving situations and architectures, it is possible to run a simulation using the only-ICE architecture model for a certain procedure, and log the output engine torque.

The torque profile acquired corresponds to the external torque demand to follow that exact procedure test.

Obviously in a power management strategy that will be implemented in the vehicle’s on board electronics this is not the correct strategy. In this case, in fact, an analytical calculation or an estimate based on look-up table is necessary. For the aim of this work, the approach previously described was implemented.

Regarding the *optimal torque*, this quantity is defined by a simple 1-D look-up table, giving as input the engine’s crankshaft rotating speed.

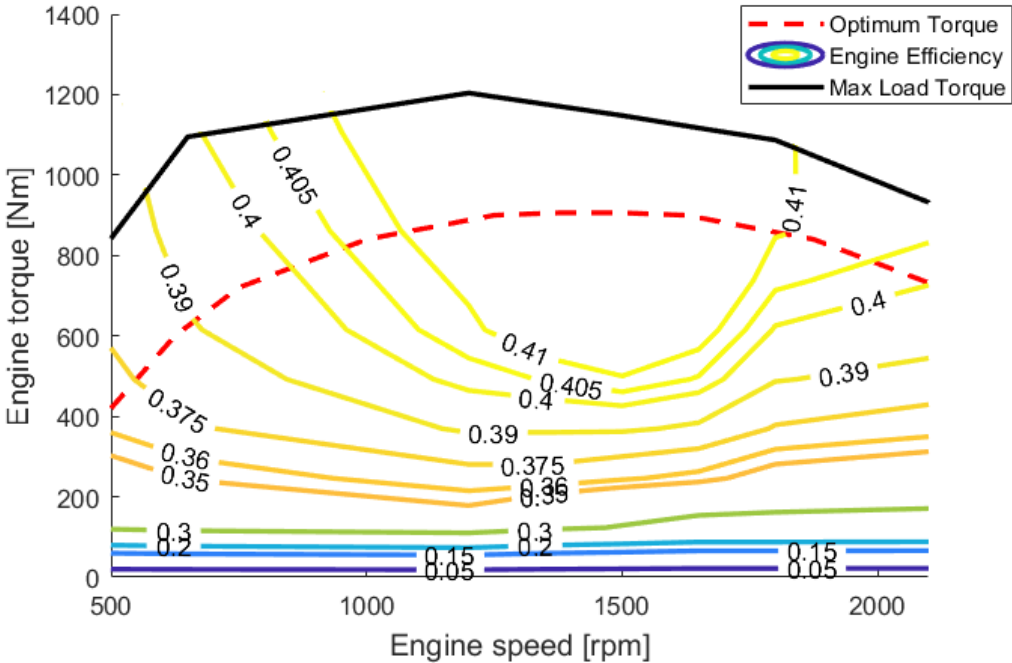


Figure 55 - Optimum engine torque curve

However, in hybrid mode, the optimal torque curve could be inappropriate for some types of driving situations. Since the highest engine efficiencies are achieved at higher loads, it can

happen that the optimal torque is always too high, while the engine load is relatively low, for example in a city speed profile. This will result in an excess of energy stored in the batteries, and therefore an excessive increase of the battery's SOC.

So, a multiplying factor has been introduced (*a*), which multiplies the optimal torque curve and scales it in order to stabilize the SOC to a goal value. Another method to reduce the SOC when the optimal torque is too high is to switch frequently to full electric mode when the vehicle is travelling at idling or low speed conditions, taking advantage of the energy previously collected at higher efficiency and reducing the SOC.

The ideal electric torque is then calculated as:

$$C_{EV_{id}} = C_{ext} - a \cdot C_{opt}$$

The obtained value is then processed according to different operating strategies that will be described below.

3.3.3.2 SOC control strategies

According to the battery's specifications, it is necessary that its SOC remains controlled in a specific range. Therefore, if during the cycle the SOC goes below 25% or above 90%, the ideal torque calculated is processed in order to force the SOC to remain in the selected range.

To do so, three parameters have been introduced: a *gain*, and two *boundaries* (upper and lower). The following table describes the choice of these parameters corresponding to the different situations:

Table 6 - SOC control strategy parameters

| Condition | Gain | Upper boundary | Lower boundary |
|--------------------------------|------|----------------|----------------|
| $SOC < SOC_{min}$ | 1.2 | 0 | N.D. |
| $SOC_{min} < SOC < SOC_{norm}$ | 1 | 100 | N.D. |
| $SOC_{norm} < SOC < SOC_{max}$ | 1 | N.D. | 100 |
| $SOC > SOC_{max}$ | 1.2 | N.D. | 0 |

If the SOC is too low ($< SOC_{min}$), the torque is limited to negative values (it is only possible to apply an electric braking torque that will charge the battery, and it is not possible to drain energy from the battery). Furthermore, the amount of braking torque is raised by 20% (gain=1.2).

If the SOC is between SOC_{min} and SOC_{norm} , the system sets an upper boundary for the motoric torque to 100 Nm (related to the engine's rotating speed), and restores the gain to 1. If the

SOC is included in the regular operating range ($SOC_{norm} < SOC < SOC_{max}$) there are no boundaries to the torque and the gain is unitary. If the SOC overcomes the SOC_{max} it will be only possible to exert a motoric torque. Therefore the lower boundary is set to 0 and the motoric torque is boosted by 20% in order to favor the battery discharge.

3.3.3.3 Powertrain mode selection

Another task for the power management subsystem is to define the vehicle’s driving mode between electric only and hybrid mode.

In the first mode the engine is shut off and the power is delivered only by the electric motor, exploiting the charge stored in the batteries. The charge is restored when the vehicle switches again to hybrid mode, by shifting up the engine’s load.

This allows to eliminate the engine’s operating points in the lower loads, increasing the engine’s efficiency. Moreover, this strategy allows to remove the idling phase.

So, the subsystem will give as an output a parameter called “mode”, which is equal to zero during the full electric mode, and equal to one in hybrid mode.

This parameter will multiply the output signals of the TruckSim model, in order to simulate the engine turning off, such as the engine output torque and power, and the fuel rate.

Furthermore, if this parameter switches to zero, the required power to follow the speed profile defined in the test procedure (which is the engine’s output power coming from TruckSim) will come from the electric machine.

So, the motoric power that goes into the battery block will switch to this value, corrected by the motor’s efficiency, as described in section 3.3.1.

The input parameter that define the powertrain mode are:

- Vehicle’s speed;
- Required power;
- Current mode.

Table 7 - Powertrain mode selection strategy

| Current mode | Vehicle’s speed | Required power | Next mode |
|--------------|-----------------|--------------------------------|-----------|
| 1 | >20 km/h | - | 1 |
| 1 | <20 km/h | > 90% of motor’s maximum power | 1 |
| 1 | <20 km/h | < 90% of motor’s maximum power | 0 |
| 0 | >30 km/h | - | 1 |
| 0 | <30 km/h | > motor’s maximum power | 1 |
| 0 | <30 km/h | < motor’s maximum power | 0 |

As it is explained in table 7, if the vehicle’s speed drops below 20 km/h and the required power (which can be related to the throttle pedal position) is less than 90% of the electric motor’s power, the powertrain switches to electric mode.

Once that the mode is 0, in order to switch back to hybrid mode, the vehicle’s speed has to raise to at least 30 km/h, or the required power has to overcome the maximum power that the electric motor can provide. This prevents the mode to flicker from 0 to 1 an excessive number of time when the threshold values of speed and torque are reached.

3.3.3.4 Simulink model

Once that the power management strategies have been defined, it was possible to implement the subsystem in the Simulink model.

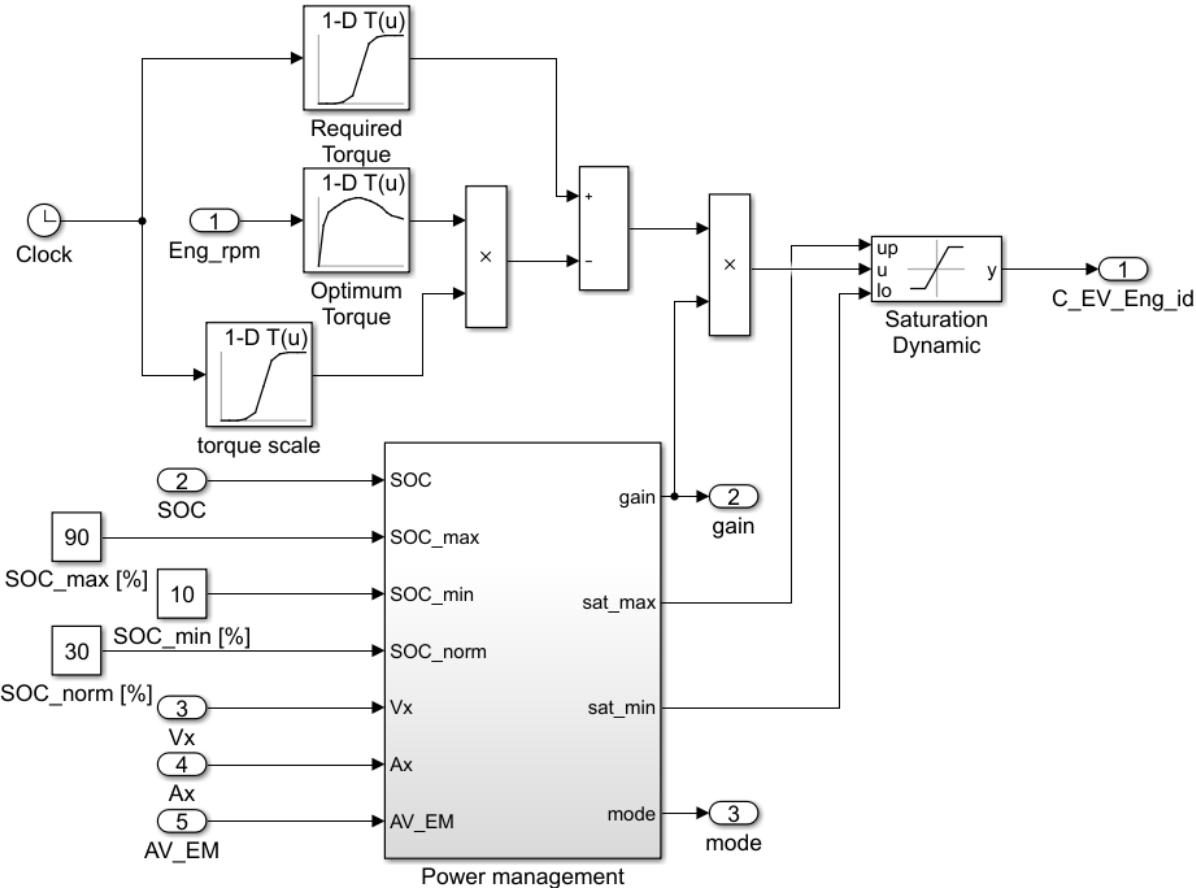


Figure 56 - Power management subsystem

The required torque value is given by a 1-D look-up table that contains the required torque profile, obtained by launching a simulation of the system where have been previously disconnected the input torque signals, and logging the output engine torque.

The optimum torque curve is implemented in another 1-D look-up table, which takes as an input the current engine rpm. The torque scale parameter is needed to scale the optimum torque curve, in order to balance the battery SOC and avoid abnormal behavior of the system.

The ideal torque referred to the engine’s angular speed is obtained as described in section 3.3.3.1, and is later multiplied by the gain and saturated by two external boundaries, calculated in a further subsystem.

This subsystem is organized in two sections: the first is dedicated to limit the ideal torque in order to implement SOC control strategies, as explained in paragraph 3.3.3.2, and the second section’s task is to define the powertrain’s operating mode.

The Simulink modelling of this subsystem is reported below:

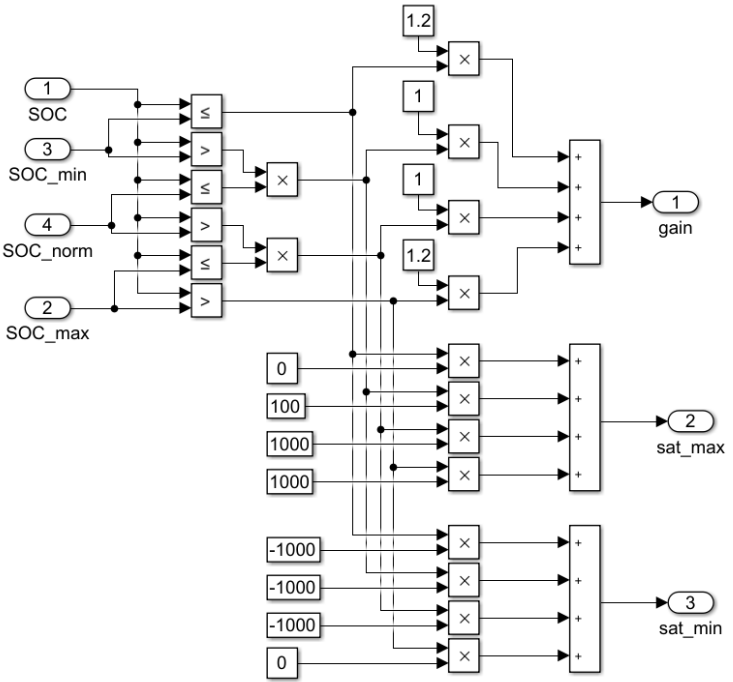


Figure 57 - SOC control strategy subsystem

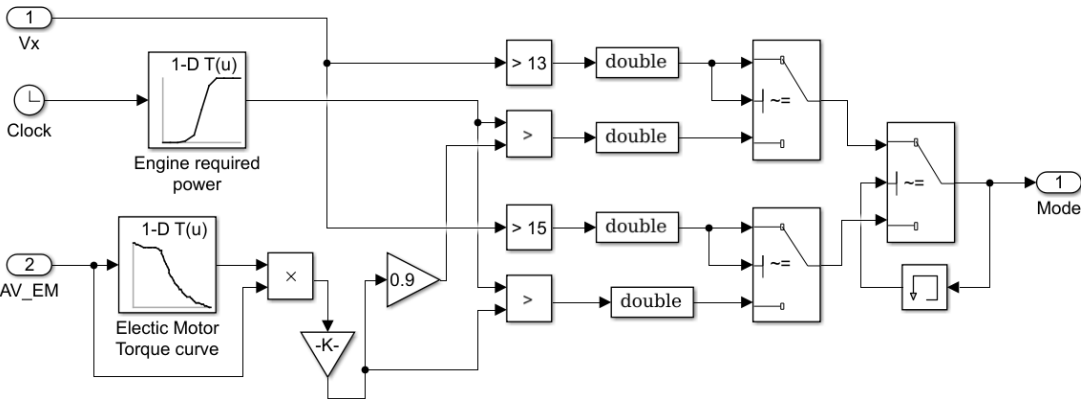


Figure 58 - Powertrain mode selection subsystem

3.3.4 Model assembling

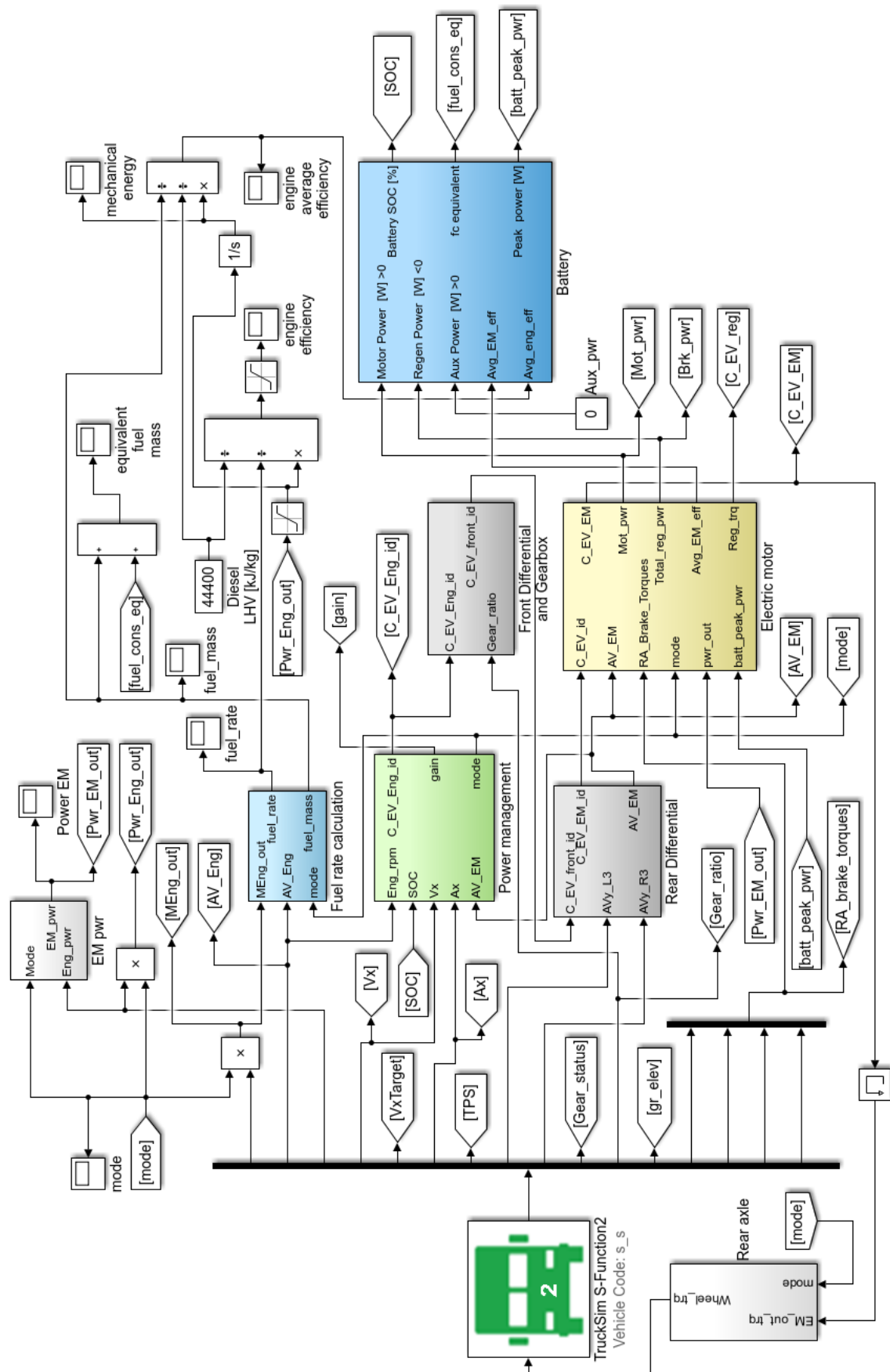


Figure 59 - Assembled Simulink model

Figure 59 reports the assembled Simulink model that simulates the complete hybrid powertrain. The signal flow can be summarized as it follows.

The TruckSim solver gives several variables as outputs, some of them are sent to signal scopes by “GoTo” flags, in order to be saved to the Matlab workspace and then processed, and some of them are sent to the model’s subsystems.

The power management block receives the engine’s rotational speed, the longitudinal speed of the vehicle and its acceleration, as well as the battery SOC (fed back from the battery model). It processes those signals as it is described in section 3.3.3 and gives as outputs the ideal electric torque referred to the engine’s rotational speed and the operating mode.

The ideal electric torque is referred to the front wheels’ speed by the front differential and gearbox block, and then to the electric machine speed by the rear differential block. The two differential block configurations are represented in the following figures:

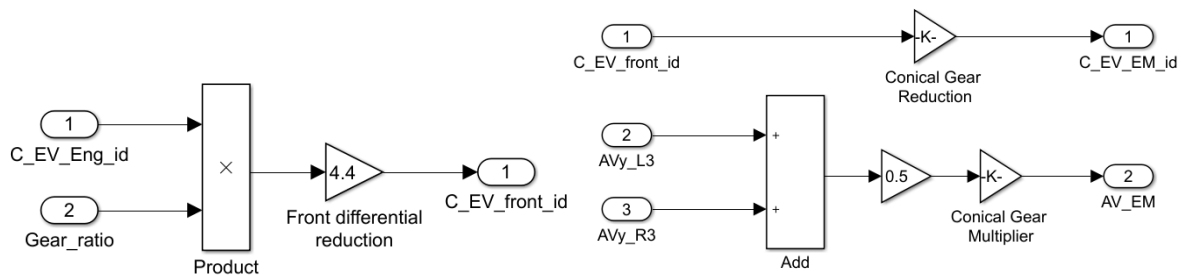


Figure 60 - Front and rear differential schematic

This value of torque is still ideal, and is sent to the Electric machine block, where it is processed according to the constraints imposed by the characteristic of the electric machine and the battery, as described in section 3.3.1. This block receives as input also the braking torque coming from TruckSim, in order to simulate the regenerative braking.

This block gives as outputs the actual electric torque, as well as the motoric and brake power, and its average efficiency (both in charging and discharging mode).

The electric torque is referred to the wheels by considering the rear differential gear reduction ratio (in the “rear axle subsystem”), and it is fed back into the TruckSim solver as a 2D input signal. The motoric and brake power as well as the efficiency are sent to the battery block.

The battery block processes these signals and determines the SOC, the equivalent fuel consumption and the peak power manageable. The SOC and the peak power are fed back respectively to the power management block and to the electric machine block, while the equivalent fuel consumption is sent to the workspace.

Finally, the fuel consumption calculation block calculates the fuel rate of the vehicle and the fuel consumption, in the same way as explained in section 3.1.7.

3.3.5 Food delivery hybrid truck modelling

The next step of the modelling procedure was to create another Simulink model to simulate the food delivery truck, in the same way as it was done for the previous only-ICE model.

The food delivery model differs from the first one by the presence of the “Auxiliary device” block, which simulates the power absorption by the external refrigeration system.

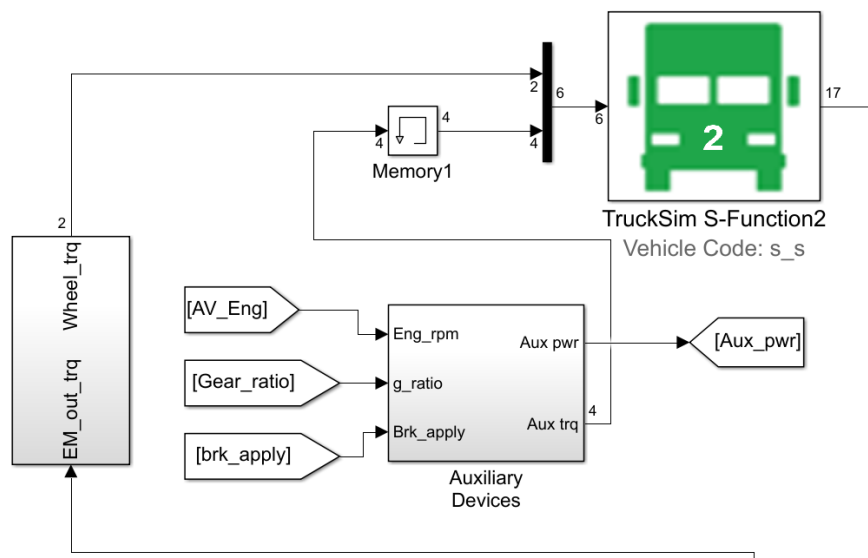


Figure 61 - Auxiliary Device block

The block is identical to the one discussed in paragraph 3.1.8, and the torque calculated are concatenated to the hybrid powertrain output signal by a mux operator, and then fed into the TruckSim solver.

Another modification to the system was the introduction of a new auxiliary power source that is connected to the battery block and simulates the power absorption during the stop and it causes a further discharge of the battery.

Furthermore, to simulate the vehicle shutdown, a new parameter has been introduced, called “torque gain”. This parameter is obtained by connecting a clock to a 1-D look-up table, and it is equal to 1 when the engine is on, while it is set to 0 during the stops.

This parameter is then multiplied by the engine output power and its output torque, as well as to the fuel rate.

Regarding the auxiliary power absorption, instead, a complementary parameter is calculated and multiplied to the auxiliary power. This new parameter is equal to 0 when the engine is on, so the power is drained directly from the internal combustion engine, and is set to 1 when the engine is off, redirecting the power flow towards the battery and draining it.

3.4 Wheel motors hybrid configuration – component sizing

After the modelling of the first hybrid configuration, the next step was to create a model for the second architecture, modifying the previous model which was taken as a base.

However, before starting to model the architecture in Simulink, it was necessary to define and size the main components of the electric axle.

3.4.1 Electric machine

The main differences between this architecture and the previous one are the number and type of electric machines, their disposition and their connection to the wheels.

This solution involves two wheel motors which are directly connected to the wheels, with no gear reduction.

Therefore, the electric machine should be able to deliver a much higher amount of torque at low speeds, and they don't require high performances at high speeds.

The absence of the differential is an advantage in terms of overall mechanical efficiency of the electric powertrain, and because there is a greater number of degrees of freedom of the system. In fact, each wheel is completely independent and driven by a specific motor, so this powertrain opens to various possibility of torque vectoring that weren't possible in the previous architecture.

Regarding the electric motor type, the ideal solution is represented by so called "frameless motors". These motors are sold as a package in which the rotor and the stator are separate and can be assembled later. The manufacturer will then design a specific case for the two components and will embed it in the machine.

These motors are meant to work as spindle motors, but their specifications fit the requirements researched for this application.

3.4.1.1 Rexroth IndraDyn H MBS272D

The electric machine chosen for this architecture was the IndraDyn H MBS272D, by the Bosch-Rexroth group.

This motor represents the state-of-the art for high-torque synchronous frameless motors, and it consists of a stator with a three-phase winding and a rotor with permanent magnets.

This solution embeds a cooling system which is self-contained in the motor, increasing the cooling efficiency and capacity. The next table resumes the specifications of the motors (Bosch Rexroth, 2018):

Table 8 - Wheel motor characteristics

| | |
|----------------------------|------------|
| Rated torque | 525 [Nm] |
| Rated speed | 500 [rpm] |
| Rated power | 27,5 [kW] |
| Rated current | 71 [A] |
| Maximum torque | 1200 [Nm] |
| Maximum current | 200 [A] |
| Maximum speed | 2000 [rpm] |
| Constant DC voltage | 620 [V] |

The motor's efficiency map has been estimated referring to similar machines with similar characteristics, as for the first solution.

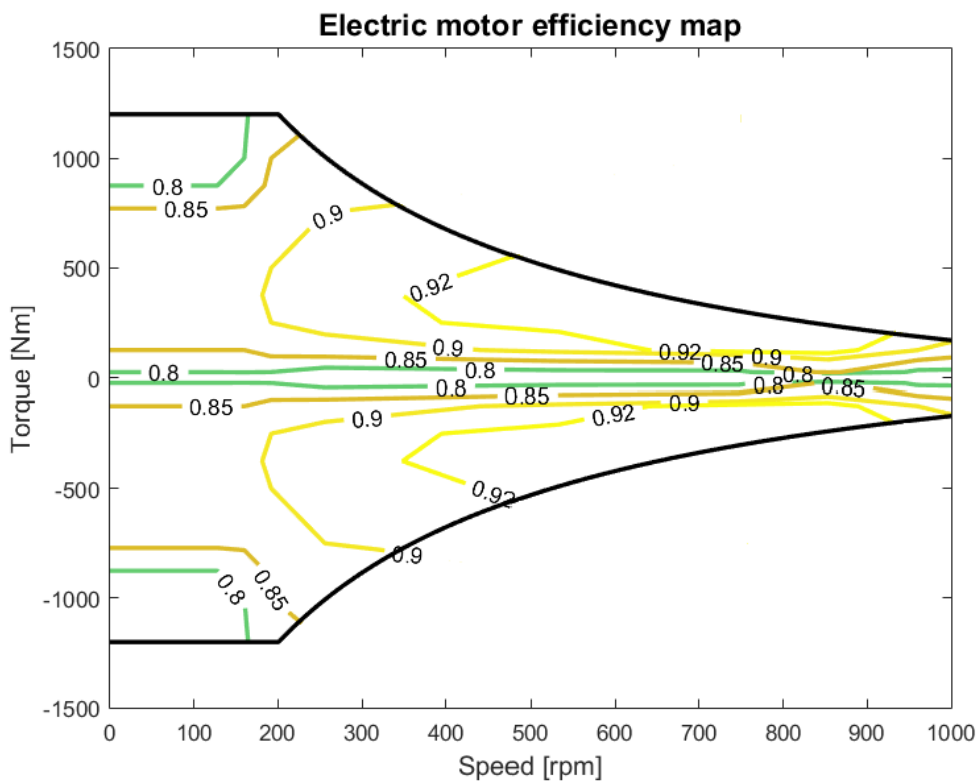


Figure 62 - wheel motors efficiency map

3.5 Wheel motors hybrid configuration – modelling in Simulink

In order to create the Simulink model, the single electric motor model has been taken as a starting point. The main difference between the two models is related to the electric machine and the mechanical connection to the wheels.

While in the first architecture model a “rear differential” block was implemented, in this model that block is missing. Therefore, the output angular speeds of the rear wheels from the TruckSim model are concatenated into a vector using a mux block and they are fed into the “wheel motors” subsystem.

Furthermore, the “rear differential” subsystem of the previous model was responsible of reducing the ideal torque in order to refer it to the electric motor speed. In this model this step is missing, because the torque that the two wheel motors have to deliver has to be referred to the rear wheels’ angular speed. So, the calculated ideal torque from the power management (C_EV_id) is directly sent as an input of the “wheel motors” subsystem, after being referred to the rear wheels.

The “wheel motors” subsystem design is represented in the following figure:

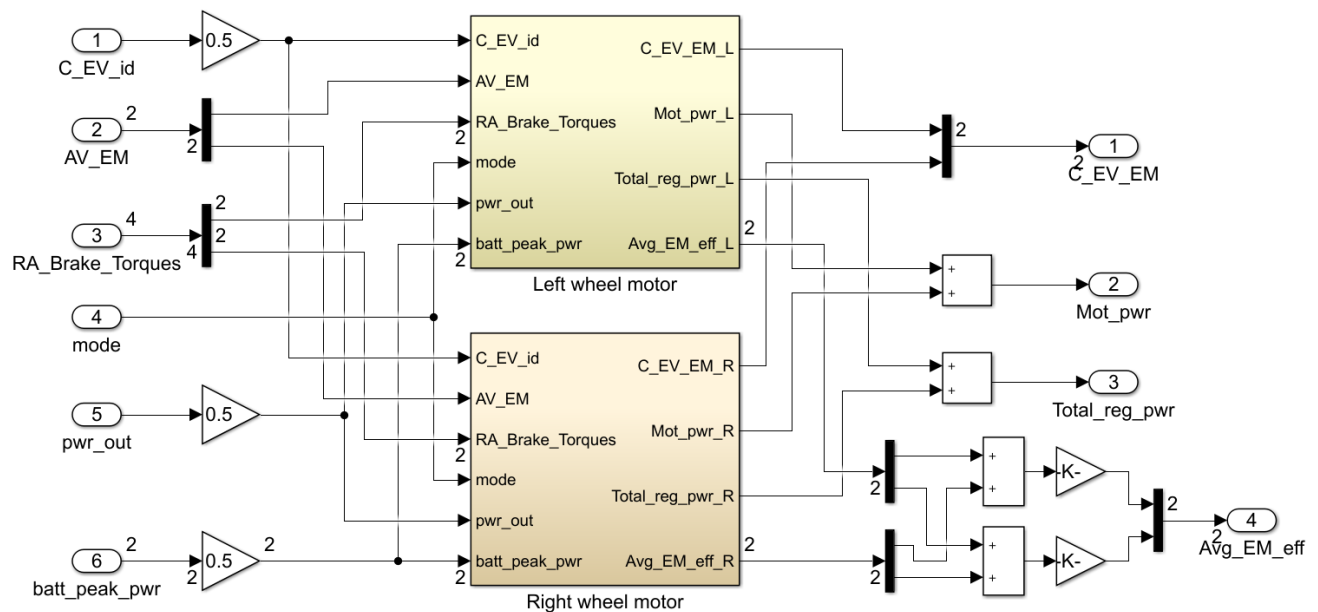


Figure 63 - Wheel motors Simulink block

It is possible to distinguish two main blocks, referring to the corresponding wheel motor. The input of the model are:

- *Ideal torque referred to the rear axle (C_EV_id)*: this is the output torque from the power management block, which is split in half and sent to the two motors, as an ideal open differential would do. However, this time the torque splitting is electronic and not mechanical.

- *Wheel motors' angular speed (AV_EM)*: the two rear wheels' angular velocities output from the TruckSim model are simply demuxed and sent to the two motors, without multiplication, since the connection between the motors and the wheels is direct.
- *Rear axle braking torques (RA_brake_torque)*: even in this case, the left and right hand side braking torques are demuxed and sent to the respective motor.
- *Mode*: this parameter represents an output from the power management block, and it defines the hybrid mode currently active, as it happens in the single EM model.
- *Engine output power (pwr_out)*: this quantity is necessary when the mode selected is full electric. In this case, in fact, the model considers the power delivered by the engine as if it has been delivered by the electric motor. For a wheel motors architecture, the overall power needs to be split in half and sent to the respective motors.
- *Battery peak power (batt_peak_pwr)*: this value takes in account the maximum power tolerated by the battery, and it is needed to saturate the output power signal, which is fed into the battery subsystem.

The structure of the two wheel motors subsystems is identical to the previous single electric machine model, shown in figure 43. The only difference is related to the torque curves and the efficiency map implemented.

Then, the output are concatenated into a vector (in case of torques), or simply added up (in case of powers) and sent as output. Regarding the motor's average efficiencies (in charge and discharge phase), the mean value for the two motors has been calculated so, as output, we have just two values, related to the charge and the discharge phase.

4. Simulations results, analysis and discussion

Once that the different architecture have been modeled in TruckSim/Simulink, it was possible to launch the simulations, acquire data and compare the different configurations.

It is important to notice that the processes of data analysis and model optimization were conducted in parallel: the correct sizing of the components and the power management design required a preliminary data analysis. In this chapter will be analyzed the final results of the simulations, ran on the definitive models.

4.1 Only-ICE architecture

First, the only-ICE configurations (whose modelling process has been discussed in section 3.1) were simulated through the procedures defined in section 2.4

4.1.1 Urban path test results

The first test ran was the urban path test, described in paragraph 2.4.2. Primarily, the vehicle's effective speed profile and the target speed have been compared, in order to confirm the validity of the run. In fact, the two profiles should be almost identical.

Plotting the two speed profiles and the difference between the two quantities, it is possible to confirm that the test was successful.

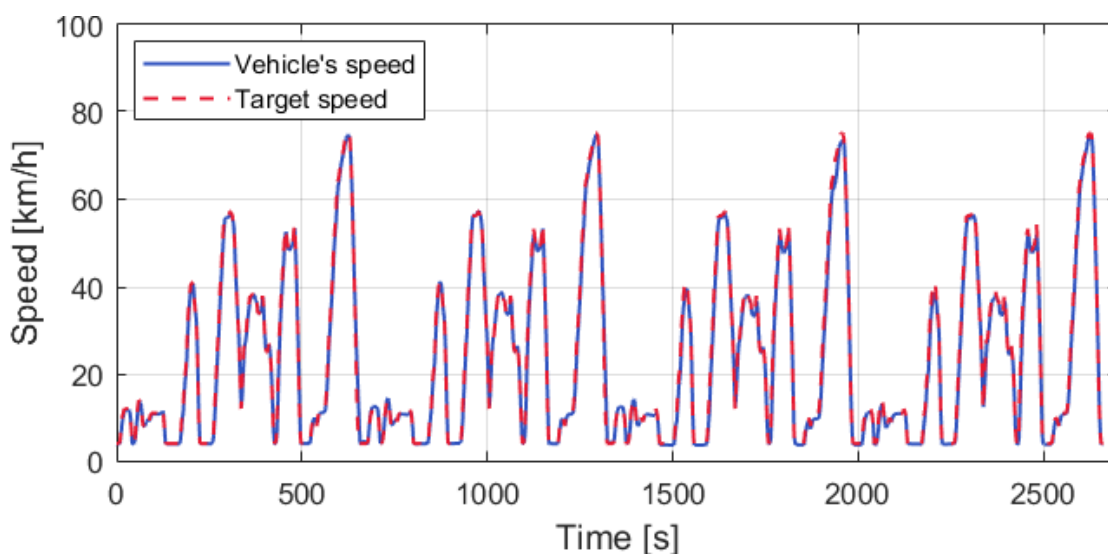


Figure 64 - Urban path test, Only-ICE, vehicle speed versus target speed

In fact, the target speed deviation remains close to 0 most of the times, except for the cases where the truck is subjected to particularly intense braking, where the speed difference can get close to 10 km/h, but for short intervals. However, the standard deviation value is equal to 1,3 km/h, which is acceptable.

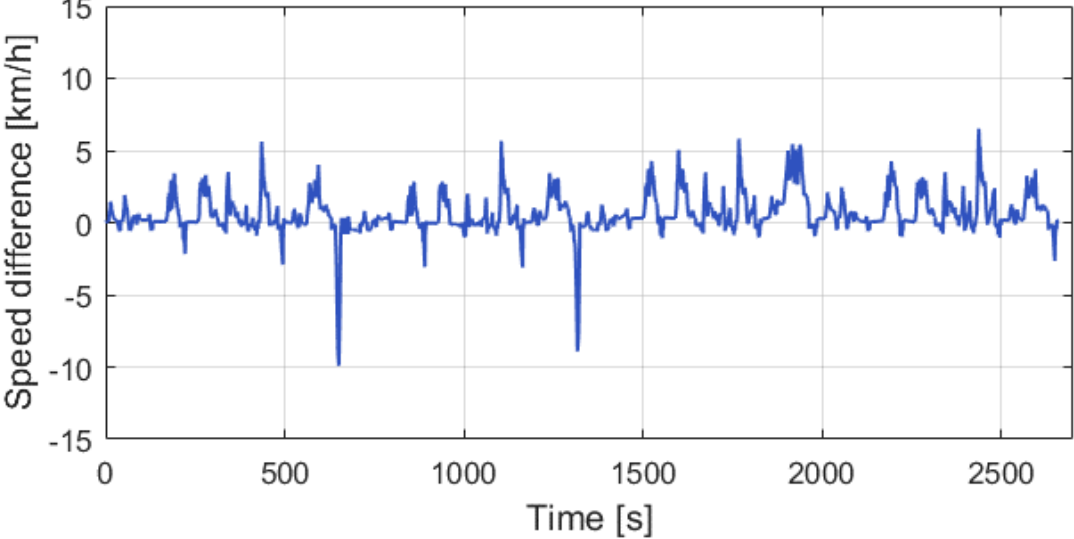


Figure 65 - Urban path test, Only-ICE, speed target deviation

The engine’s output torque becomes negative (close to -200 Nm) during the braking phase, because of the engine and driveline’s inertia. However, at the most intense accelerations and at the highest speed phase corresponds a higher load, and the output torque can overcome 1000 Nm (for example between 500 and 650 simulation seconds, where the truck rapidly accelerates until reaching 80 km/h).

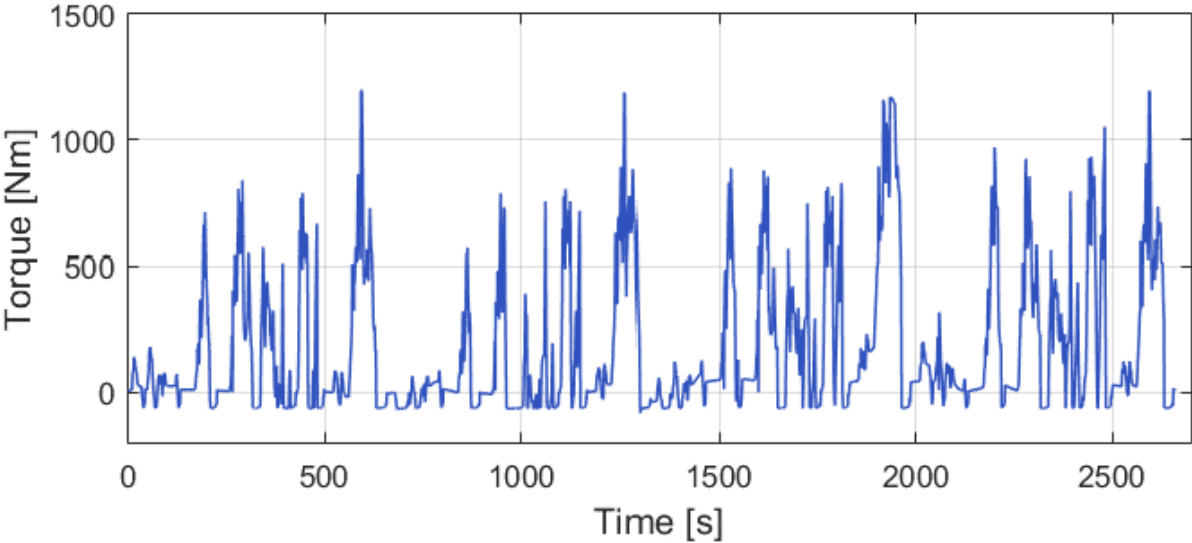


Figure 66 - Urban path test, Only-ICE, engine's output torque

Another interesting plot to analyze is the engine's overall efficiency trend. Even in this case, it is clear how the engine runs at very different values of efficiency, from 0 to slightly above 40%. The average efficiency throughout the entire drive cycle is equal to 37%, which is a really good value anyways.

This happens because the high load operating points corresponds both to highest efficiency and to highest output power. Therefore, since the average efficiency can be intended as an weighted average on the output mechanical energy, those operating points have a greater "weight" over the low load operating points, which corresponds to a lower efficiency as well.

The dashed line reported in the following graph represents the engine's average efficiency, while the blue trace reports the instantaneous overall efficiency.

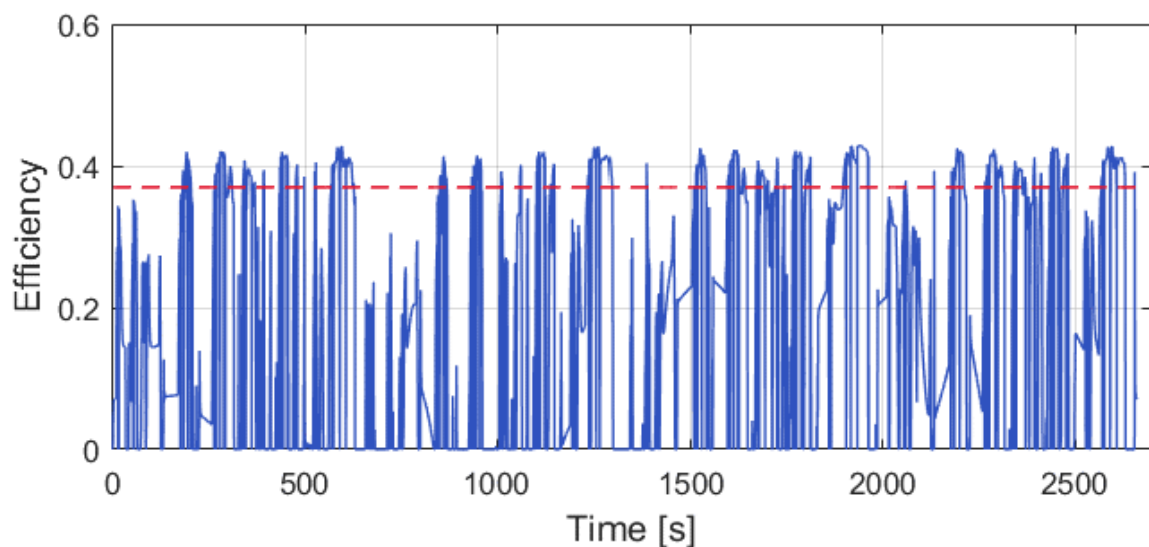


Figure 67 - Urban path test, Only-ICE, engine's overall efficiency

In figure 68 it is possible to analyze a scatter plot of the operating points of the engine during the cycle.

During the most demanding acceleration phases the engine operates towards the optimal efficiency area, however it is clear how the engine operates for a considerable amount of time at low loads and, therefore, at low efficiencies.

This indicates that a hybrid powertrain can contribute to eliminate the operating points at low efficiency by involving the electric axle, charging the battery by further shifting towards the higher part of the map the other operating points.

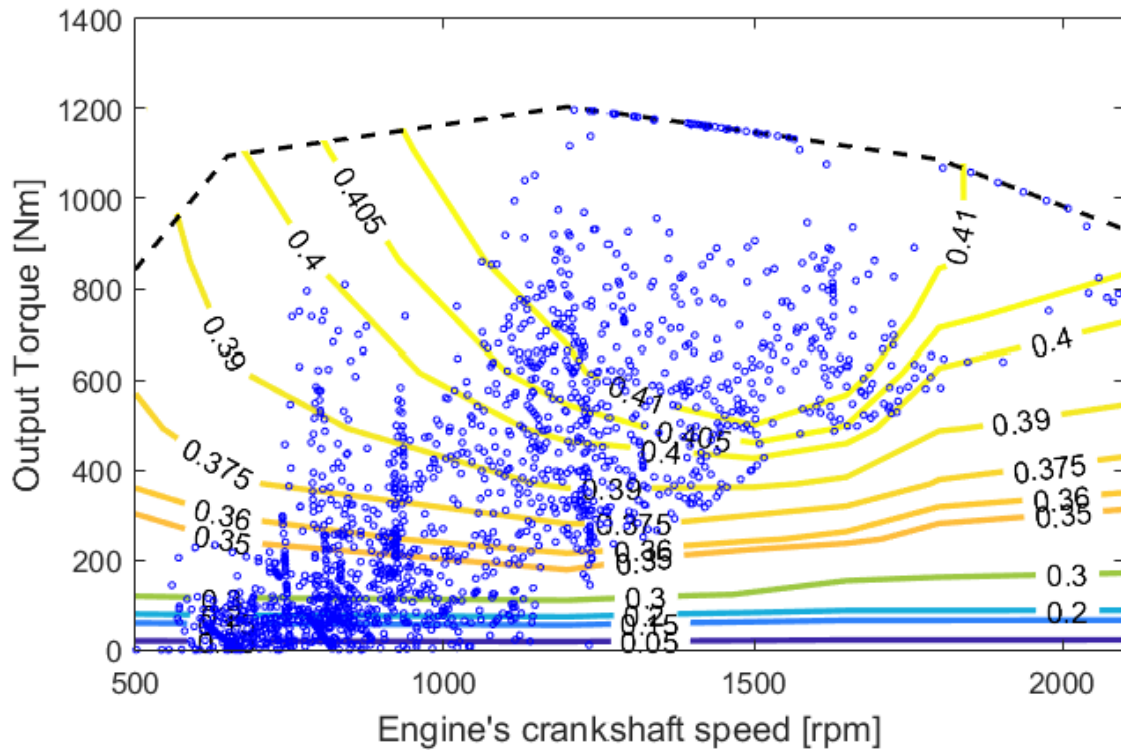


Figure 68 – Urban path test, Only-ICE, engine's operating points

Finally, the cumulated fuel consumption throughout the cycle is reported. It is noticeable how the slope of the function varies with time. In particular, a greater slope is associated with more demanding external conditions, which cause the engine to operate at higher loads, and this determines a higher fuel rate.

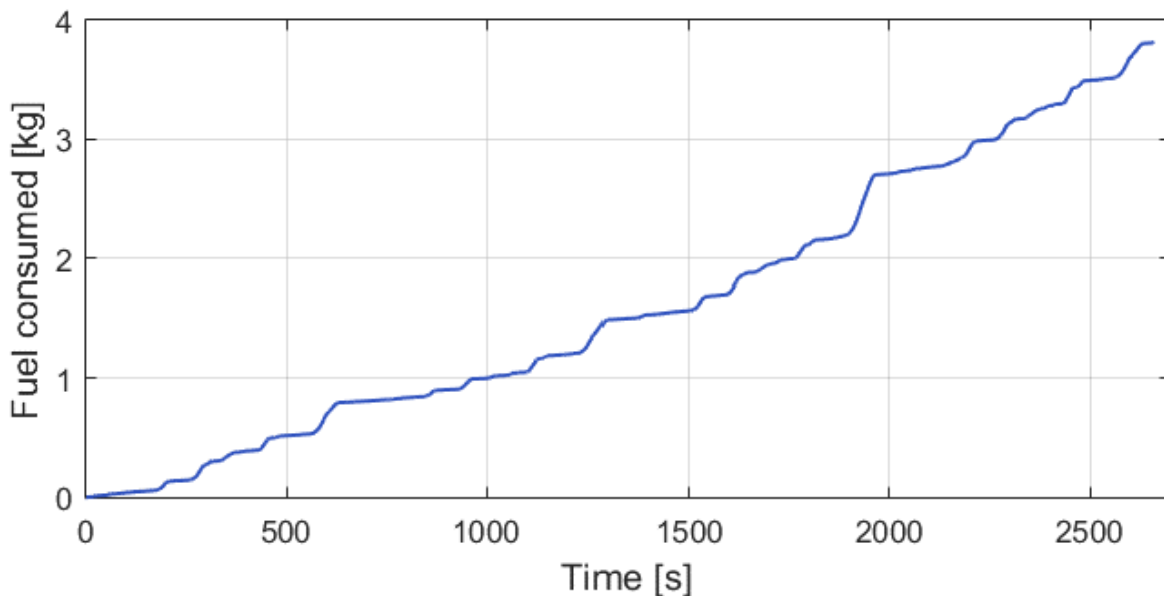


Figure 69 - Urban path test, Only-ICE, cumulated fuel consumption

The following table resumes the main results obtained by simulating the urban path cycle on the only-ICE architecture:

Table 9 - Urban path, Only-ICE, test results

| Urban path test results – Only ICE architecture | |
|--|-----------|
| Average output torque | 167,21 Nm |
| Average output power | 22,3 kW |
| Average fuel rate | 1,4 g/s |
| Mass of fuel consumed | 3816 g |
| Volume of fuel consumed | 4,57 l |
| Average specific fuel consumption | 3,88 km/l |
| Total output mechanical energy | 62668 kJ |
| Average engine efficiency | 37% |

4.1.2 Food delivery path test results

Once that the model has been predisposed, and the data relative to the speed profile and road elevation (discussed in paragraph 2.3.4) have been included in the TruckSim model, it was possible to run the simulation and process the results.

The final results were obtained by carrying out two separate calculations and then merging the results.

The first calculation regarded the procedure's phases during which the truck has a speed different from zero. The results of this part of the simulation were obtained by launching the Simulink simulation and setting to zero the instantaneous variables calculated when the truck performs a stop (such as the output power and torque, the fuel rate, and so on). Therefore, the cumulated variables remained constant during the stops.

The second calculation was carried on Matlab, and regarded the phases during which the truck performed a stop for the food delivery action. The choice to not carry on a single simulation was made because using the first approach for both phases would result in an unstable model and therefore would provide incorrect results. Furthermore, during the stopping phase, the instantaneous variables are much simpler to estimate.

During this phase, the instantaneous variables were calculated separately in Matlab. In particular, the instantaneous idling fuel rate was calculated by interpolating the fuel rate table, giving as an input the vehicle's idle speed (700 rpm), and the engine's crankshaft output torque, which changed based on the auxiliary load cycle.

Analyzing the vehicle's speed profile and the deviation from the target speed, we can observe how the model is working fine and the truck is able to follow the entire speed profile without problems.

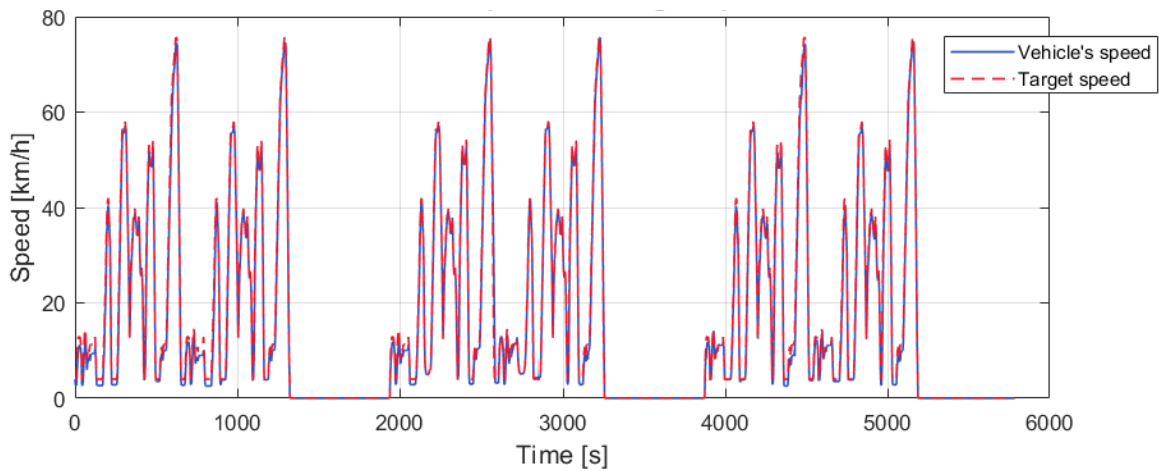


Figure 70 - Food delivery test, Only-ICE, vehicle's speed versus target speed

An interesting observation can be done by looking at the engine's overall and average efficiency. While in the previous test the engine's average efficiency was definitely high (above 36%), due to the variety of high load working points exploited during the test, in this test the average efficiency drops to 33%. This is due to the stop phase, during which the engine keeps running in order to power the auxiliary devices.

It has to be remembered that the engine's overall efficiency is defined based on the output power, and therefore it drops to zero during the stops. However, if we consider the auxiliary power as a useful effect, including it into the output power, the engine's efficiency during the idling phase is still equal to 29%, which is not an optimal value.

In the next figure, the engine instantaneous overall efficiency is compared to the average efficiency throughout the cycle.

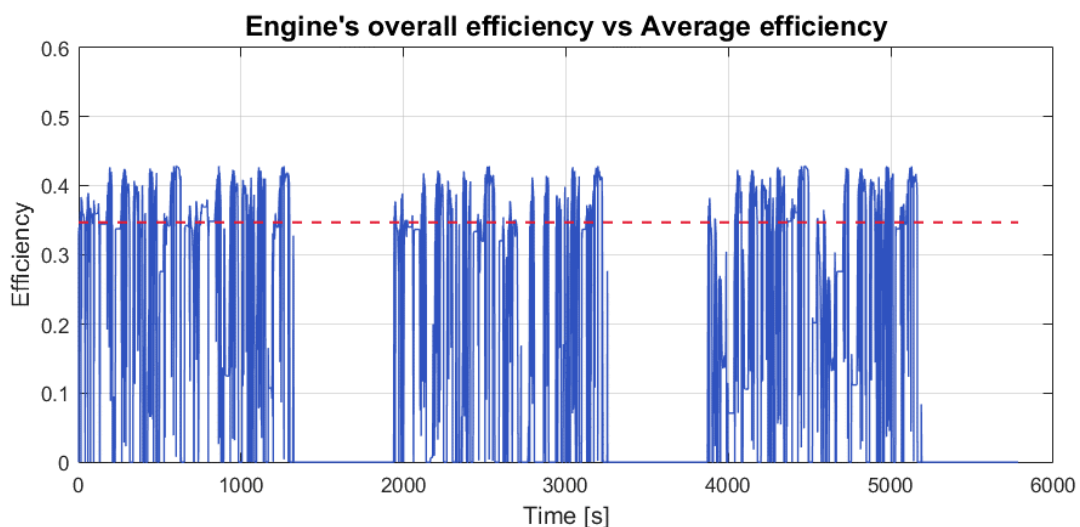


Figure 71 - Food delivery test, Only-ICE, engine's overall efficiency

Finally, we report the mass of fuel consumed during the test, and a summarizing table of the obtained results.

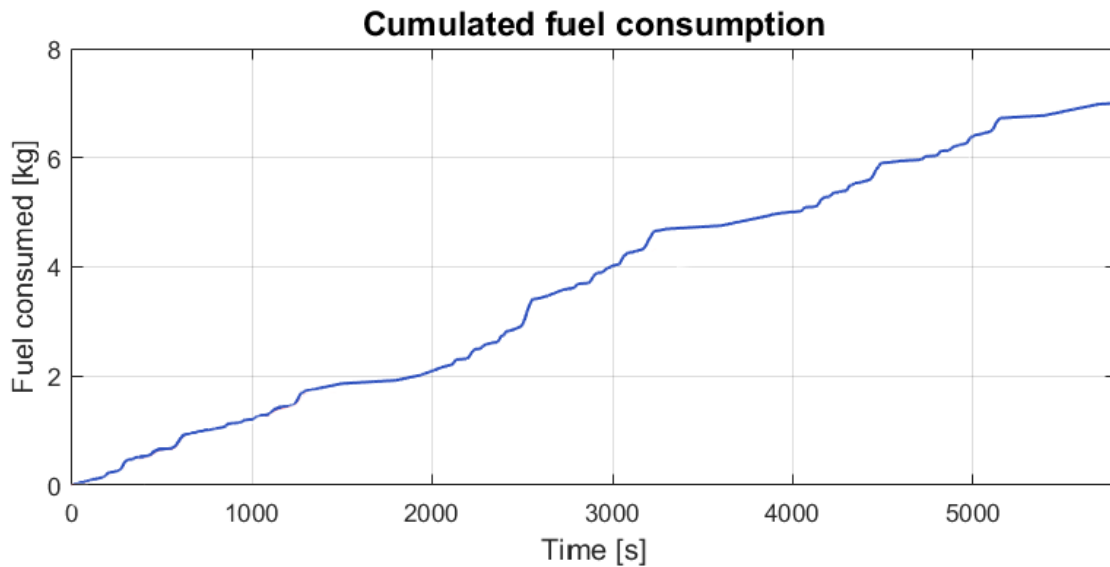


Figure 72 - Food delivery test, Only-ICE, cumulated fuel consumption

Table 10 - Food delivery test, Only-ICE, test results

| Food delivery test results – Only ICE architecture | |
|--|-----------|
| Average output torque | 165 Nm |
| Average output power | 20,15 kW |
| Average fuel rate | 1,21 g/s |
| Mass of fuel consumed | 6997 g |
| Volume of fuel consumed | 8,38 l |
| Average specific fuel consumption | 3,29 km/l |
| Total output mechanical energy | 102700 kJ |
| Average engine efficiency | 33% |

4.1.3 Cruising path test results

The last test conducted was the cruising test, described in paragraph 2.4.4. The actual speed profile and the target speed profile match perfectly, with a target speed deviation absolute value that rarely exceeds 2 km/h. This is due mainly to the absence of hard braking or acceleration phases in the test.

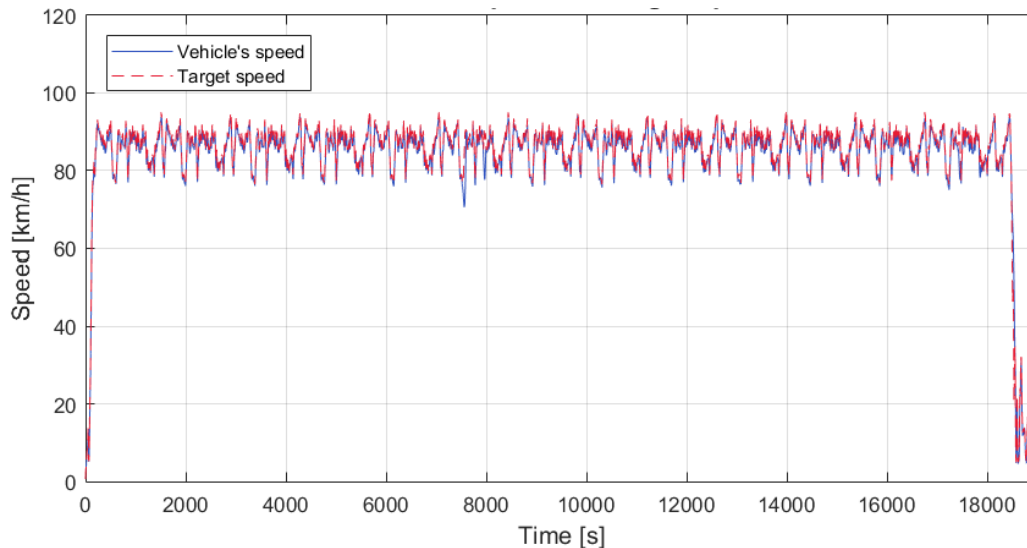


Figure 73- Cruising test, Only-ICE, vehicle's speed versus target speed

As supposed previously during all the duration of the test the engine's efficiency is sufficiently high, since during the cruising mode the internal combustion engine works at high loads and therefore it delivers low specific fuel consumption. In fact, as it can be observed from figure 74, the engine's average efficiency reaches 40%, while the peak efficiency is just slightly higher. We can conclude that in this mode the engine is working in optimal conditions. A hybrid powertrain could not be useful in this situations.

Furthermore, during the test the vehicle's speed oscillates around a constant value, and therefore the fuel consumption does not vary a lot. This can be observed in figure 75, noticing that the cumulated fuel consumption is almost linear (except in the final phase).

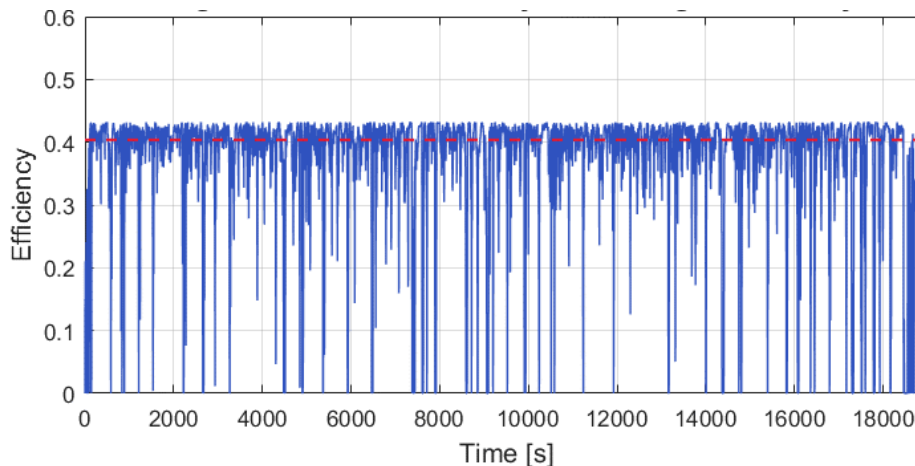


Figure 74 - Cruising test, Only-ICE, engine's efficiency

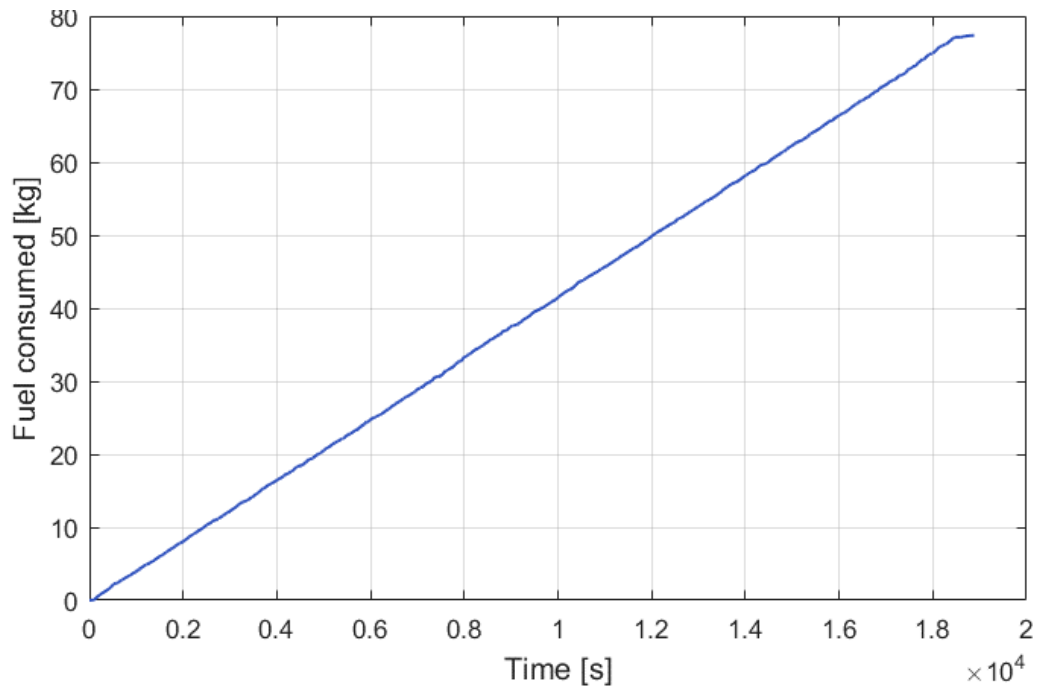


Figure 75 - Cruising test, Only-ICE, cumulated fuel consumption

Finally, a summary table is reported to review the results from this test procedure.

Table 11 - Cruising test, Only-ICE, test results

| Urban path test results – Only ICE architecture | |
|---|-----------|
| Average output torque | 492 Nm |
| Average output power | 74 kW |
| Average fuel rate | 4,1 g/s |
| Mass of fuel consumed | 77650 g |
| Volume of fuel consumed | 93 l |
| Average specific fuel consumption | 4,75 km/l |
| Total output mechanical energy | 1403 MJ |
| Average engine efficiency | 40,68% |

4.2 Single electric motor architecture

After that the only-ICE configuration has been modeled and simulated, the next step was to set up and run the simulation for the first hybrid configuration. The procedures implemented are identical to the first test, and this allows to compare the simulation results with the previous configuration.

4.2.1 Urban path test results

The first procedure tested, as in the only-ICE architecture case, was the city profile. Before launching the simulation, an important step was the choice of the main parameters that regulate the power management of the system in Simulink.

This procedure was not conducted in a single step, but instead an iterative approach was chosen. The simulations were launched multiple times, and the results were analyzed, with particular attention to the engine efficiency, the battery SOC and the engine's operating points, modifying the power management parameters time after time.

This approach does not ensure that the parameters chosen constitute the best possible choice that allows to obtain the best performance from the system, but it represents a valid approach to estimate the potential of the system.

A further optimization of the power management strategy and of its main parameters is required in order to obtain the optimum solution to the problem.

The iterative approach has led to the choice of the following parameters for the power management strategy and the component sizing:

Table 12 - First configuration model parameters

| | |
|--|---|
| Rear differential gear ratio | 12 |
| Battery capacity | 6048 Wh |
| Battery banks | 2 |
| Cell per banks | 48 |
| Minimum SOC | 30% |
| Initial SOC | 50% |
| Maximum SOC | 80% |
| Electric mode lower speed threshold | 20 km/h |
| Electric mode upper speed threshold | 30 km/h |
| Electric mode lower power threshold | 90% of maximum motor power |
| Electric mode upper power threshold | Maximum motor power |
| Optimum torque gain | 0.55 for the first half 0.63 for the second half |

In the following graphs the trends of the vehicle's speed, the powertrain's operating mode, the battery SOC and the engine's torque versus the simulation time are reported. The last quantity is compared to the engine's output torque of the only-ICE vehicle.

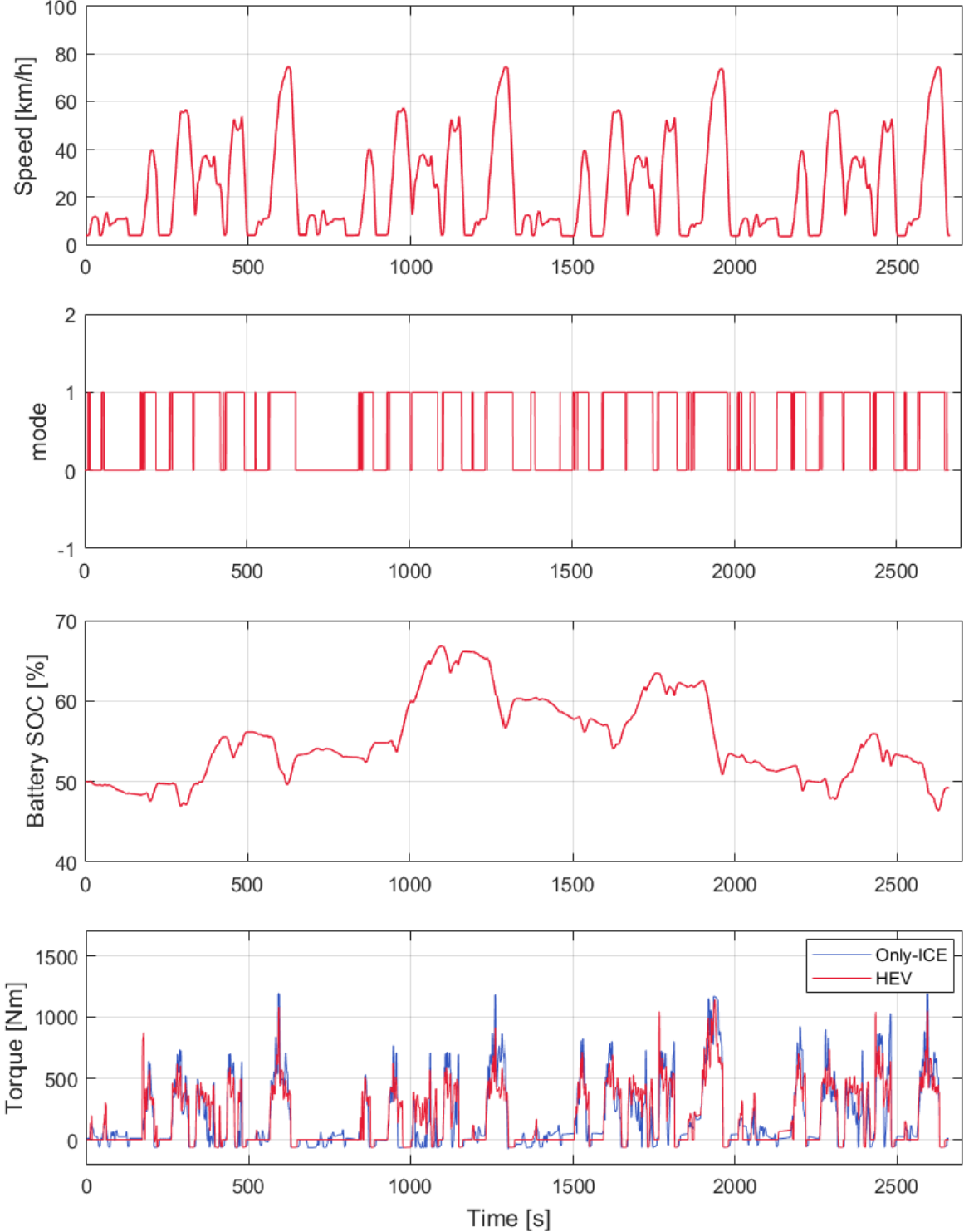


Figure 76 - Urban path test results, first configuration

In order to verify the reliability of the results, the two speed profiles of the two configurations have been confronted and their difference has been calculated. The speed difference value is reported in the following graph.

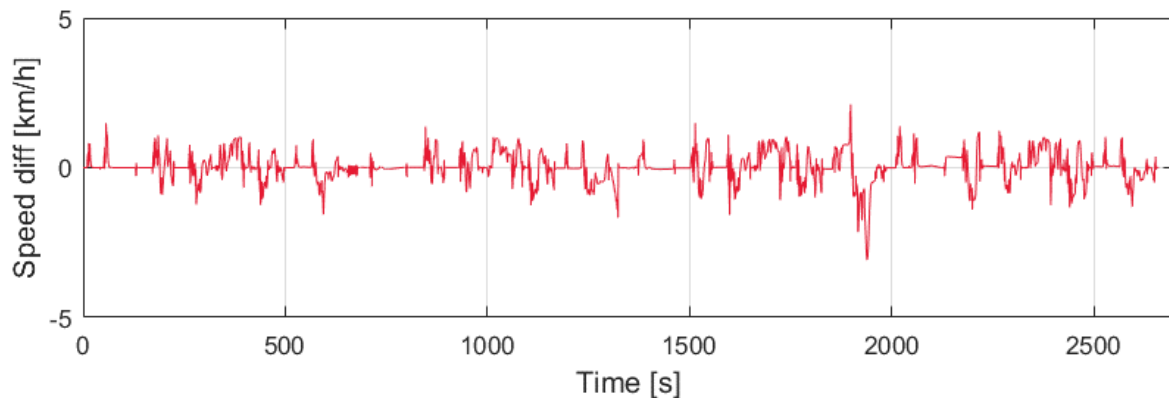


Figure 77 - Speed difference, Only-ICE vs HEV

This value oscillates between 1 and -1 km/h, and it exceeds quite rarely the absolute value of 2 km/h. The standard deviation value of this quantity is 0.46 km/h, and therefore the speed profiles of the two configurations are sufficiently close.

Since the speed profile of the urban path alternates intervals characterized by strong accelerations and high velocities to intervals where the vehicle's speed and required torque are relatively low, it is possible to notice how the powertrain switches quite often from a hybrid operating mode to a full electric operating mode.

This allows to significantly reduce the time in which the engine operates at low loads and low efficiency, exploiting the battery charge to drive the vehicle. The charge is then recovered by regenerative braking and by increasing the loads at which the engine works during the hybrid mode.

Analyzing the battery SOC trend, it is possible to note that the battery is properly sized, and the difference between the maximum and minimum values of SOC reached is about 15%. Furthermore, it is clear from the graph how the battery SOC is increased when the vehicle is subjected to hard decelerations because of regenerative braking and when the truck runs at medium-low loads. Instead, it decreases when the powertrain switches to full electric mode, and during strong accelerations. This indicates that the power management strategy is working properly.

Finally, it is possible to note that the engine torque drops to zero during the full electric mode because the engine is turned off. At the same time, at medium-low loads the HEV vehicle torque overcomes the only-ICE architecture torque, in order to increase the engine's efficiency and charge the battery. At low loads the torque is lower in the HEV case, in order to balance the SOC and provide combined power during demanding accelerations.

In the following graph the operating points of the engine are confronted between the two configurations:

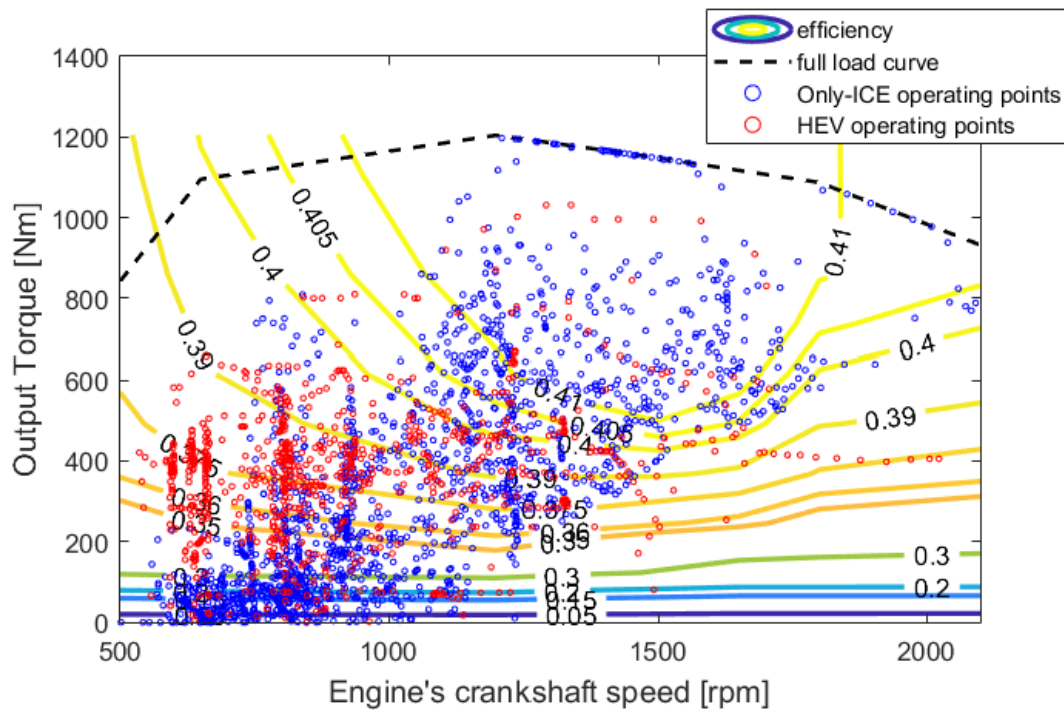


Figure 78 - Engine operating points, ICE vs HEV

As expected, it is clear how the density of the HEV configurations' operating point is much higher at medium-high loads, while in the low efficiency area it is possible to see only blue dots, which refer to the only-ICE configuration.

This contributes to raise the average efficiency of the engine. Reporting this value over time for the two configurations, in fact, we have:

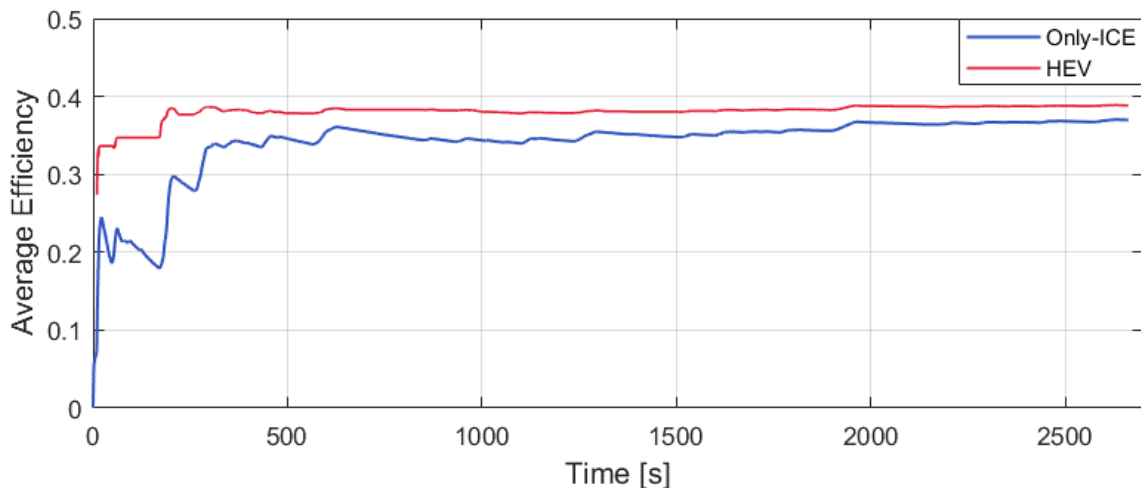


Figure 79 – Urban path test, first configuration, Engine average efficiency

The following plot represents the distribution of the engine's efficiency throughout the cycle. On the x axis we have the efficiency, while on the y axis we have the frequency normalized to the maximum frequency.

It is possible to notice how in the HEV configuration every operating point at low load is excluded because of the activation of the full electric mode. Therefore, the distribution is more concentrated towards higher values of efficiency.

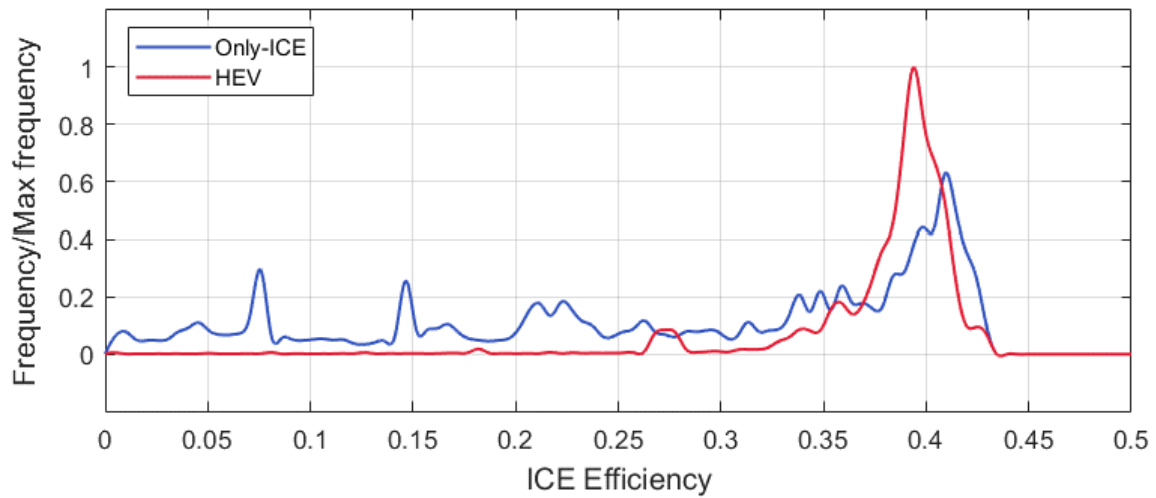


Figure 80 – Urban path test, first configuration, Engine efficiency distribution

The following graph reports the electric motor's operating points during the test.

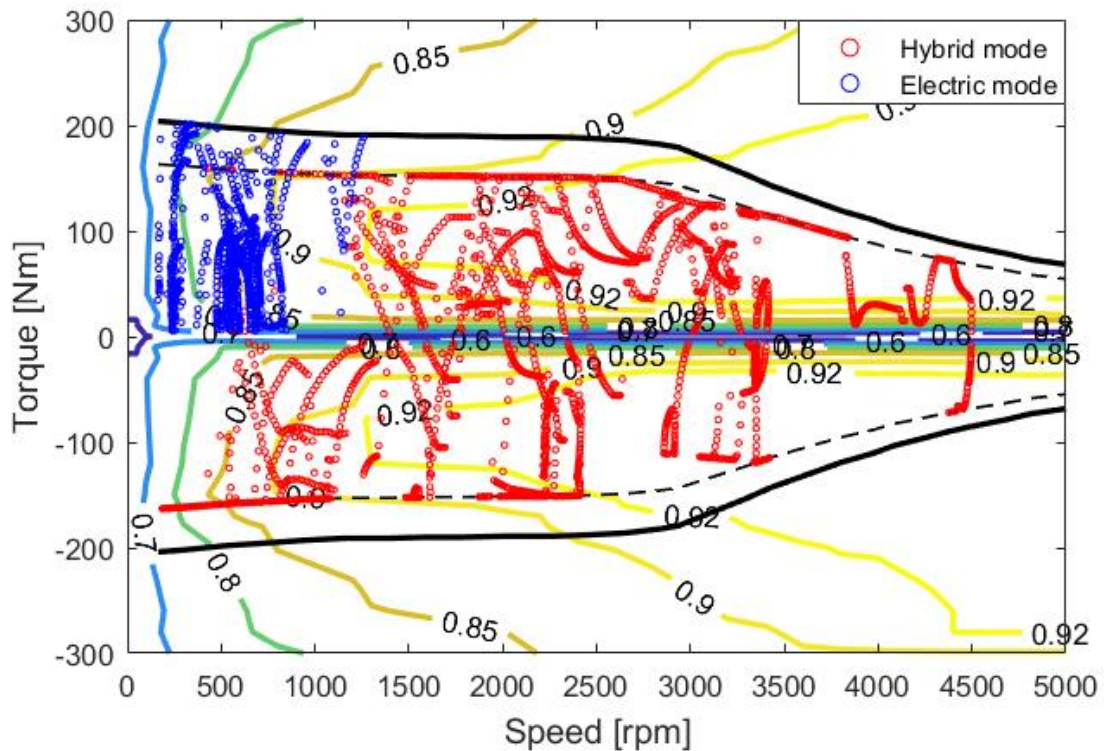


Figure 81 – Urban path test, first configuration, EM operating points

It is clear how the electric machine works in its entire operating map. Regarding the hybrid mode, it is evident a points thickening towards the dashed line in the negative torque area. This line represents 80% of the motor’s maximum power (imposed as a limit in the model). This thickening is mainly due to regenerative braking.

Along with the increasing ICE efficiency effect, the electric axle introduces another advantage over the conventional vehicle that contributes to reduce the fuel consumption during the cycle, which is the reduction of the required overall mechanical energy due to regenerative braking.

In fact, with this strategy it is possible to increase the battery SOC by exploiting part of the vehicle’s kinetic energy during the braking phase. This energy is then used to drive the electric axle and it is then converted again into kinetic energy.

The effect is the reduction of the mechanical energy required to complete the procedure. Integrating the engine’s output power, it is possible to calculate this value. The two values are confronted in the graph below:

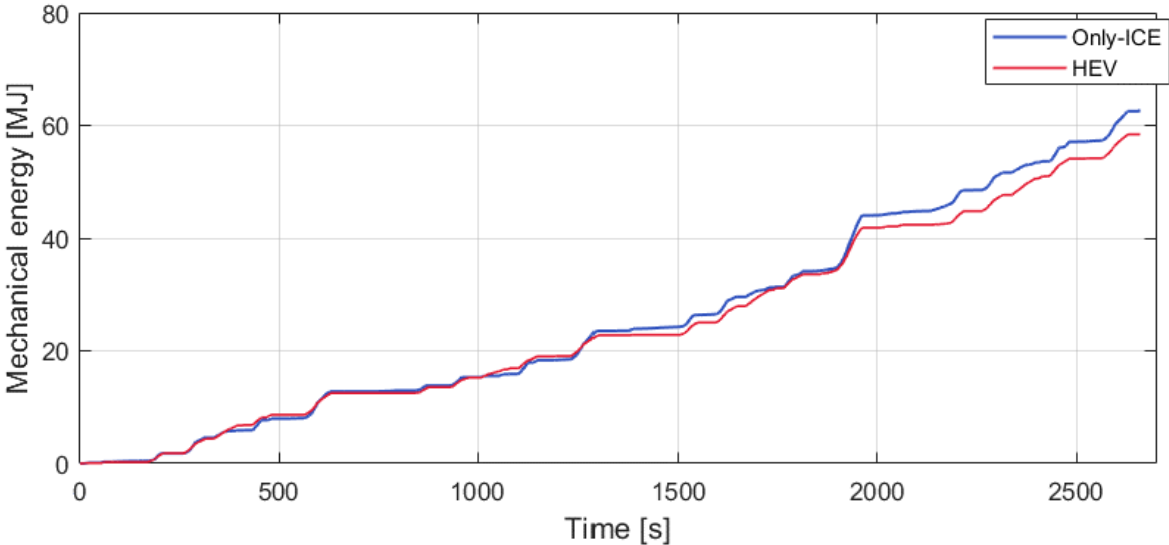


Figure 82 – Urban path test, first configuration, overall mechanical energy

These two positive effects contribute to an overall reduction of the fuel consumption throughout the cycle. In fact, the cumulated fuel consumption can be expressed as:

$$m_{fuel} = \frac{E_u}{\eta_u H_i}$$

Where E_u is the mechanical energy and it is reduced, and η_u is the engine’s overall efficiency, which is increased.

As a result, confronting the cumulated fuel consumption throughout the cycle, we have:

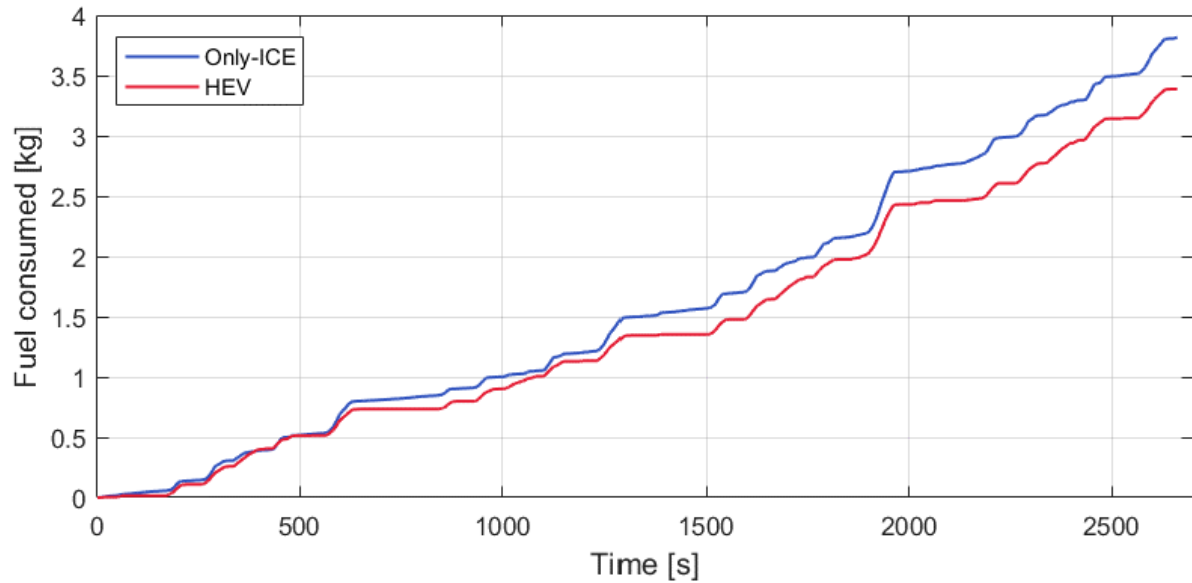


Figure 83 – Urban path test, first configuration, Cumulated fuel consumption confrontation

Finally, the results are summarized in the following table:

Table 13 – Urban path test, first configuration, results confrontation

| | Only ICE | HEV | Difference |
|--|----------|----------|---------------|
| Electric mode operating time | - | 1866 s | - |
| Hybrid mode operating time | - | 795 s | - |
| Minimum battery SOC | - | 46,4% | - |
| Maximum battery SOC | - | 66,8% | - |
| Overall engine output mechanical energy | 62,67 MJ | 58,43 MJ | -6,8% |
| Average overall engine efficiency | 37% | 38,85% | +5% |
| Fuel consumption | 3,82 kg | 3,39 kg | -11,3% |
| Equivalent fuel consumption | 3,82 kg | 3,41 kg | -10,7% |

4.2.2 Food delivery test results

In this paragraph the results obtained by simulating the first hybrid configuration on the food delivery test procedure will be analyzed. The trends of the vehicle's speed, the powertrain's operating mode, the battery SOC and the engine's torque versus the simulation time are reported in the following graphs. The last quantity is compared to the engine's output torque of the only-ICE vehicle.

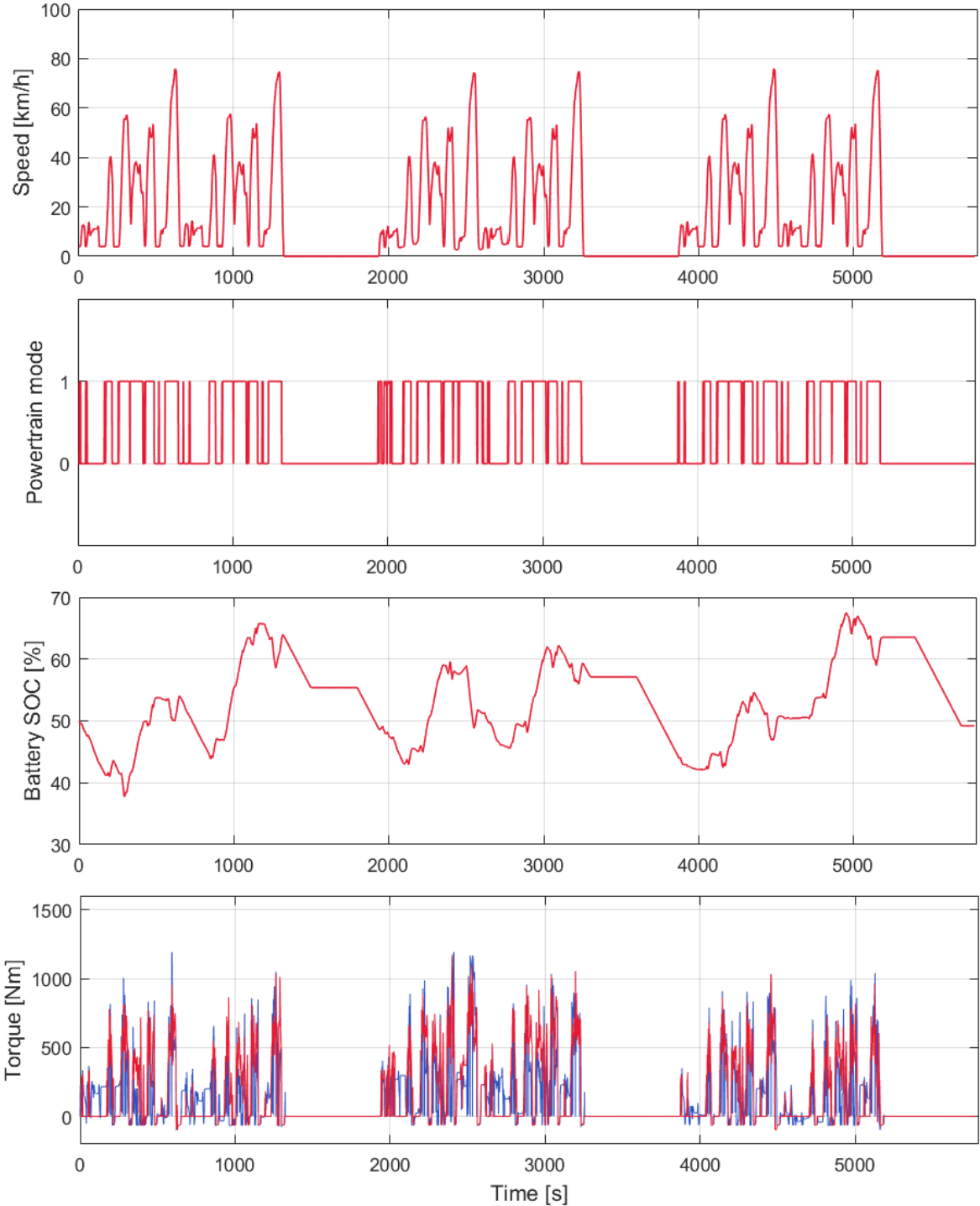


Figure 84 – Food delivery test results, first configuration

As in the previous case, there is a strong correspondence between the speed profile and the powertrain operating mode, and this allows to eliminate the low efficiency engine operating points and the idling phase, increasing the overall engine efficiency.

This case presents a fundamental difference compared to the simple urban path test, which is the external power demand by the refrigeration system. When the powertrain mode is set to “hybrid mode”, the power request is satisfied by the engine, while when the operating mode switches to “full electric mode”, the power request is addressed by the battery.

The single cycles are interspersed with pauses that represent the food delivery phase. Here, the hybrid configuration allows to obtain a huge advantage compared to the conventional architecture. Here, in fact, the engine is off and the power demand from the auxiliary system is satisfied by the battery, using the energy that has been previously stored at much higher efficiencies.

In terms of overall mechanical energy, this represents an apparent disadvantage: in fact, we notice that during the normal vehicle advancement, the electric axle works most of the time as a generator, in order to increase the battery SOC and to have sufficient energy for the food delivery pause. So, the output mechanical energy demand from the engine increases (and it’s balanced by the energy recuperation by regenerative braking).

However, the advantages on the engine’s efficiency largely compensate the higher request of mechanical energy. In fact, in the conventional architecture, during the pause we have a useful output power from the engine equal to zero (the power delivered to the auxiliary system is not considered as useful power), but we have fuel consumption. So, the engine works at 0% efficiency, and this has a strong impact on the average efficiency.

In the hybrid case, instead, the engine is turned off. So the average efficiency remains constant during this phase since the output power is zero, but at the same time the fuel consumption drops to zero as well (it is not possible to define an instantaneous overall efficiency in this phase).

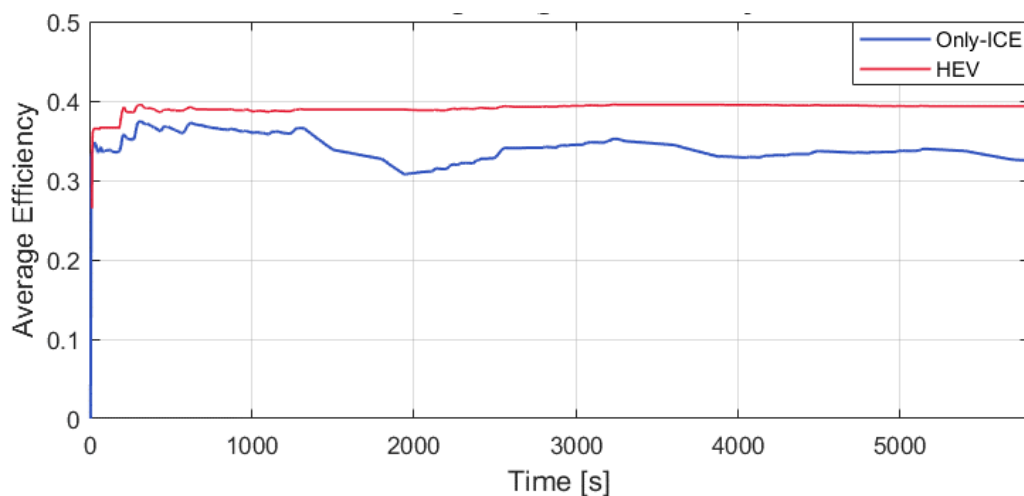


Figure 85 – Food delivery test, first configuration, average efficiency

The mechanical energy request throughout the cycle remains almost identical, because of the compensation of the two effects due to regenerative braking and energy storing into the batteries to power the auxiliary devices, as discussed before.

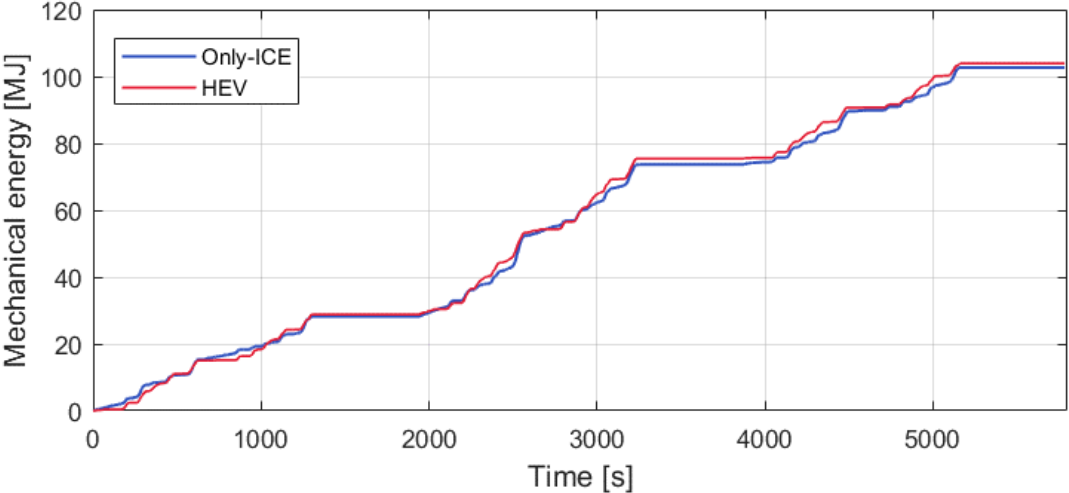


Figure 86 – Food delivery test, first configuration, Output mechanical energy

The considerable improving of the engine’s average efficiency caused a noticeable reduction of the cumulated fuel consumption:

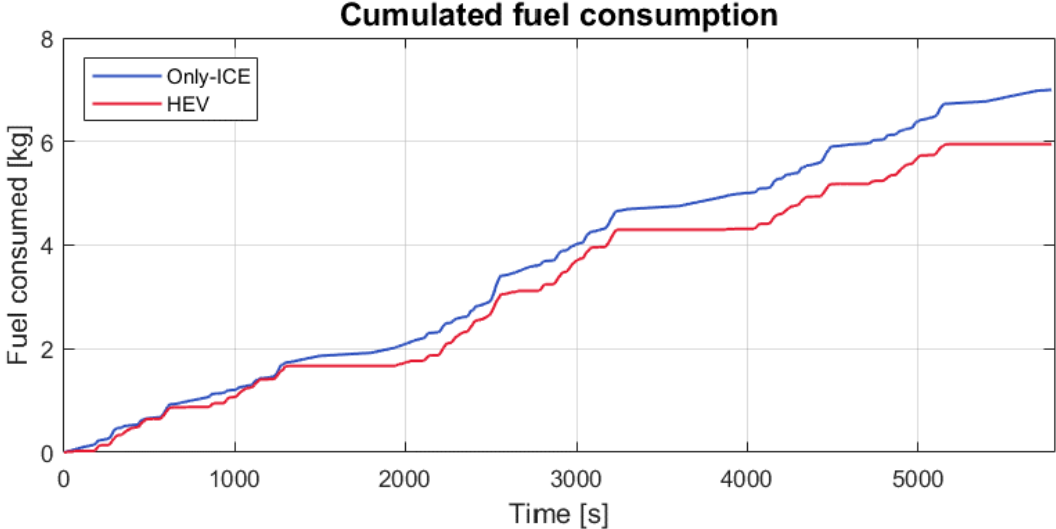


Figure 87 - Food delivery test, first configuration, Cumulated fuel consumption

Table 14 - Food delivery test results, first configuration

| | Only ICE | HEV | Difference |
|--|----------|----------|----------------|
| Electric mode operating time | - | 3453 s | - |
| Hybrid mode operating time | - | 2331 s | - |
| Minimum battery SOC | - | 37,7% | - |
| Maximum battery SOC | - | 67,5% | - |
| Overall engine output mechanical energy | 102,7 MJ | 103,8 MJ | +1,07% |
| Average overall engine efficiency | 33% | 39,34% | +19.2% |
| Fuel consumption | 6,997 kg | 5,95 kg | -14,96% |
| Equivalent fuel consumption | 6,997 kg | 5,973 kg | -14,63% |

4.2.3 Cruising test results

The last analyzed scenario regarded the cruising test, described in paragraph 2.4.4. Theoretically, this situation is not ideal for a hybrid powertrain for several reasons.

First, the engine operates already in its maximum efficiency area, since the vehicle travels at high speeds and high loads. Then, since the speed profile fluctuations are not as noticeable as in an urban profile, there is much less chance to recover mechanical energy through regenerative braking. Finally, for most of the cycle the speed is high, so the mode will be permanently hybrid.

However, there is still some possibility to increase the engine's overall efficiency. In fact, in a real cruising speed profile the speed is not always constant and the road presents an elevation which varies over time. Therefore, the engine will change its operating points during the vehicle's advancement, eventually reaching the low efficiency area.

By the use of the battery as an energy storage device, it could be possible to stabilize the engine's operating points towards the high efficiency area and increase (even if slightly) the engine's overall efficiency.

However, the powertrain itself introduces some energy losses in the process of converting mechanical energy into electrical energy and then into chemical energy to store in the battery and vice versa.

This will increase the mechanical energy demand throughout the cycle. This test aims to evaluate whether if the advantages in terms of efficiency (if any) will overcome the energy losses due to energy conversion. If that's the case, this indicates that the hybrid mode can be used even in a cruising path. If this possibility does not occur, in the power management

strategy an option to recognize a cruising maneuver and deactivate the system has to be taken into consideration.

Running the simulation in Simulink, the following results in terms of speed profile and battery SOC can be obtained.

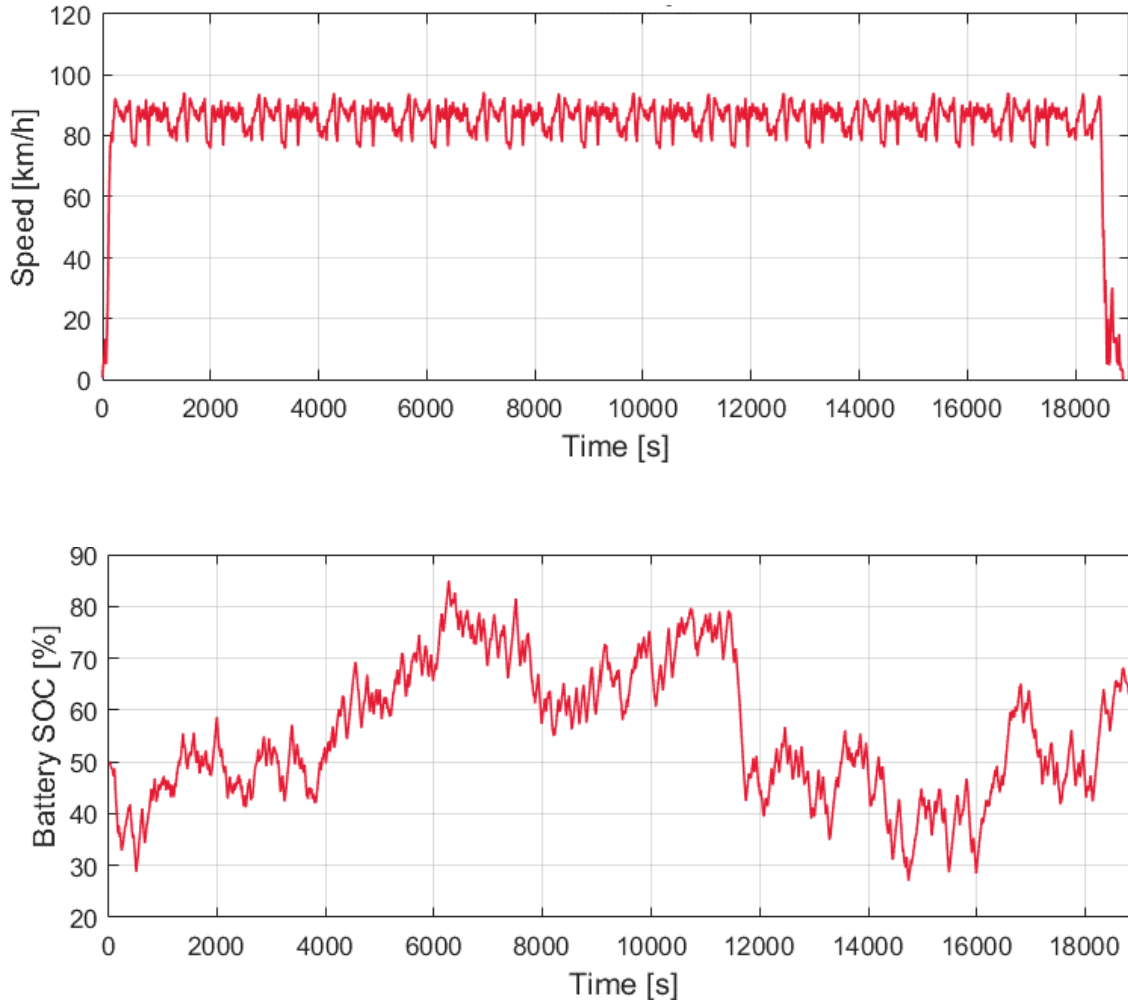


Figure 88 – Food delivery test, first configuration, vehicle’s speed and battery SOC

It is possible to notice how the SOC trend is very variable, and it follows the road elevation trend and the load fluctuations. However, it remains into the accepted range between 30% and 90%, therefore the power management does not intervene in order to bring back the SOC value into the optimal range.

As expected, the powertrain works in order to force the engine’s operating points towards the lower part of the maximum efficiency area, which is not too shifted towards high loads in order to prevent the SOC from going towards the upper boundary.

As a result, reporting the scatter plot of the engine operating points for the Only-ICE configuration and for the hybrid powertrain vehicle, it is possible to notice how the first ones are more disperse throughout the torque range, while the second ones tend to concentrate towards around 600 Nm value.

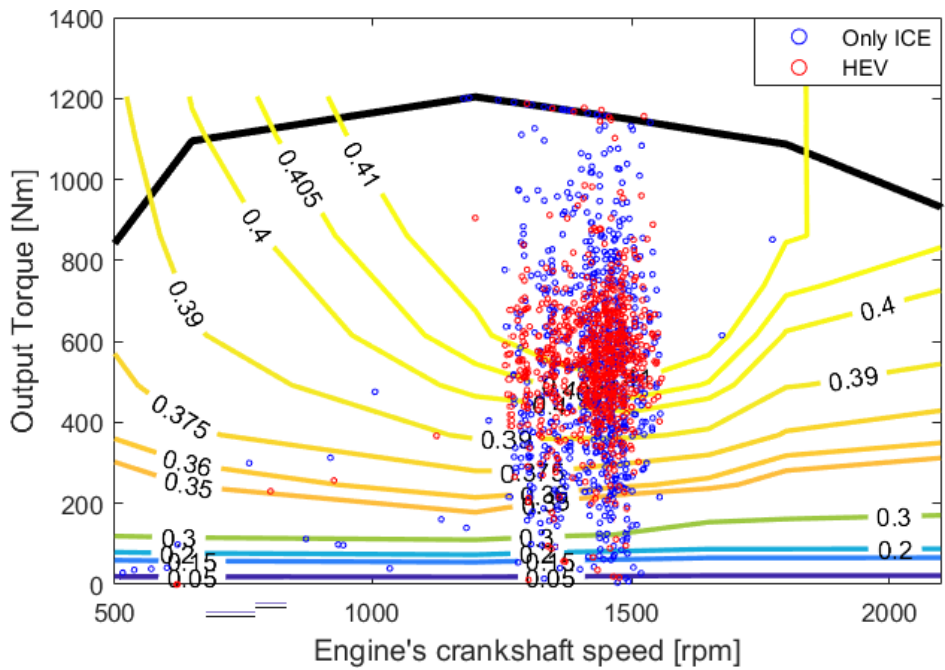


Figure 89 – Cruising test, first configuration, Engine operating points confront

As a result, it is possible to assist to a slight increase in the average engine's efficiency throughout the cycle. However, since the conventional vehicle already operates at high load and really close to the optimal efficiency area, the difference between the two values is almost negligible.

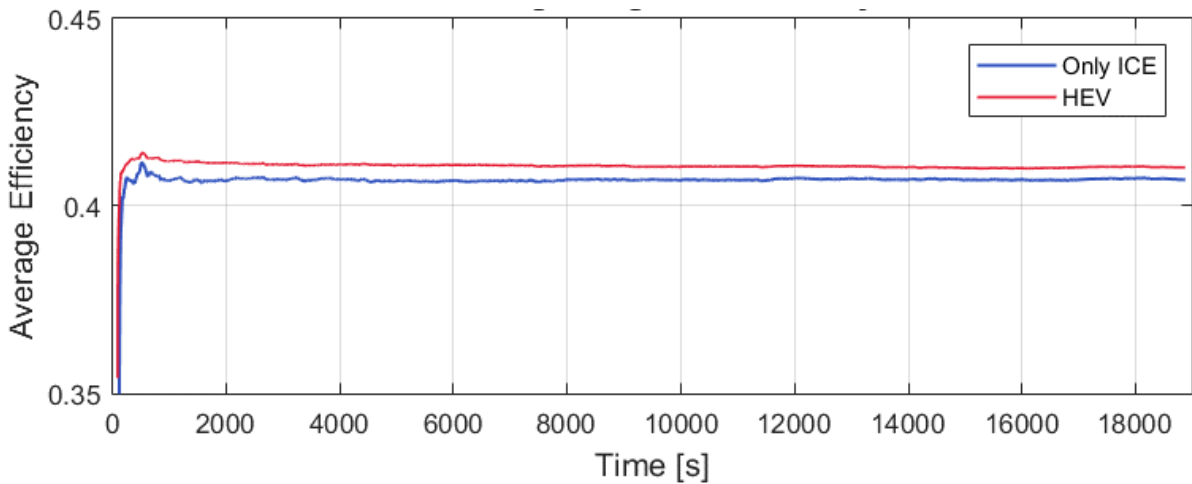


Figure 90 – Cruising test, first configuration, Engine average efficiency confront

As discussed before, however, an increase in the demand of mechanical efficiency due to energy conversion from the electric axle has to be expected. This is evident in the following plot.

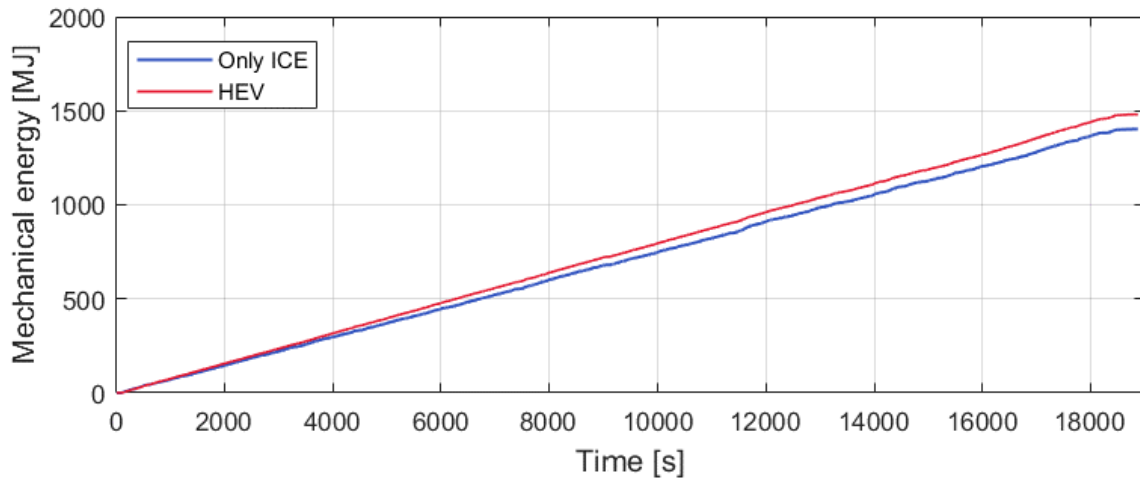


Figure 91 – Cruising test, first configuration, Mechanical energy confront

As a result, it seems that the energy losses overcome the small gain on the energy efficiency. This results in a worse fuel consumption.

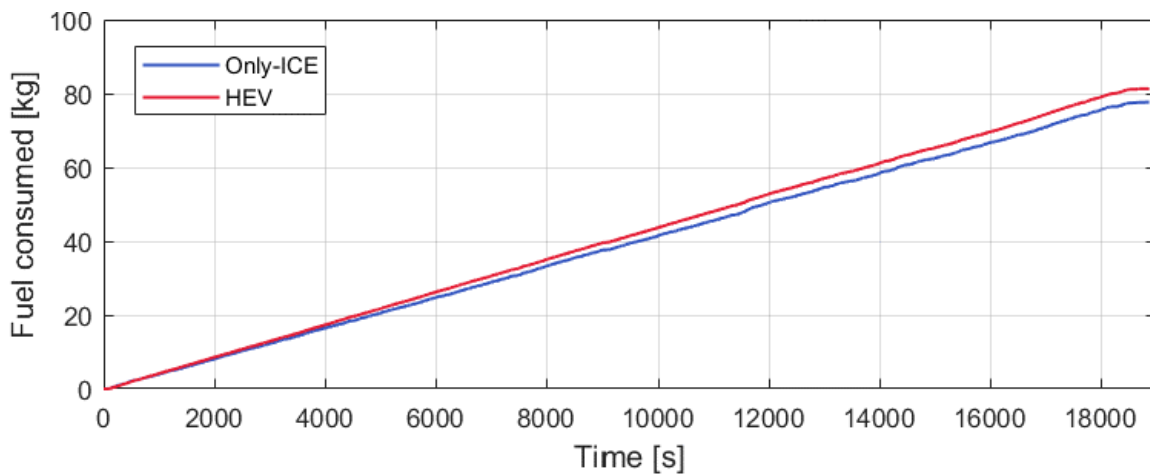


Figure 92 – Cruising test, first configuration, Cumulated fuel mass confront

This test has then highlighted the limitation of a hybrid system for this type of applications. In fact, if the vehicle is used exclusively for long cruising itineraries, this system could also be counterproductive.

Therefore, it is necessary to implement a power management strategy that recognizes a cruising path and switches to only Internal Combustion Engine mode, while the hybrid and full electric modes can be activated in other situations, like the ones described in the previous sections, where the system has proven to potentially guarantee really interesting results.

The following table summarizes the results obtained in this last test.

Table 15 – Cruising test results, first configuration

| | Only ICE | HEV | Difference |
|--|-----------------|------------|-------------------|
| Minimum battery SOC | - | 27% | - |
| Maximum battery SOC | - | 85% | - |
| Overall engine output mechanical energy | 1403 MJ | 1480 MJ | +5,5% |
| Average overall engine efficiency | 40,68% | 41,01% | +0,81% |
| Fuel consumption | 77,65 kg | 81,29 kg | +4,68% |
| Equivalent fuel consumption | 77,65 kg | 80,52 kg | +3,7% |

4.3 Wheel motors architecture

The further step was to simulate the second hybrid architecture, characterized by the wheel motors configuration.

The procedure analyzed was the urban path test, since it is already evident from the previous analysis that the system does not provide the desired results on a highway cruising scenario.

4.3.1 Urban path test results

The initial approach to simulate the architecture was to set the same parameters in the power management strategy used in the first configuration, in order to highlight the differences.

The greater power of the wheel motors determine a bigger hybridization factor for the vehicle. Therefore, the system offers a better opportunity to perform the ICE load shift strategy seen before, and it is able to store a greater amount of energy by regenerative braking.

As a matter of fact, if the power management strategy remains unchanged, the only effect is an increase in the battery SOC over time compared to the previous solution.

This means that at the end of the cycle the powertrain has stored a greater amount of energy in the batteries in respect to the first configuration.

So, it is possible to change the parameters in order to obtain the same final SOC and see how this affects the results.

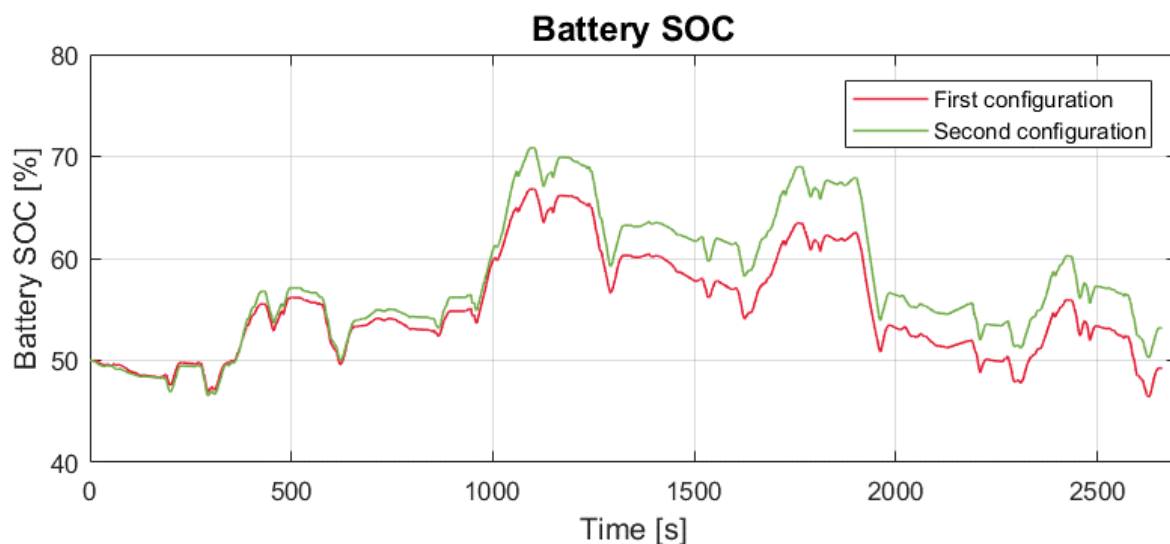


Figure 93 - SOC confrontation, first vs second configuration

The iterative approach has led to the choice of the following parameters for the power management strategy and for the component sizing:

Table 16 – Second configuration model parameters

| | |
|--|---|
| Battery capacity | 6048 Wh |
| Battery banks | 2 |
| Cell per banks | 48 |
| Minimum SOC | 30% |
| Maximum SOC | 80% |
| Electric mode lower speed threshold | 20 km/h |
| Electric mode upper speed threshold | 30 km/h |
| Electric mode lower power threshold | 90% of maximum motor power |
| Electric mode upper power threshold | Maximum motor power |
| Optimum torque gain | 0.53 for the first half 0.63 for the second half |

The following graphs represent a confrontation of the trends of the vehicle's speed, the Battery SOC, and the engine's average efficiency, between the two hybrid configurations.

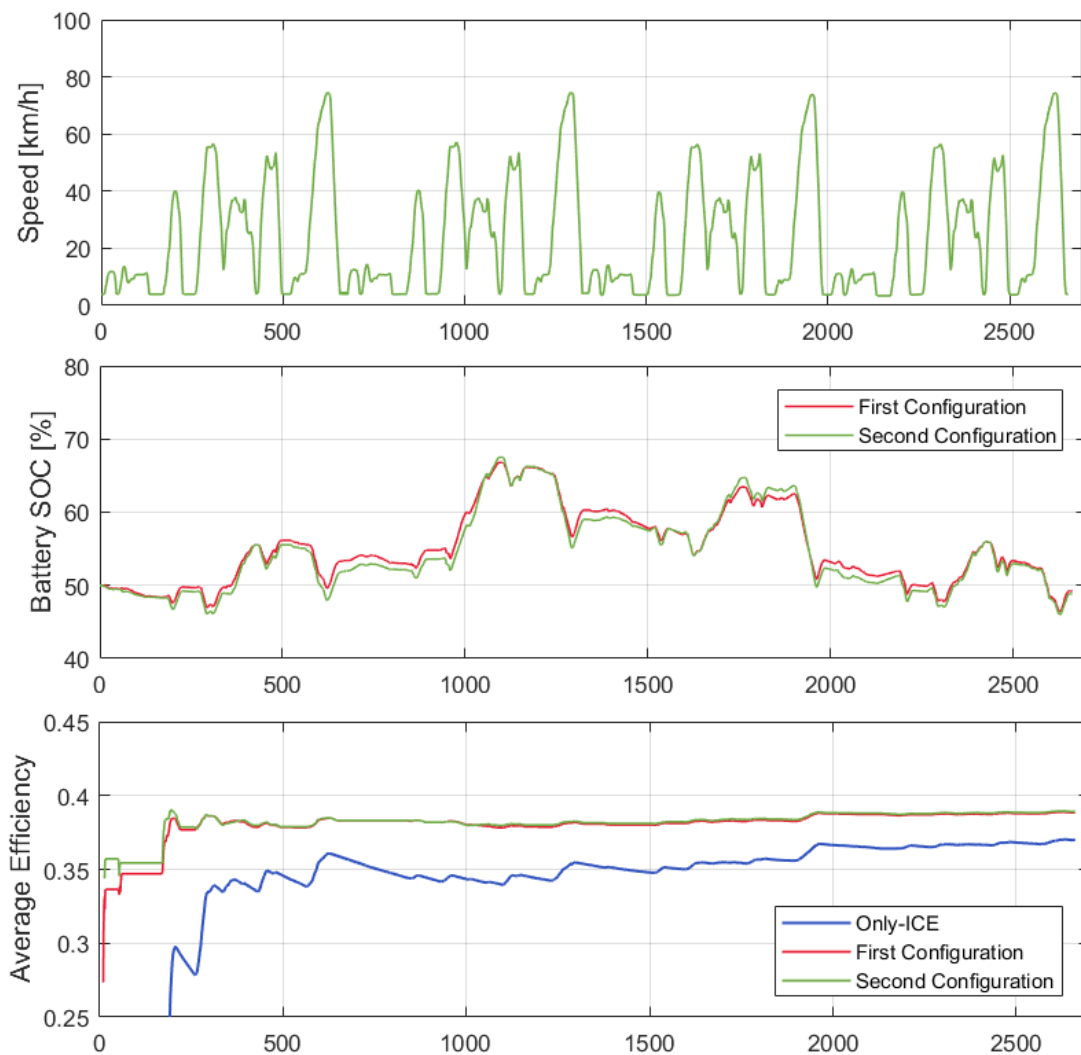


Figure 94 – Second hybrid configuration graphs

Due to the higher efficiency of the electric powertrain and the slightly higher hybridization factor, it is possible to increase the energy stored in the battery throughout the cycle.

However, if the power management parameters are set in order to obtain a final SOC identical to the previous configuration, this results to a slight reduction of the mechanical energy required for the procedure and a slight increase of the average overall efficiency of the ICE.

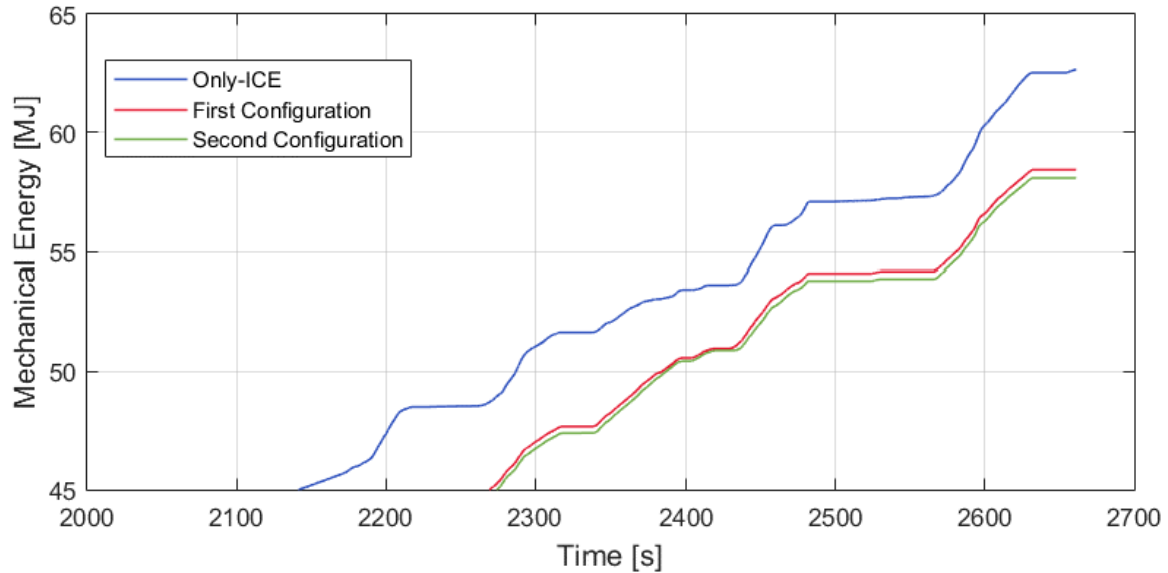


Figure 95 – Second configuration, Mechanical energy confrontation

Plotting the operating points of the electric machine, we obtain:

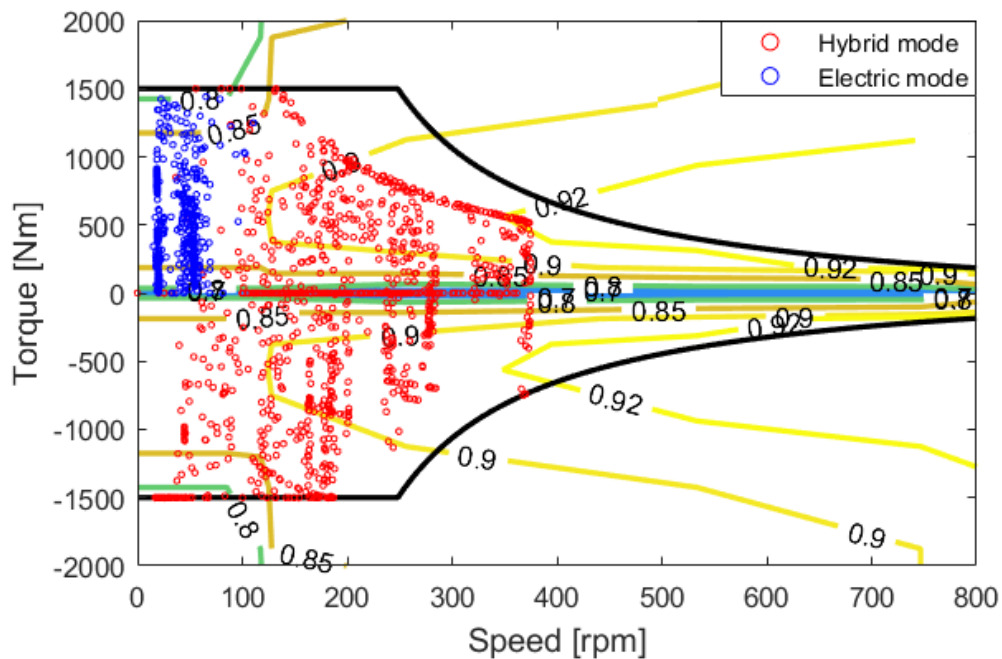


Figure 96 – Second configuration, Electric motor operating points

It can be noticed that in hybrid mode not all the motor’s operating field is exploited, both in traction and in regeneration mode.

This is due to the limitation of the maximum electric power that the battery can handle, which was not evident in the single electric motor case.

Therefore, the cumulated fuel consumption is further reduced, as it can be seen in figure 97. However, it has to be pointed out that the reduction in terms of fuel consumption is not relevant, and the two configuration can be considered almost equivalent.

Regarding the second configuration, the best strategy would be to maintain the same power management parameters as the first architecture, and take advantage of the extra energy stored in the batteries by increasing the full electric mode speed boundaries.

However, in the urban cycle presented in this work, the vehicle does not explore sufficient speed conditions in order to take advantage from this change in the full electric mode limits, therefore the improvements cannot be investigated.

The following graph reports the fuel consumption trends of the three architecture analyzed.

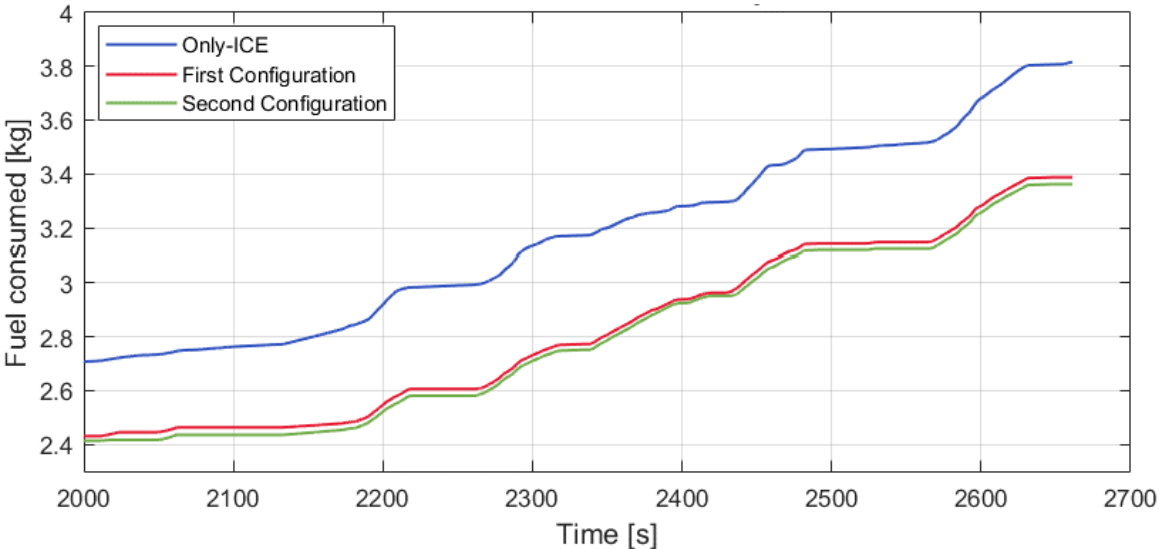


Figure 97 – Second configuration, Cumulated fuel consumption confrontation

Finally, the results of the test are summarized in the following table.

Table 17 – Second configuration, test results

| | HEV 2 | Only ICE | Difference | HEV 1 | Difference |
|--|---------|----------|----------------|----------|---------------|
| Electric mode operating time | 1972 s | - | - | 1866 s | - |
| Hybrid mode operating time | 689 s | - | - | 795 s | - |
| Minimum battery SOC | 46% | - | - | 46,4% | - |
| Maximum battery SOC | 67,5% | - | - | 66,8% | - |
| Overall engine output mechanical energy | 58 MJ | 62,67 MJ | -7,45% | 58,43 MJ | -0,73% |
| Average overall engine efficiency | 38,92% | 37% | +5,19% | 38,85% | +0,18% |
| Fuel consumption | 3,36 kg | 3,82 kg | -12,04% | 3,39 kg | -0,88% |
| Equivalent fuel consumption | 3,39 kg | 3,82 kg | -11,25% | 3,41 kg | -0,6% |

4.3.2 Urban path test results with re-sized battery pack

In section 4.3.2 it has been highlighted how the motors' capabilities could not be completely exploited due to the limitations from the battery pack in terms of peak power, both in charge and in discharge mode.

The problem could be solved by increasing the peak current that the battery pack can handle. In this test, the number of battery modules in parallel has been increased from 2 to 3, switching from a capacity of 6048 Wh to 9072 Wh.

The following results show the impact of an increase in the number of battery modules to the powertrain's performance throughout the urban test.

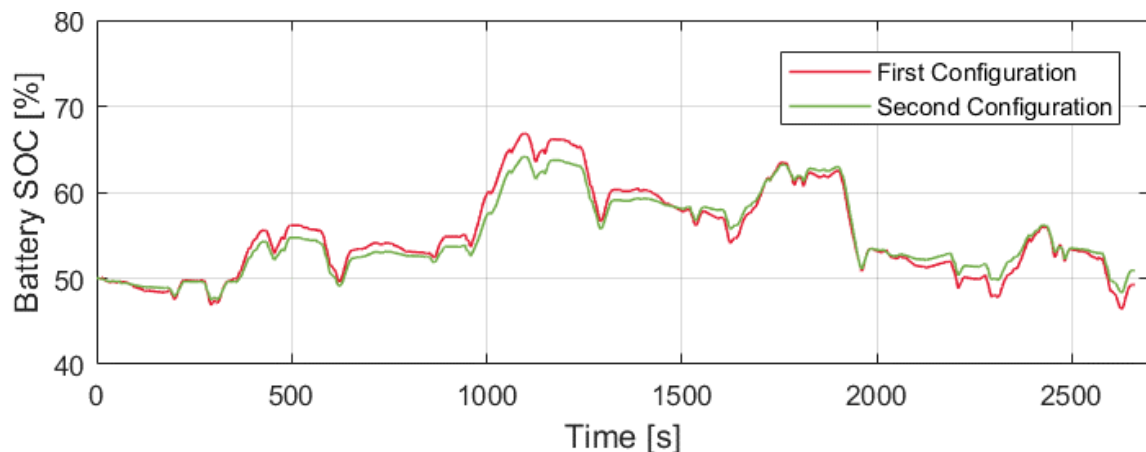


Figure 98 – Second configuration with resized battery pack, Battery SOC

The first noticeable effect of an increase of the capacity of the battery pack is a more stable SOC: an equal amount of energy stored will result in a reduced delta-SOC.

Furthermore, it can be clearly seen how the hyperbolic trend representing the torque limitation related to the maximum power handled by the battery is pushed up towards the maximum torque delivered by the motor. This means that the motor's capabilities of storing energy in generator mode and reducing the idling phase in motoric mode is enhanced.

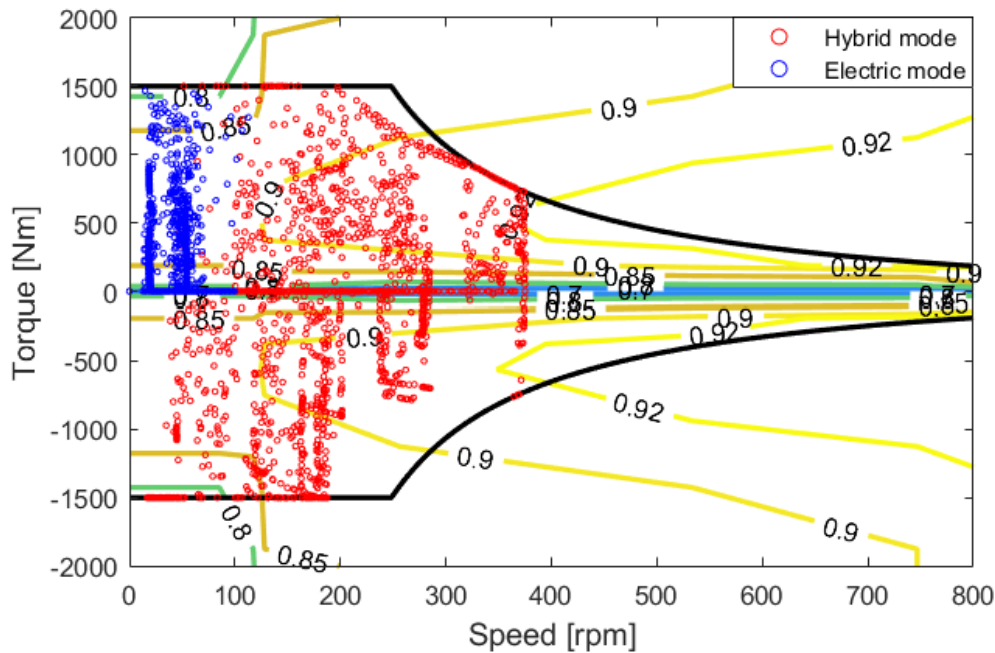


Figure 99 – Second configuration with resized battery pack, Electric motor operating points

This results in a noticeable advantage in terms of mechanical energy reduction throughout the test, as shown in figure 100.

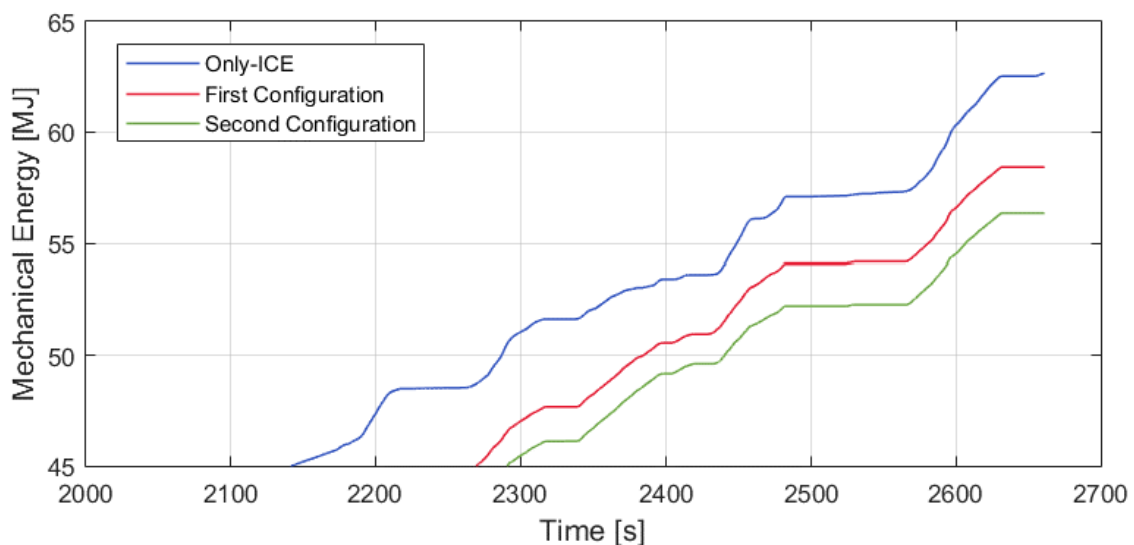


Figure 100 – Second configuration with resized battery pack, Mechanical energy

This has an impact to the overall fuel consumption, which is further reduced in respect to the first configuration and to the smaller battery pack.

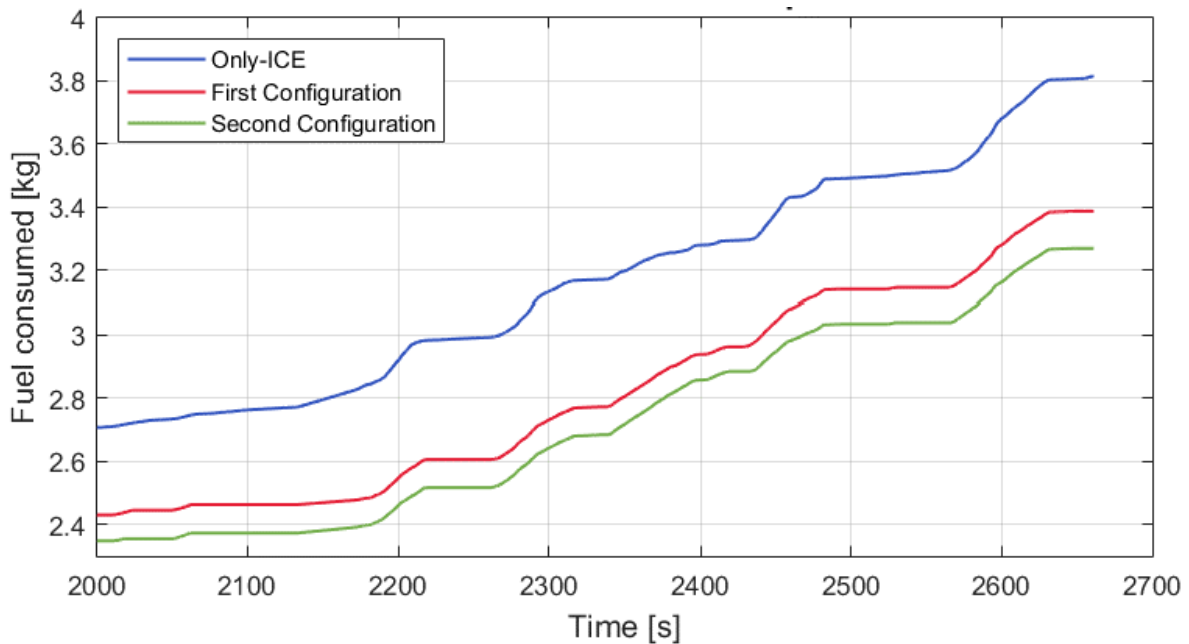


Figure 101 – Second configuration with resized battery pack, Cumulated fuel consumption

Finally, the results of the test are summarized in the following table.

Table 18 - Urban test results, second configuration with resized battery pack

| | HEV 2 | Only ICE | Difference | HEV 1 | Difference |
|--|----------|----------|----------------|----------|---------------|
| Electric mode operating time | 1664 s | - | - | 1866 s | - |
| Hybrid mode operating time | 1016 s | - | - | 795 s | - |
| Minimum battery SOC | 47,5% | - | - | 46,4% | - |
| Maximum battery SOC | 64,12% | - | - | 66,8% | - |
| Overall engine output mechanical energy | 56,35 MJ | 62,67 MJ | -10,08% | 58,43 MJ | -3,55% |
| Average overall engine efficiency | 38,92% | 37% | +5,19% | 38,85% | +0,18% |
| Fuel consumption | 3,26 kg | 3,82 kg | -14,65% | 3,41 kg | -4,4% |

5. Design feasibility study

In this chapter a feasibility study of the design of the two configurations analyzed so far will be carried on, in order to highlight the possible solutions for the modification of the rear axle that will embed the electric powertrain.

This is a preliminary study, and a rough sizing of the components will be done, so as to point out the critical issues of the design problem.

Furthermore, the study will be addressed to the structural axle, the tires, the electric machine (or machines) and the connection between the machine and the wheels. Components such as the battery pack, the power conversion unit and the suspensions will not be included in the study.

5.1 Single electric motor feasibility study

The first configuration analyzed is the single electric motor architecture. In this solution, the electric machine has to be coupled to the wheels through an open differential, with a conical gear reduction and a gear ratio of 12:1.

The starting point for the electric axle is a regular tractive axle that receives the torque from a driving shaft connected to the vehicle's torque coupler, and then splits it to the wheels through a differential.

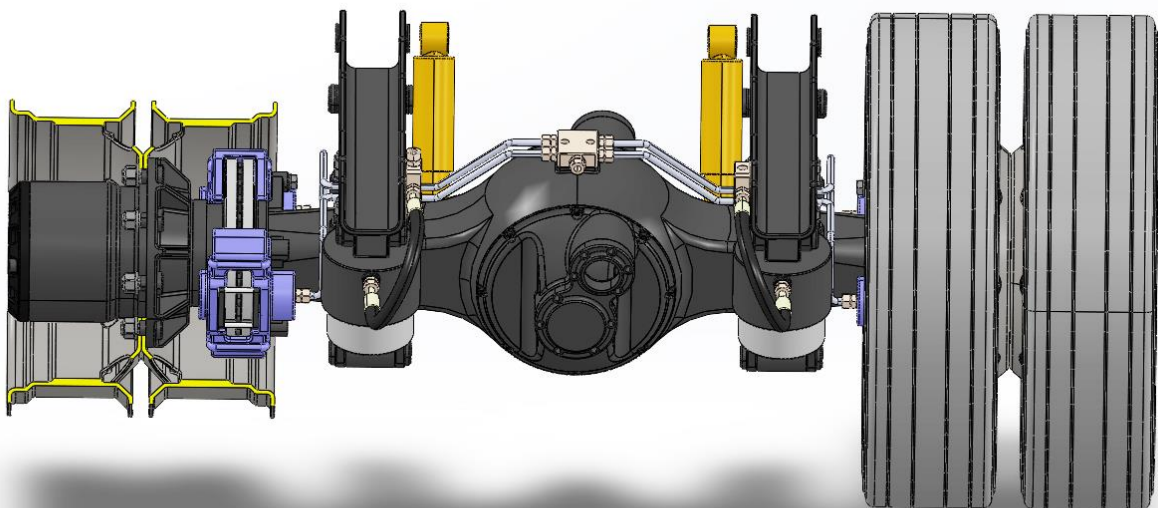


Figure 102 - Conventional axle rendering

The axle can be converted into an electric axle by modifying the front cover and installing the electric motor on the new cover. For assembly reasons, a mounting flange is required in order to allow the access on the front bolts and ease assembly and disassembly operations.

The following figure reports a proposal of design for the connection between the electric machine and the axle.

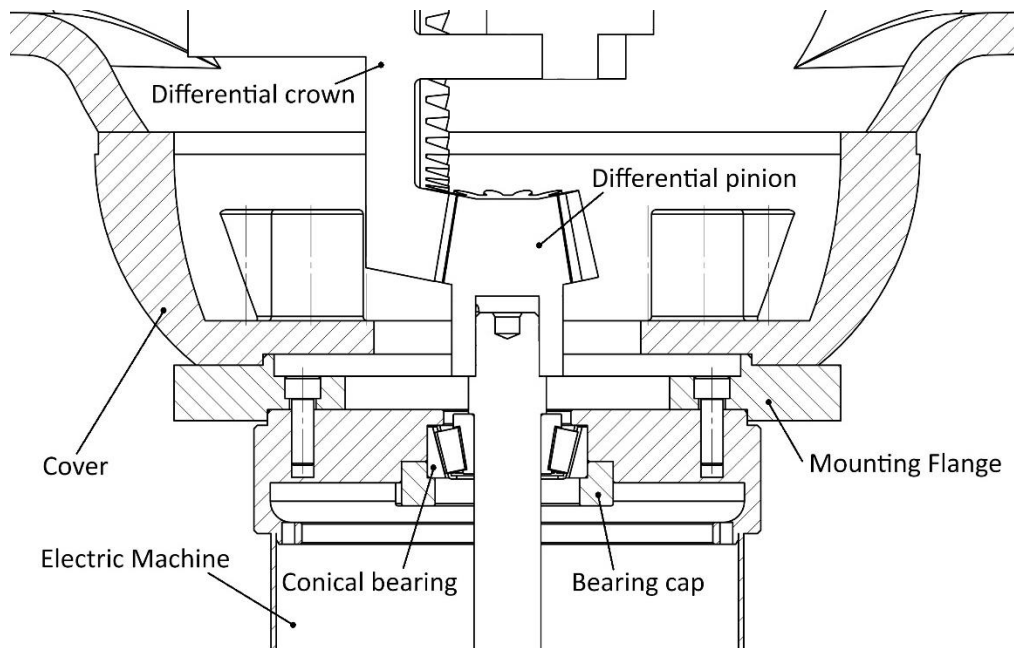


Figure 103 - Mechanical connection between EM and differential

The main elements of the assembly are:

- **Electric machine:** the electric machine represented in the assembly is the HPEVS AC-51. The machine's rotor is connected to a central shaft, supported by two conical bearings mounted with an "O" disposition. The shaft is then connected to the differential pinion.
- **Conical bearings:** in order to sustain the axial force generated by the differential conical gear coupling, it is necessary to substitute the original ball bearings of the motor with two conical bearings. The bearings should be mounted with an "O" disposition, since the axial force is external and directed towards the center of the motor.

In order to achieve this disposition, the edges of the bearing have to be constrained. The external edge is constrained by a shoulder on the shaft, while the internal edge is constrained by a bearing cap, which bolts to the inner side of the motor. The motor originally provided a bearing cap for the ball bearings, therefore the substitution of the bearing and the introduction of the new cap is a relatively simple operation, and requires limited machining processing on the motor's shaft and inner flange.

- **Differential pinion:** the final element that has to be mounted on the motor's shaft is the pinion that will gear with the differential's crown, transferring the power to the wheels. The differential pinion can be connected to the motor's shaft with a shrink-fitting technique.
- **Mounting flange:** in order to facilitate the assembling and disassembling operations of the motor, and to ease the maintenance operations, it is necessary to provide a mounting flange that is connected to the motor and can be bolted to the axle cover.

The flange has to be provided with ridges that can facilitate the centering operations. Regarding the motor connections, the default motor bolt seats can be used, minimizing the intervention of the motor's structure.

- **Axle cover:** this component substitutes the original cover of the axle, and it has to provide special stud seats in order to assemble the motor's mounting flange.

The cover can be then bolted to the main body of the axle.

This simple, yet effective design, allows the connection of the electrical machine to the differential and then to the wheels. The intervention on the axle is not much invasive, and it allows to retrofit this architecture to an existing vehicle, without major mechanical changes.

However, it is necessary to design a housing for the battery pack and the power conversion system. These components can be housed in the truck's payload, sacrificing a small part of the payload's capacity.

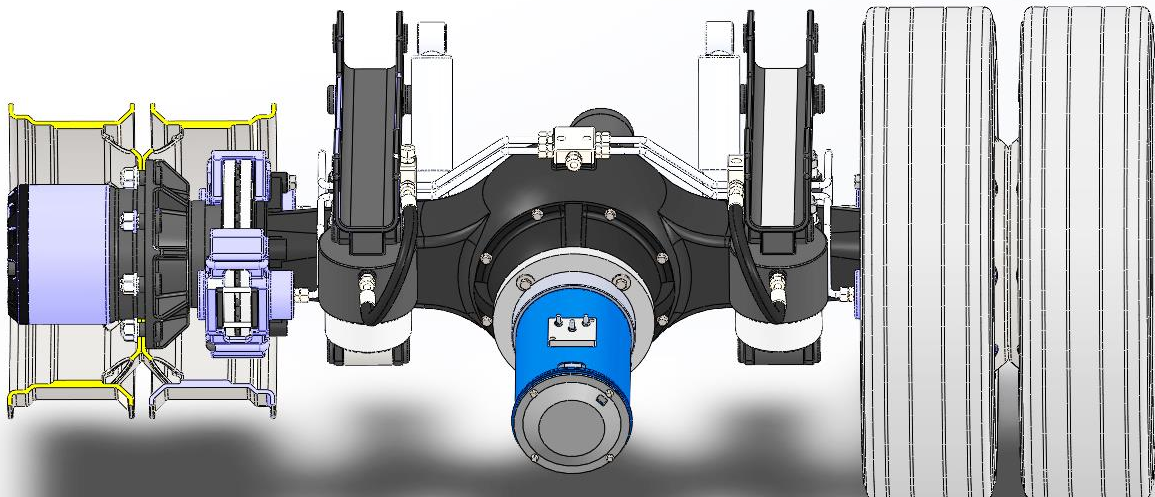


Figure 104 - Electric axle rendering

5.2 Wheel motors architecture feasibility study

In this section the design problem of the second hybrid configuration will be addressed, proposing a possible design idea.

Unlike the single electric machine configuration, in this case the rear axle cannot be simply modified, but it has to be completely redesigned, in order to provide housing to the frame less wheel motors.

Furthermore, in order to guarantee the necessary maintenance operation for the motors and to facilitate the assembling and disassembling procedures, it is necessary to make sure that the motor can be separated from the rest of the assembly independently, without having to disassemble the entire wheel hub.

The proposed design solution for the electric rear axle is characterized by a re-designed structural axis, with a semi-cylindrical shape in order to provide enough space for the electric machine, which is connected to a main hub. The hub houses the wheel shaft and its conical bearings, while the shaft is connected to the wheel hub and to the brake disk.

The electric motor is mounted on the other side of the main hub, and can be disassembled simply by removing dedicated bolts. The link between the motor's rotor and the wheel shaft is a fluted connection.

The following figure represents a section of the assembly. The main components are listed in the table below.

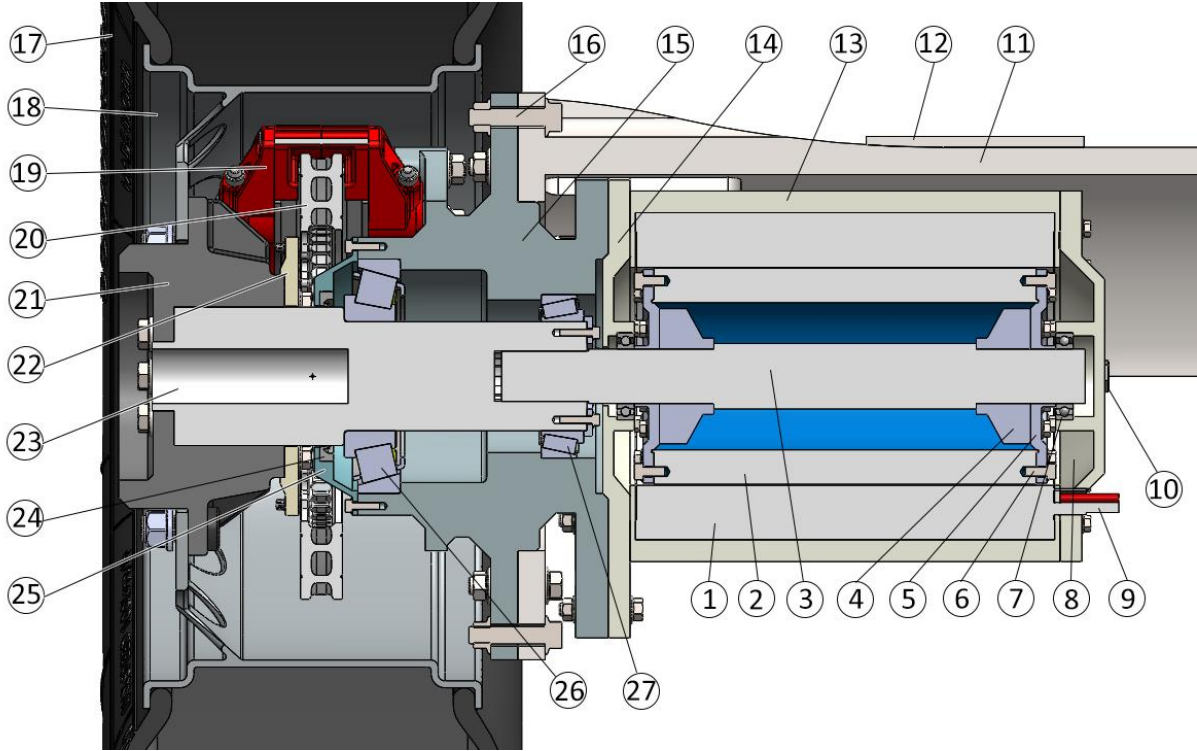


Figure 105 - Wheel motor configuration assembly

Table 19 - List of components

| Component number | Component description |
|-------------------------|---|
| 1 | Electric machine stator |
| 2 | Electric machine rotor |
| 3 | Electric machine shaft |
| 4 | Mounting support for the motor's shaft |
| 5 | Mounting flange connecting the rotor to the shaft |
| 6 | Mounting bolts |
| 7 | Electric motor shaft ball bearings |
| 8 | Electric machine rear cover |
| 9 | Power wires |
| 10 | Refrigeration system outlet |
| 11 | Structural axle |
| 12 | Suspension support |
| 13 | Electric machine housing |
| 14 | Electric machine front cover |
| 15 | Main hub |
| 16 | Hub-axle connecting bolts |
| 17 | Tire |
| 18 | Wheel |
| 19 | Brake caliper |
| 20 | Brake disk |
| 21 | Wheel hub |
| 22 | Brake disk support flange |
| 23 | Wheel shaft |
| 24 | Retaining ring |
| 25 | Bearing cap |
| 26 | First conical bearing |
| 27 | Second conical bearing |

The main assembly can be divided into three different sub-assemblies, that can be assembled separately during the mounting phase, and then they can be connected together. The main sub-systems are:

- **Wheel subsystem:** it includes the wheel, the tire, the wheel hub, the main shaft, the brake disk and caliper, and all the minor connecting components such as mounting flanges and bolts.
- **Main hub subsystem:** this sub-assembly includes the main structural hub, which provides support to both the wheel and the electric motor subsystems, and connects to the structural axle.
- **Electric machine subsystem:** it comprehend the rotor, the stator, the motor's shaft, the complete housing, the ball bearings and the secondary mounting elements. This sub-assembly is completely independent from the afore mentioned, and it can be disassembled separately just by removing the mounting bolts that link it to the main hub.

In the following sections the single subsystems will be analyzed separately, highlighting the mounting sequence and describing the single components more in detail.

5.2.1 Wheel subsystem

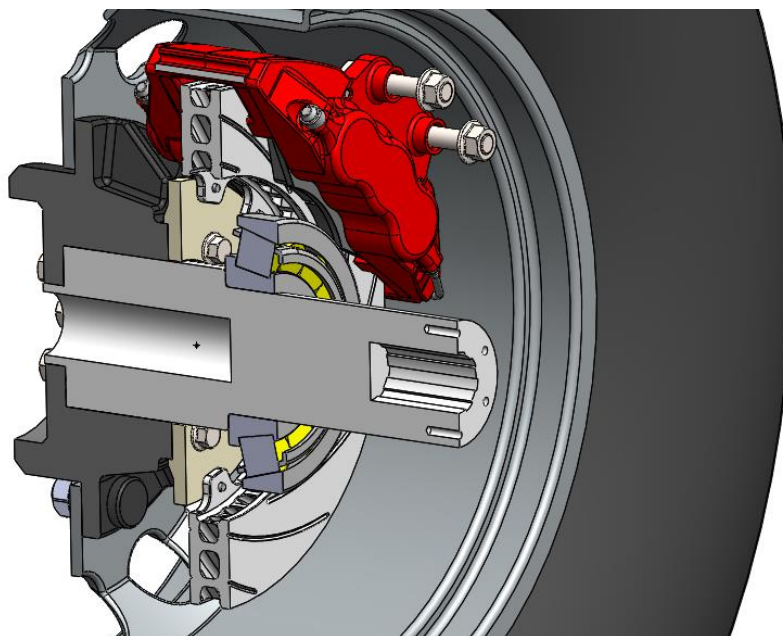


Figure 106 - Wheel assembly

The first subsystem that can be assembled is the wheel subsystem. In particular, the first elements that can be connected together are the wheel shaft and the wheel hub by six studs accessible from the front of the tyre.

Then, the braking disk support flange can be mounted to the wheel hub, and the braking disk is then mounted to the flange.

The next component that can be assembled on the wheel shaft is the first conical bearing, through a shrink-fitting technique. A dedicated shoulder on the wheel shaft allows to constrain the bottom left edge of the bearing.

Finally, the brake disk and caliper and the tire have to be assembled after that the subsystem has been connected to the main hub, as described in the following section.

5.2.2 Main hub subsystem

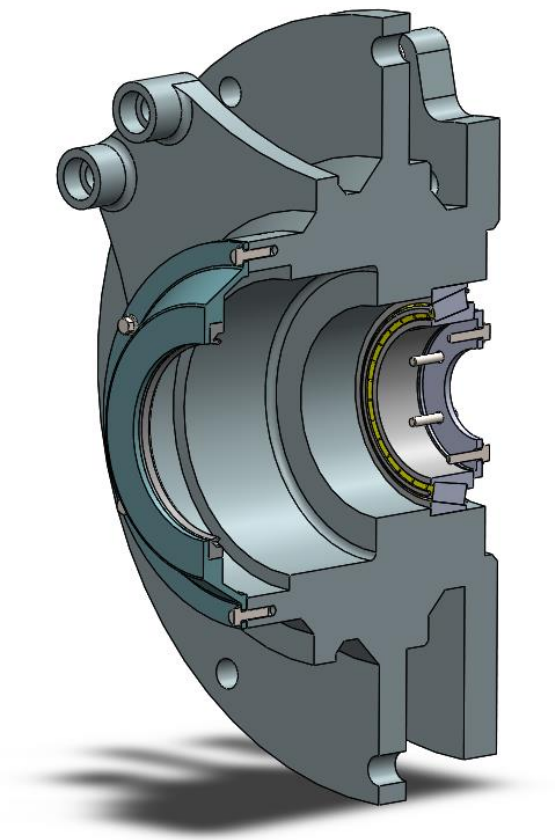


Figure 107 - Main hub assembly

The second subsystem analyzed is the main hub subsystem. The main hub is a structural element which is responsible of providing support to the wheel subsystem, the braking system, and the electric machine subsystem.

Furthermore, this element is connected to the structural axle, and transmits the vertical and the axial forces generated by the weight of the vehicle and by its interaction with the ground.

The sub-assembly is composed by the main structural element (hub), the bearing cap and its retaining ring, the second conical bearing and its retaining flange.

In terms of assembling phase, the first element that can be mounted to the hub is the conical bearing, through a shrink-fitting procedure.

Later on, the wheel subsystem can be coupled with the hub, and finally the bearing cap (previously coupled with the retaining ring) can be fitted to the hub.

The last elements that can be assembled are the components of the braking system and the tire.

Once that the two subsystems have been assembled together, they can be bolted to the structural axle. The last element remaining is the electric machine sub-assembly, that can be assembled independently from the previous ones.

5.2.3 Electric machine subsystem

This sub-assembly comprehends all the components related to the wheel motor, such as the stator, the rotor, the shaft, the housing and covers, bearings, and the mounting elements such as flanges and supports.

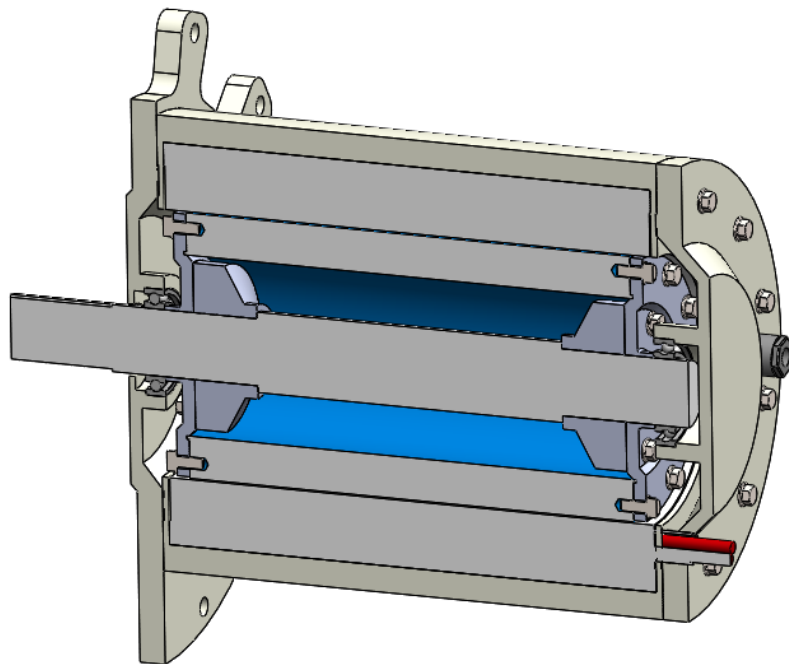


Figure 108 - Electric machine assembly

The sub-assembly can be assembled and then mounted directly to the external flange of the wheel hub, after that this has been bolted to the rear axle.

Then, it is necessary to connect to the motor the power wires coming from the power converting system, and the pipes from the refrigerant circuit.

As in the previous architecture, some space has to be dedicated to house the battery pack and the power management block. It is possible to sacrifice a small amount of the payload capacity to house these components.

The following figure represents a rendering of the complete assembly of the axle.

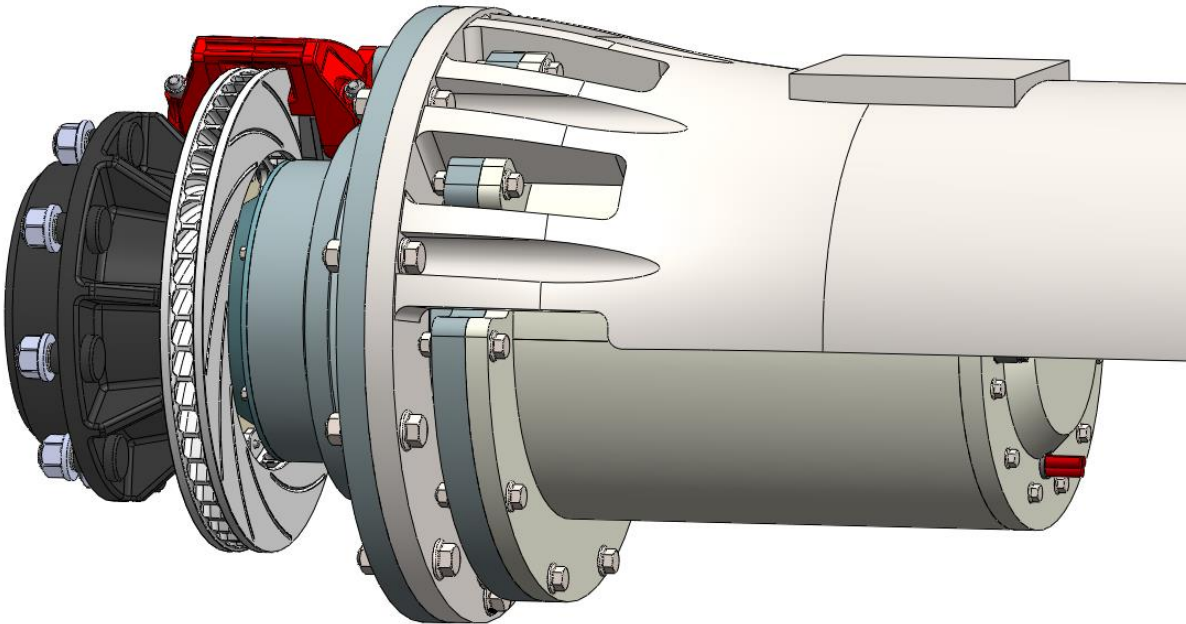


Figure 109 - Complete assembly

6. Conclusions and future work

6.1 Conclusions

The goal of the present work was to create a mathematical model of two Parallel Hybrid architectures for Medium/Heavy Duty Service Vehicles and to analyze their performances in different “real life” scenarios.

The configurations analyzed were two “through the road” parallel hybrid architectures (also referred as P4 configurations). The first one characterized by a single electric machine connected to the wheels through a differential, and the second one characterized by two wheel motors directly connected to the wheels and working independently.

Both the hybrid powertrains are constituted by an Internal Combustion Engine that delivers the torque to the front axle and to the first rear axle, and by an electric powertrain that provides the torque to the second rear axle. The connection between the two power sources is provided by the constraints imposed by the road, and so there is no direct mechanical connection. A power management system is responsible of splitting the power between the two sources depending on the driving conditions.

The class of vehicles taken as a reference is Class 5 according to the US GVWR classification. Those vehicles are also referred as “medium duty trucks”, and the category includes vehicles such as the Ford F-550, RAM 5500, GMC 5500 and so on.

Therefore, vehicle’s features used to generate the models were taken from the Ford F-550, while the ICE chosen is a Detroit Diesel S50, an 8.5 liter unit capable of delivering a maximum power of 205 kW.

The component sizing for the electric powertrain has been conducted in parallel with the simulations, through an iterative process. For the first configuration, an HPEVS AC-51 electric machine has been chosen, capable of delivering a maximum power of 55 kW, while for the second configuration, two Bosch-Rexroth IndraDyn H MBS272D, with a rated power of 27,5 kW each, have been taken as a reference. Both configurations are equipped with a lithium-ion battery pack with a capacity of 6048 Wh.

The first step of the work was to create a mathematical model of the vehicle, in all his configurations of interest: only-ICE, ICE and single electric motor, ICE and wheel motors. This was possible using the software TruckSim by “Mechanical Simulations”, coupled with Matlab/Simulink. This combination has allowed the realization of the hybrid architectures, which were not immediately available in the TruckSim suite.

The hybrid powertrain Simulink model is made up by different functional subsystem interacting with each other and with the TruckSim block. The main one are: a power management block, which integrates a simple rule-based strategy to determine the electric torque to be delivered; an electric machine block, which simulates the electric motor/generator behavior, determining the actual torque delivered, the electric power

request or supply and the behavior of the regenerative braking system; a battery subsystem, which describes the behavior of the battery pack and allows to determine relevant quantities such as the battery SOC; and other auxiliary blocks that are required to describe mechanical devices of the powertrain, or are necessary to calculate some quantities of interest and facilitate the post-processing phase.

The afore-mentioned models were then put to the test into different scenarios. The first one is an urban city route, which describes a real-life itinerary of a truck in an urban environment. The second one is a food-delivery procedure, in which the vehicle is engaged in a sequence of advancement and stop phases. This procedure was important to test the behavior of the system in the management of auxiliary devices, compared to a regular ICE architecture. Finally, the last scenario was a cruising test on a highway, in order to evaluate the powertrain's behavior in a high speed situation.

In the urban test, it was possible to observe how the electric powertrain succeeds in assisting the ICE and optimizing its functioning.

In fact, it was noted how, with an appropriate calibration of the power management parameters and an appropriate sizing of the powertrain components, the ICE operating points are shifted towards higher efficiency areas, using the battery as an energy buffer and the electric machine as a motor/generator. In order to balance the SOC, however, the power management engages a full electric mode when the vehicle speed is sufficiently low, when the required torque does not exceed the maximum torque delivered by the motor, and when the battery has a sufficient SOC. This strategy has allowed to remove the engine operating points from the lowest efficiency area, due to idling or low speed coasting conditions.

This has resulted in an increase of the overall engine efficiency, from an average value of 37% of the only-ICE configuration to a value of 38,85% for the first configuration and 38,92% for the second configuration.

Moreover, the hybrid powertrain has allowed to implement a regenerative braking strategy, which can be used to recover part of the energy dissipated during braking maneuvers. This has allowed to lower the overall requested energy to complete the whole procedure, despite the fact that the losses of the electric powertrain during the energy conversions contribute to increase this value. However, we assist to a reduction of the mechanical energy required from 62,67 MJ of the only-ICE configuration to 58,43 MJ of the single electric motor architecture and 58 MJ of the wheel motors architecture.

These two effects combined together result in a perceptible reduction in fuel consumption. In fact, the first hybrid architecture has allowed to obtain a fuel saving of 10,73%, while the fuel saving for the second architecture is 11,25%.

The wheel motors architecture allows to have a better fuel economy due to the slightly greater hybridization factor provided, and because of the better efficiency of the frame less motor. However, the advantage is not considerable as expected if the battery pack is not changed. This can be explained by the absence of a gear reduction between the wheel motors and the wheels. So, it is difficult to take advantage of the full capabilities of the motors, especially at low speeds, where the maximum power delivered by the motors drops drastically.

However, it has been observed that if the maximum current that the battery pack could handle is increased, the advantages of the wheel motors architecture increase significantly. In these conditions, in fact, the architecture can provide a reduction of the mechanical energy required of 10,08% in respect to the only-ICE architecture and 3,55% compared to the first configuration. This results in a fuel saving reduced by 14,65% compared to the conventional vehicle, and by 5,6% compared to the single EM architecture.

The second procedure has the task to simulate the different management of auxiliary devices with a hybrid powertrain. If in conventional architectures the auxiliary devices are directly powered by the engine, reducing its organic efficiency and forcing the engine to idle when the vehicle performs a stop, in a hybrid architecture the auxiliary devices can be powered separately by the electric powertrain's battery pack.

This strategy allows to reduce drastically the idling time of the ICE, increasing its efficiency. In a simulated real life scenario in which the vehicle has to alternate an urban path to a food delivery stop phase, the advantages provided by the hybrid architecture are evident.

The first configurations allows the engine to increase its overall efficiency from 33% to 39,3%, resulting in a fuel saving of 14,63%.

The last scenario was the highway cruising procedure. This situation is the least favorable for a hybrid powertrain, since the engine runs already at good efficiencies, and the braking maneuvers are almost absent. However, the oscillations in speed and road slope determine a dispersion in the engine's operating points.

The hybrid powertrain can still optimize the engine's operation, but it is not previously evident if the advantages in the engine's load shifts are able to compensate the losses due to energy conversion.

As a matter of fact, it results that in this situation the hybrid mode is not effective. In fact, despite there is a really slight increase in efficiency, from 40,7% to 41%, there is also an increase in the mechanical energy required, that goes from 1403 MJ to 1480 MJ. This results in an increase of the fuel consumption by 3,7%.

Therefore, it is convenient to introduce a cruising recognition strategy in the power management in order to spot a highway cruising phase, and switch the powertrain to full ICE mode.

The two hybrid configurations have therefore shown an interesting potential in terms of fuel economy for Service Vehicles frequently employed in urban journeys. The wheel motors architecture does not seem to ensure consistent advantages in terms of fuel saving, unless the battery pack is resized to ensure a bigger peak power handled by the system.

Furthermore, the wheel motors architecture allows an independent management of the two wheels, opening to torque vectoring and stability control strategies; the main disadvantage of this solutions resides in higher costs and complexity of the system.

In the last part of the work the two architectures have been analyzed from a design point of view, in order to have an overview of the feasibility of the two systems. As mentioned before,

the second solution is the most complex, and it requires a complete re-design of the entire axle. The first architecture, instead, is relatively simple to implement, and requires minor modifications of the existing tractive axle in order to convert it into an electrically powered one.

6.2 Future work

From this starting point, it may be possible in the future to further develop the hybrid powertrains models, and test them on board of a concept vehicle.

In terms of future work, one of the first problem to face would be a better optimization of the current power management strategy. In fact, in this work the power management is simple and rule-based. In every scenario, with an iterative process, it was possible to tune the parameters of the power management in order to optimize the system's performance.

However, the optimization process of the parameters is much more complex and requires a dedicated work. This could lead to further results in terms of fuel economy, and maybe can highlight further differences between the two architectures.

Moreover, it has to be noticed that the power management parameters were chosen specifically for a given test procedure, which was known a prior. A strategy to recognize a certain driving pattern is necessary when the power management is integrated on board, since the itinerary and the speed profile that the vehicle will face are not known a prior on a real driving scenario.

In order to implement the models in the vehicle's on board electronics, it is necessary to modify some of the input parameters and how they are acquired. For example, in these models the required torque and power, used to determine the electric torque to be delivered and the powertrain mode, were previously calculated by running a simulation of the only-ICE configuration and then logging the data in specific arrays.

In an on-line model, these parameters have to be estimated relating them to the throttle position input.

Finally, another interesting analysis would be to confront the results obtained in this work with a power management strategy oriented to minimize the engine-out pollutant emissions rather than minimizing the fuel consumption.

In conclusion, this work has shown how hybrid powertrains have a great potential in optimizing the operation of vehicles, increasing their overall efficiency. Not only in passenger car applications, where this technology is slowly gaining a consistent market share, but also in commercial applications, especially for service vehicles engaged in challenging itineraries in an urban context.

In these applications, the parallel "through the road" solutions analyzed seem to be promising in terms of simplicity, effectiveness, and possibility to be retro-fit to older vehicles.

Bibliography

- Block, D., Harrison, J., Brooker, P., Center, F., & Dunn, M. (2015). Electric vehicle sales for 2014 and future projections. *Electric Vehicle Transportation Center*.
- Buecheler, D., Bolvashenkov, I., & Herzgov, H. (2009). Verification of the Optimum Hybridization Factor as Design Parameter of Hybrid Electric Vehicles. *Vehicle Power and Propulsion Conference*, 847-851.
- Chau, K., & Wong, Y. (2002). Overview of power management in hybrid electric vehicles. *Energy Conversion and Management, Volume 43, Issue 15*, 1953-1968.
- Durbin, T., Johnson, K., Miller, J., Maldonado, H., & Chernich, D. (2008). Emissions from heavy-duty vehicles under actual on-road driving conditions. *Atmospheric environment*, 4812-4821.
- Ehsani, M., Gao, Y., & Emadi, A. (2010). *Modern electric, hybrid electric, and fuel cell vehicles*. CRC Press.
- Ferrari, G. (2014). *Motori a combustione interna*. Società editrice Esculapio.
- Galvagno, E., Morina, D., Sorniotti, A., & Velardocchia, M. (2013). Drivability analysis of through-the-road-parallel hybrid vehicles. *Meccanica*, 351-366.
- Khajepour, A., Fallah, S., & Goodarzi, A. (2014). *Hybrid and Electric Vehicles - Technologies, Modelling and Control: A Mechatronic Approach*. Wiley.
- Lukic, S., & Emadi, A. (2004). Effects of drivetrain hybridization on fuel economy and dynamic performance of parallel hybrid electric vehicles. *IEEE Transaction on Vehicular Technology*, 385-389.
- Mechanical Simulation. (2018). *TruckSim demonstration manual*. Tratto da carsim.com.
- Miller, J., Ehsani, M., & Gao, Y. (2005). Understanding power flows in HEV eCVT's with ultracapacitor boosting. *IEEE Vehicle Power and Propulsion Conference*.
- Nelson, F. (2000). Power requirements for batteries in hybrid electric vehicles. *Journal of power sources 91*, 2-26.
- Pacejka, H. (2005). *Tyre and Vehicle Dynamics*. Butterworth-Heinemann.

- Shancita, I., Masjuki, H., Kalam, M., Fattah, I., Rashed, M., & Rashedul, H. (2014). A review on idling reduction strategies to improve fuel economy and reduce exhaust emissions of transport vehicles. *Energy conversion and management*, 794-807.
- Somà, A., Bruzzese, F., & Viglietti, E. (2015). Hybridization Factor and performances of Hybrid Electric Telescopic heavy vehicles. *Tenth International Conference on Ecological Vehicles and Renewable Energies*.
- Yang, Y., Arshad-Ali, K., Roeleveld, J., & Emadi, A. (2016). State-of-the-art electrified powertrains-hybrid, plug-in, and electric vehicles. *International journal of powertrains*, 1-29.

Sitography

- Bosch Rexroth. (2018). *Rexroth IndraDyn H MBS272D User manual and technical specifications*. Retrieved from Bosch Rexroth: https://www.boschrexroth.com/country_units/america/united_states/sub_websites/brus_dcc/documentation_downloads/ProductDocumentation/CurrentProducts/Motors/IndraDyn_H/29789502.pdf
- Ford. (2018). *Ford F-550-XL technical specifications*. Retrieved from Ford: <https://www.ford.com/commercial-trucks/chassis-cab/models/f550-xl/>
- *Heavy Heavy-Duty Diesel Truck (HHDDT) schedule by California Air Resources*. (n.d.). Retrieved from Dieselnet: <https://www.dieselnet.com/standards/cycles/hhddt.php>
- HPEVS. (n.d.). *HPEVS Peak and Continuous power Graphs for AC-51*. Retrieved from HPEVS: <http://www.hpevs.com/hpevs-ac-electric-motors-power-graphs-ac-51.htm>